SANDIA REPORT

SAND91—0184 • UC—603
Restricted Distribution by Sponsor
Printed January 1991

Potential Impacts of Iraqi Use of Oil as a Defensive Weapon

H. W. Church, M. W. Edenburn, W. Einfeld, D. Engi, S. A. Felicetti,
T. H. Fletcher, G. S. Heffelfinger, K. D. Marx, J. T. McCord,
D. A. Northrop, J. R. Waggoner, N. R. Warpinski, B. D. Zak,
P. W. Moore, L. D. Potter

Prepared by
Sandia National Laboratories
Albuquerque, New Mexico 87185 and Livermore, California 94550
for the United States Department of Energy
under Contract DE-AC04-76DP00789
Office of Foreign Intelligence

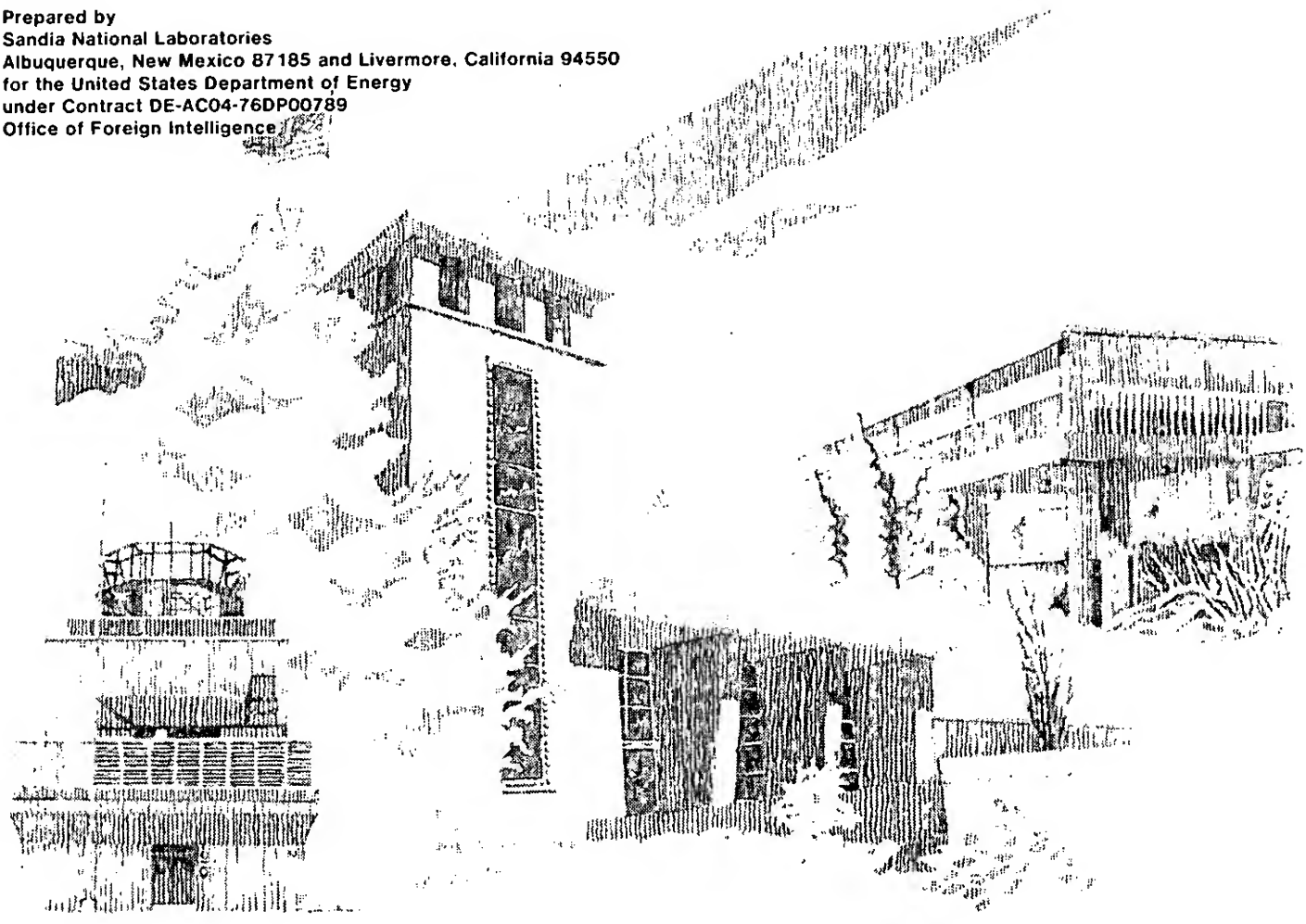

SF2900Q(8-81)

Issued by Sandia National Laboratories, operated for the United States Department of Energy by Sandia Corporation.

SAND91-0184
Distribution Restricted by Sponsor
Printed January 1991

Distribution
Category UC-603

POTENTIAL IMPACTS OF IRAQI USE OF OIL AS A DEFENSIVE WEAPON

H. W. Church, M. W. Edenburn, W. Einfeld, D. Engi
S. A. Felicetti, T. H. Fletcher, G. S. Heffelfinger, K. D. Marx
J. T. McCord, D. A. Northrop, J. R. Waggoner
N. R. Warpinski, and B. D. Zak
Sandia National Laboratories
Albuquerque, NM 87185

P. W. Moore
Tech. Reps., Inc.
Albuquerque, NM 87110

L. D. Potter
Albuquerque, NM 87110

Sponsored by the
Office of Foreign Intelligence
Department of Energy

This page intentionally left blank

EXECUTIVE SUMMARY

A multidisciplinary team studied the potential atmospheric optical effects, ecological stresses, and reservoir damages that would result from the demolition of wellheads in Kuwaiti oil fields and from the discharge or ignition of oil from nonreservoir sources such as oil storage tank farms, man-made oil-filled trenches, pipelines, and oil tankers. Base-case and worst-case scenarios for the oil fields were considered: in the base-case scenario, 300 wellheads in Kuwait were destroyed and 50% of these were ignited; in the worst-case scenario, all 900 wellheads were destroyed and 80% of these were ignited. The approach in this study was to perform a series of time-phased analyses, each stage of which generated not only immediate results, but also the requisite inputs, or source terms, for the succeeding stage. Hence, reservoir analyses provided source terms for combustion analyses in addition to estimates of reservoir damage; combustion analyses defined combustion products, posed oil-filled trench issues, and provided source terms for atmospheric processes; atmospheric analyses generated potential optical effects and provided source terms for ecological analyses that, in turn, provided estimates of ecological stresses.

Midday light levels are expected to be several orders of magnitude less than on a moonlit night due to extinction of sunlight by soot within a corridor tens of kilometers wide downwind (probably southeast) from burning trenches. Darkening under plumes from oil fields will vary from modest to more intense than darkening under plumes from the trenches. Maximum degradation of visibility is expected between ground level and 2 km altitude at distances of 5 to 30 km from the sources. Reduced visibility will exist over 100 km from the sources. Major degradation is also expected in the infrared region of the spectrum; consequently, electro-optical instrumentation will be affected. Use of a line source rather than a two-dimensional array of wells is a source of uncertainty (a factor of two or three in optical depth) in these estimates as are meteorological conditions.

In all scenarios, airborne pollutants created by burning oil are not expected to produce major health effects in the large population centers, except possibly on a small number of sensitive individuals. Downwind of the fire trenches, pollutant concentrations may be sufficient to cause nausea and eye and respiratory system irritation in unprotected individuals. Oil spilled over the ground will kill vegetation and is a threat to shallow aquifers and coastal wells. Most vegetation is expected to recover within a year. Oil (77 times the amount of the Exxon Valdez spill) discharged from tankers, pipelines, or on-shore storage tanks into the Gulf will cause major damage to the marine ecology, to the fishing industry, and to desalination facilities in four countries. Detailed quantitative aspects of the damage are uncertain.

Extensive, irremediable losses from reservoir damage are not expected. However, oil losses due to uncontrolled flow could amount to as much as 7 to 10 Mbbl/day in the worst-case scenario and 5 to 6 Mbbl/day in the base-case scenario. The number of wells affected and the time required to regain control of them are uncertain.

Given the Iraqi Pipeline to Saudi Arabia (IPSA) as the only source of oil, fire trenches can be filled in roughly 145 hours if there is no seepage. Based on current estimates of oil seepage, the trenches may not be fillable simultaneously, but preconditioning with oil to reduce seepage may allow them to be filled and maintained at a full level. If the trenches contain no oil, IPSA-limited burning can occur along trench feeder lines at about one-sixth the intensity of oil-filled trenches, resulting in still significant concentrations of pollutants and degradation of visibility. Most uncertain are soil properties (seepage rates) from the trenches and the potential for use of added sources of oil (e.g., Southeast Field).

CONTENTS

FIGURES

TABLES

This page intentionally left blank

I. INTRODUCTION

The first objective of the preliminary analyses documented here was the determination of the **reservoir damage** from the demolition of wellheads in Kuwaiti oil reservoirs and the **ecological stresses (ecostresses)** from discharges from blown wellheads and nonreservoir sources such as oil storage tank farms, man-made oil-filled trenches, pipelines, and oil tankers. The second objective was to determine the **optical characteristics** of the atmosphere (a mixture of air, volatiles, combustion products, etc.) that would result from the discharge and combustion of oil from both reservoir and nonreservoir sources. Figure I-1 is a simplified map of Kuwait showing reservoir and nonreservoir sources, some critical facilities that could be affected, and the probable direction in which combustion products would be blown.

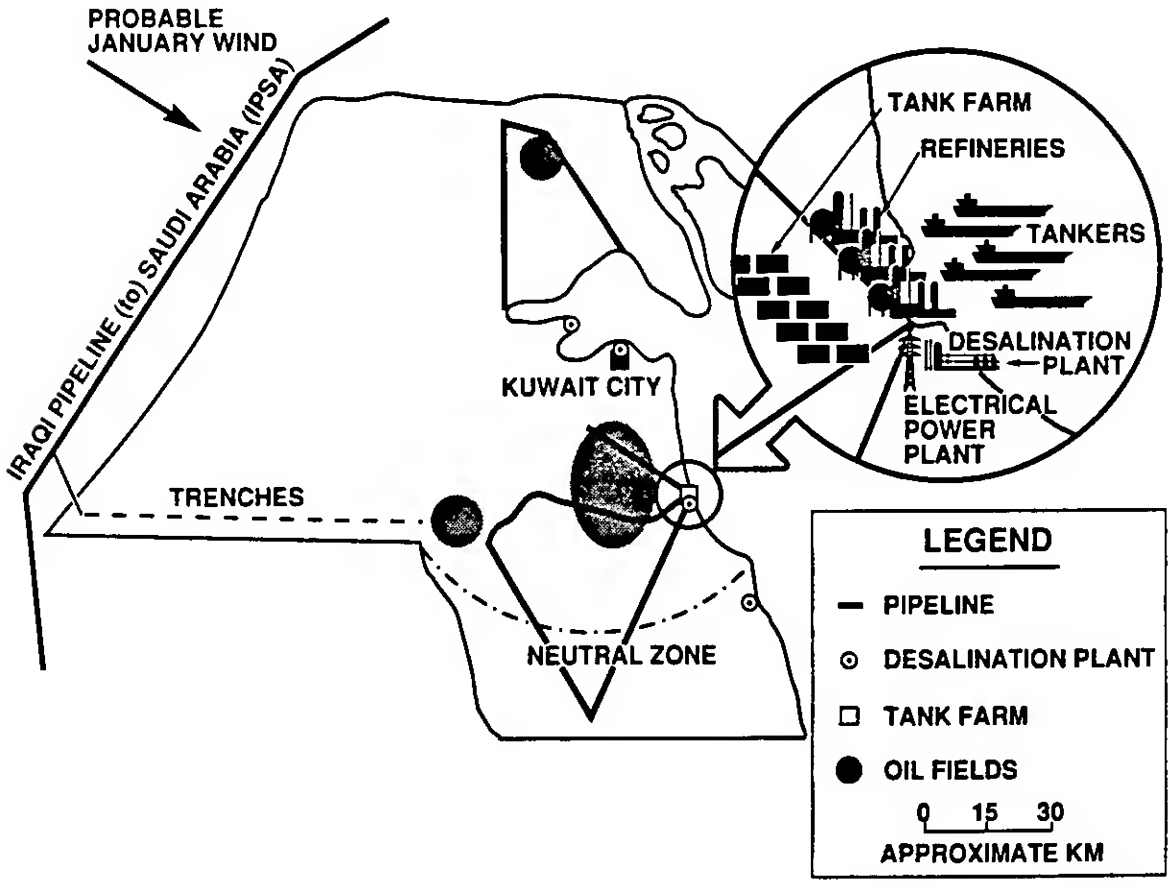

Figure I-1. Map of Kuwait Showing Sources.

For reservoir sources, the results and recommendations in this report refer to the four cases, or scenarios, shown in Figure I-2.

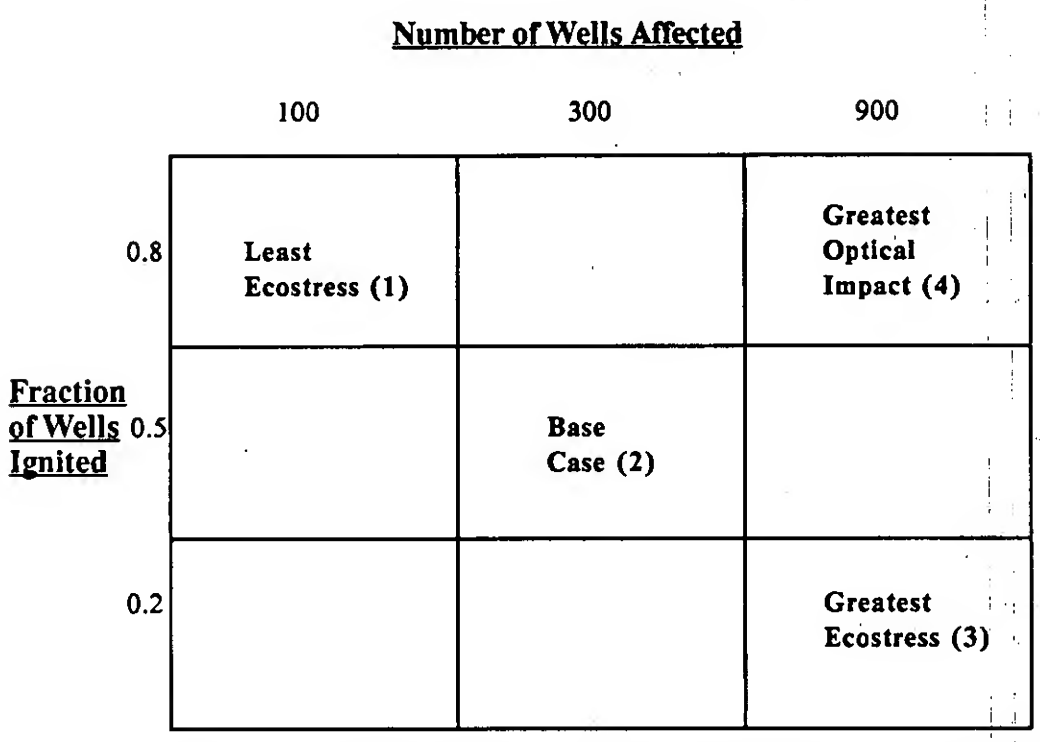

Figure I-2. Selection Matrix for the Four Scenarios Considered in the Analyses.

The four scenarios were selected from the matrix above by identifying

- The base-case scenario (#2) from among the nine combinations—demolition of 300 wellheads (250 in the Southeast Field and 50 in the West Field)[1] with 50% of these wells ignited[2] ;
- The two extremes in terms of expected ecostresses—demolition of 100 wellheads (80 in the Southeast Field and 20 in the West Field) with 80% ignited (#1, least environmental stress) and demolition of 900 wellheads with 20% ignited (#3, greatest environmental stress);
- The scenario (#4) deemed likely to produce the greatest optical impact—demolition of 900 wellheads with 80% ignited.

1 Reliable sources suggested the base-case number of wells affected.

2 Selection of the base-case scenario also used an expert's (Joe Bowden of Wild Well Control) estimate of the expected fraction of wells that might be ignited within a field.

The worst-case scenarios, the 900-well scenarios, represent the successful demolition of every wellhead in the Kuwaiti (Southwest, West, and North) fields. The greatest ecostress occurs for the lowest fraction of ignited wells because unburned oil is a greater ecological threat than the products of oil combustion.

The results presented here, for both reservoir and nonreservoir sources, are more descriptive than prescriptive. Little effort has been made to examine and prescribe means for controlling or allaying reservoir damage and ecostresses. The recommendations include a discussion of the principal uncertainties (i.e., those that are likely to have the greatest impact on the results) and identify subsequent analyses to reduce these uncertainties.

This page intentionally left blank

II. APPROACH

A multidisciplinary team performed the preliminary analyses needed for this report. Included in the team were project analysts with knowledge and experience in Petroleum Engineering (including Geomechanical and Reservoir Engineering), Combustion Engineering, Atmospheric Science, Chemical Physics, Ecology, Toxicology, Oil Well Control Technology, Intelligence Gathering, and Systems Analysis.

Figure II-1 shows the principal components of the project and their interactions. Component analyses were necessarily staggered; reading from left to right in Figure II-1 gives a sense of the sequences in this 30-day study.

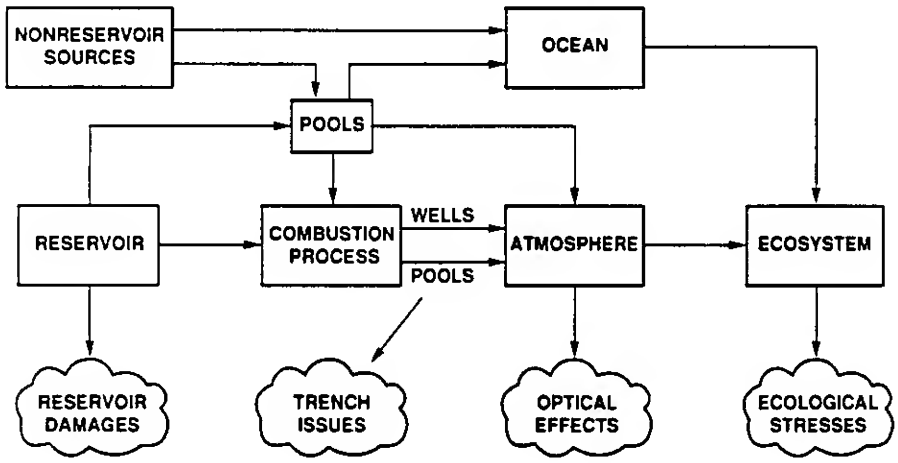

Figure II-1. Project Components and Interactions.

Reservoir sources are the reservoirs in all producing Kuwaiti fields. Nonreservoir sources include pipelines, gathering stations, tank farms, oil-filled trenches, and oil tankers. Pools are any collection of oil from reservoir and nonreservoir sources that is directly exposed to the environment and potentially threatens it.

Reservoir, nonreservoir, combustion, atmospheric, and ecosystem analyses were performed in rapid time-phased fashion so that the results from each stage could be assessed for immediate impact and then quickly passed on in the form of inputs, or source terms, to succeeding stages. Hence, reservoir analyses provided estimates of reservoir damage and source terms—estimates of uncontrolled oil flow rates, gas-to-oil ratios, and oil droplet sizes—for pool and combustion analyses. Unignited pools, including oil-filled trenches and oil mists generated by high-pressure blowout at wellheads, are a direct source to the atmosphere of organic volatiles, toxic gas, and respirable oil droplets. In this connection, the problem of filling trenches with oil

was also considered. Combustion analyses defined combustion product sources to the atmosphere. Included were pollutant production rates and injection heights for burning wellheads, oil-filled trenches, and tank farms. Atmospheric analyses provided estimates of concentrations of pollutants downwind of both burning and nonburning sources. From these results, the scope and severity of optical effects were estimated. Ecosystem analyses took account of estimated downwind atmospheric pollutant concentrations and, in conjunction with certain limited-response data, estimated the expected threat to plant and human life. Large-scale oil discharges into the Persian Gulf were considered in terms of the threat to the marine ecosystem and also the threat to freshwater supplies generated at coastal desalination facilities in Kuwait and nearby countries.

III. RESULTS

RESERVOIR ISSUES

RESERVOIR DAMAGE

If any of the well blowout scenarios occur, damage to the reservoir will be caused by the subsequent uncontrolled production in the form of lost oil (and gas) reserves, lost reservoir drive mechanism, and lost well productivity from near-wellbore formation damage. The severity of the damage will depend on the number of blowouts in a given reservoir, the duration of uncontrolled production, the properties of the reservoir, and the properties of the crude oil.

Lost Oil Reserves

Appendix A lists the estimated production from blown wells in various representative regions of Kuwait. Most of Kuwait's production comes from the Burgan oil field in the southeast. With a large number of wells, tremendous well productivity, and strategic location, the Burgan wells are an attractive and likely target for destruction. If all the wells in this field are destroyed, 6.7 million barrels of oil (and 19 billion cubic feet of gas from the gas cap) will be lost each day in this field alone. If all wells in Kuwait are destroyed, these numbers rise to 10 million barrels of oil (and 28 billion cubic feet of gas) each day. This represents roughly 0.01% of Kuwait's current estimated reserves (95 billion barrels of oil) lost each day, or 1% every 100 days. While this scenario is overly pessimistic, the permanent loss of oil and gas reserves can be significant to both the Kuwaiti economy and the environment. Table III-1 lists lost reserves for various numbers of blowout wells. Worst-case and best-case scenarios are included for each number of blowout wells to give a range of possible losses.

Table III-1. Rate of Oil (and Gas) Reserve Loss

		Number of Blowout Wells			
Damage Scenario		100	300	522	900
Worst Case*	Oil	1.98	6.10	9.20	10.00
(no damage)	Gas	5.92	18.20	26.00	28.10
Best Case	Oil	1.59	4.84	7.25	7.25
(damaged)	Gas	4.73	14.40	22.30	22.30

Oil rate in millions of barrels per day
Gas rate in billions of cubic feet per day

* "Worst Case" from the perspective of loss of gas and oil reserves is when there is no damage to the casing or reservoir to restrict maximum flow.

Figure III-1 shows losses of oil reserves under normal, controlled-production conditions[1] and under base-case (300 damaged wells), worst-case (900 undamaged wells), and best-case (100 damaged wells) conditions[2] assuming that these uncontrolled wells are gradually brought under control at a rate of 48 wells per year. This control rate is based on a reasonable estimate of the number of well-control crews that might be available and the mean time to control a well.

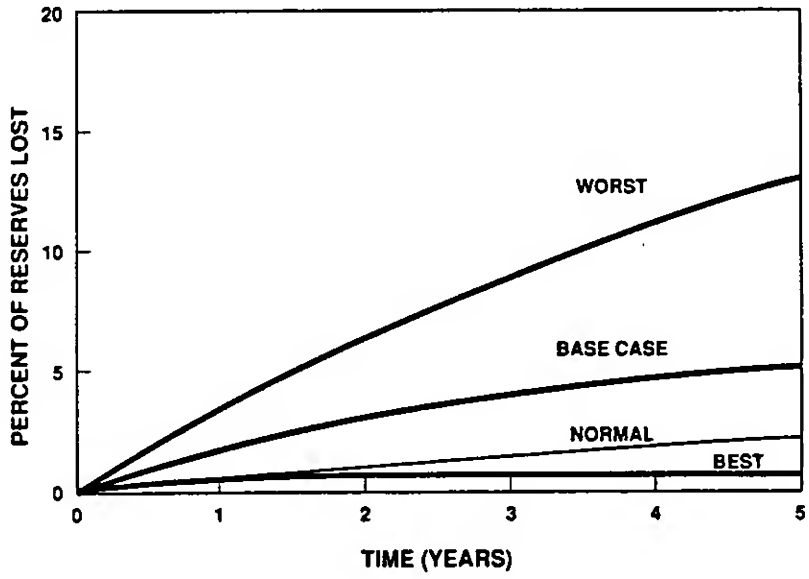

Figure III-1. Estimated Reserve Loss.

Lost Reservoir Drive Mechanism

The loss of oil and gas reserves is accompanied by the loss of reservoir energy needed to produce the oil and gas. The degree of loss depends on the reservoir drive mechanism in a given reservoir. Figure III-2 shows a qualitative comparison of the loss of reservoir drive energy for normal and uncontrolled production. As the reservoir pressure drops, the production from the wells also drops. When the pressure drops below the bubble point of the crude oil, gas comes out of solution in the reservoir. At the very high rates of production considered, the free gas will be produced, further reducing the pressure. Eventually, these wells will stop producing, as when all the air is let out of a tire. Once this occurs, efforts to raise reservoir pressure through gas or water injection are possible, but are very expensive.

---

1 Controlled production takes place at fully functioning wellheads; uncontrolled production takes place when these wellheads are blown.

2 "Worst Case" from the perspective of loss of gas and oil reserves is when there is no damage to the casing or reservoir to restrict maximum flow, and "best case" is when damage to the casing or reservoir restricts maximum (uncontrolled) flow.

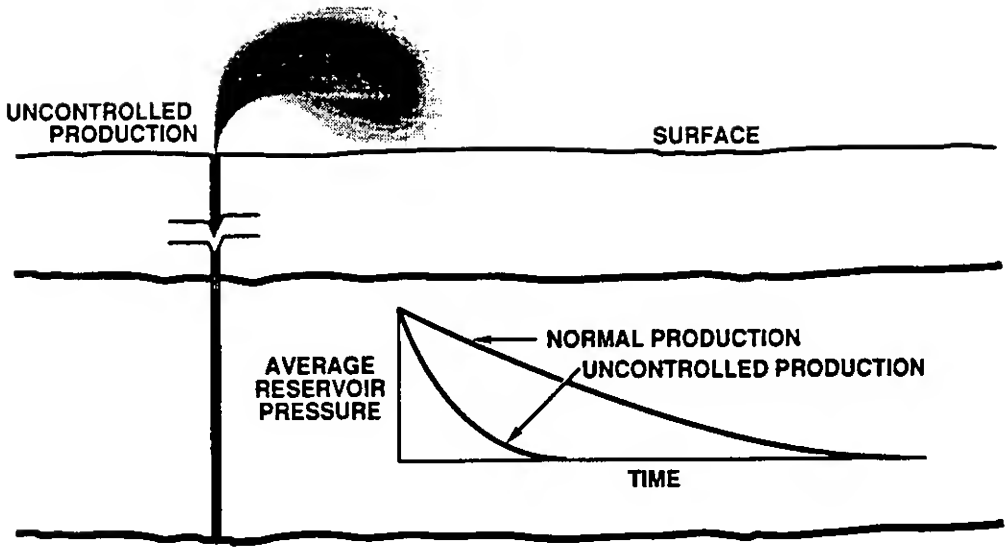

Figure III-2. Loss of Reservoir Drive Mechanism.

In the large Burgan oil field, a very strong water aquifer replaces 95% of the oil that is produced, thereby maintaining the average reservoir pressure. In about 20% of the reservoirs, however, only a small amount of water, if any, comes in from the aquifer as oil is produced, so reservoir pressure declines. These depletion-type reservoirs will be very sensitive to uncontrolled production, but quantitative estimates of depletion reservoir pressure drawdown depend on reservoir size, pressure, and productivity, and can be calculated during a follow-on to this project. Loss of these reservoirs would jeopardize 170,000 barrels of oil per day, or 10% of prewar production capacity.

Lost Well Productivity

The productivity of an oil well depends on the permeability of the near wellbore reservoir, the fluids in this region, and the condition of the tubulars in the well. The effect of uncontrolled production affects each of these areas and ultimately affects the temporal production characteristics of the well. Unfortunately, these effects are very difficult to quantify even when good data are available, so the following discussion is necessarily qualitative. Figure III-3 illustrates some of the effects of uncontrolled production.

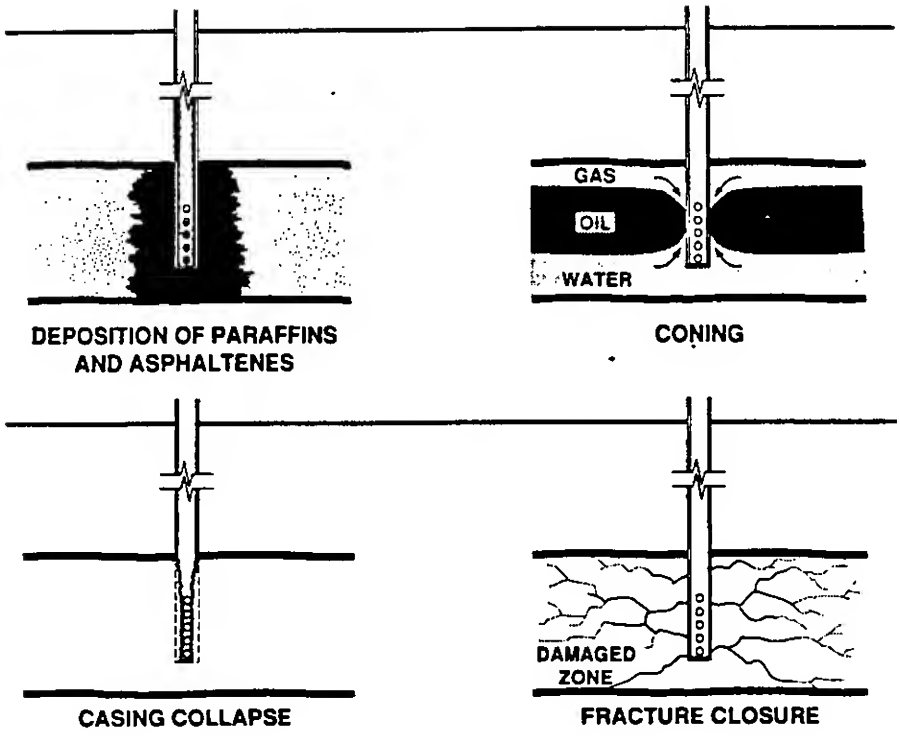

Figure III-3. Well Loss Mechanisms.

Permeability Damage. Damage to the near wellbore permeability can occur during uncontrolled flow because of asphaltene and paraffin deposition on the rock, casing, and tubing and because of rock collapse and fracture closure. The severity of both of these loss mechanisms depends on the fluid and rock properties and varies from well to well and reservoir to reservoir.

Asphaltenes and paraffins are components of the crude oil that are deposited as temperature and/or pressure drops. A temperature drop occurs if large amounts of gas flow through the perforations into the casing. Both of these drops can cause the formation, casing, and tubing to be coated with a thick layer of waxy or tarry material that can inhibit the flow of oil and gas.

With respect to the amount of reserves lost, deposition is actually beneficial, because the blowout production rate will decrease with time. However, long-term deposition may result in the loss of the well or extensive remediation to make it productive again.

The likelihood of this scenario depends on the well. Some wells have asphaltene deposition problems, and their production is likely to decrease with time. Wells without this problem experience some paraffin deposition because Kuwaiti crude oil

is a waxy crude. As likely as deposition problems are, it is impossible to quantify them or depend on them to minimize lost reserves and reservoir drive.

Another source of permeability damage is rock matrix collapse and fracture closure as the pressure drops near the wellbore. Many of the deeper reservoirs are known to have an abnormally high pressure. In these reservoirs, the pore pressure of the fluid in the rock helps to support the rock matrix. When the pore pressure drops, this support is removed and the rock matrix collapses. This provides a compaction drive mechanism that will slow the drop in reservoir pressure, but the resulting rock compaction decreases the permeability of the reservoir and is probably not reversible. Reservoirs with normal pressures will probably not experience a significant rock compaction problem.

Several of the reservoirs are known to be highly faulted and fractured and are susceptible to a damage mechanism similar to matrix compaction. As the pressure in the fracture declines, the fracture closes. Depending on the contribution of the fractures to the overall reservoir permeability, a significant and permanent drop in permeability may result.

If wells in depletion reservoirs flow uncontrolled for a long time, causing reservoir pressure to drop significantly, the rock damage mechanisms will occur. While the damage is nonreversible, it should not result in damage severe enough to make the well unusable. Also, the damage will affect the near wellbore region, not the whole reservoir, so new wells can be drilled and the predamage productivity of the reservoir can be regained.

Fluid Encroachment. When the pressure in the wellbore drops significantly, as in a blowout, the wellbore acts like a sink for all reservoir fluids. This sink leads to coning of water from the water aquifer and gas from the gas cap, when each are present. When coning occurs, fluid production into the wellbore changes from single-phase oil flow to multiphase flow of oil, water, and/or gas. This is, again, beneficial for conserving oil because producing more water means leaving more oil in the ground, but an extended shut-in period is required to recover from the coning as gravity segregates the fluids again. While the effect is reversible, it may thus take longer than desired to reverse the condition.

This is most likely to be a problem in the reservoirs with a good water drive, such as the Burgan oil field in the southeast and the Burgan reservoirs in the northern fields. Some of the depletion-type reservoirs have a mat of tar or impermeable strata separating the water and oil zones and thus should not experience a problem with water coning.

Tubular Damage. Tubular damage can occur as the result of collapse or erosion. Collapse of the tubing, or casing, can occur with the large pressure drops expected in the wells. This is not considered likely, but is possible. Erosion will occur to

some degree from particles in the fluid stream flowing in the tubing near the speed of sound. Collapse of the rock near the wellbore will result in more sand entering the tubing string through the perforations. For the two months to over a year that some wells will flow uncontrolled under these conditions, permanent loss of the tubulars in the well will likely occur.

BLOWOUT EFFLUENT CHARACTERISTICS

Our results indicate that the oil and gas effluent venting from the wellheads will contain an oil mist consisting of droplets sufficiently small that little will fall in the immediate vicinity of the well. Figure III-4 shows an oil mist generated just after the wellhead is blown on a high-pressure well on an average January afternoon (wind speed is about 10 knots). **Because of droplet evaporation,** only a small fraction will be carried more than a kilometer or two downwind of nonburning well blowouts. Since gravitational settling will not rapidly separate the oil mist from the methane, the jet of effluents will be negatively buoyant because of the droplet mass load, rather than positively buoyant like methane. Hence, the effluent cloud would behave like a heavy gas. In the absence of convective activity (under low wind conditions at night or under cloud cover), the cloud would sink towards the ground and form a dense high-concentration blanket that disperses less rapidly than neutrally buoyant or positively buoyant effluent releases.

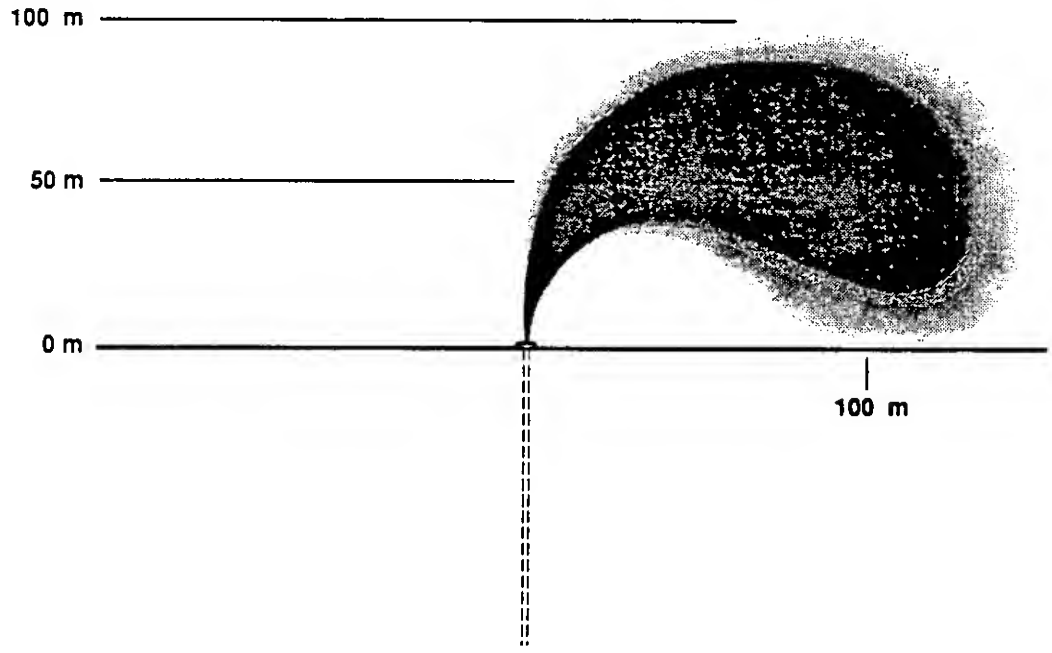

Figure III-4. Oil Mist from a High-Pressure Well.

The results also suggest that virtually all of the oil mist generated will be inhalable, and that much of it will be respirable (depositing in the lungs). Hence, the hazard is substantially greater than if the droplets were larger.

Much of the oil mist will be in the submicron size domain, which is most effective for light scattering. If the particles were ten times larger, visibility obscuration would be down a factor of ten for the same mass concentration of oil droplets. Electro-optical systems operating in the near and middle infrared regions will also be affected, but systems operating at longer wavelengths will be less affected. However, because of droplet evaporation, the optical effects of oil mist from nonburning wellheads will be localized. The infrared optical effects of the organic vapors will be much more widespread.

Should a blowout with these characteristics catch fire, virtually all the fuel can be expected to burn in the jet, much like a blowtorch. Burning droplets probably would not fall back to the surface. Combustion will likely be considerably more efficient than combustion in crude oil pools. That is, the amount of soot generated per unit mass of fuel burned will likely be lower. The optical effects of soot from oil combustion are discussed later.

COMBUSTION CALCULATIONS

A number of models for dispersion of smoke plumes in the atmosphere use stack height as one of the input parameters. If the velocity and/or stack temperature of the plume are very high, an effective stack height is used that accounts for the momentum and buoyancy of the plume. In an oil well fire from a moderate or high-pressure reservoir, enormous pipe exit velocities (as high as Mach 1) are encountered because of the volume of natural gas expelled with the oil. The high pipe exit velocity and towering flame from an ignited blowout well need to be translated into an effective stack height for use in these dispersion models.

A two-dimensional, steady-state fluid dynamics and combustion code was used to describe the combustion behavior of the natural gas and oil from typical Kuwaiti wells. The code was originally developed for treatment of pulverized coal combustion in boilers (Smith et al., 1980; Fletcher, 1983) but was modified for this project to treat oil droplets instead of coal particles. The side walls were replaced with an air inlet along the vertical sides of the computational domain, and the air flow rate was set to five times the amount required for stoichiometric combustion of the oil and natural gas (Koseki and Yumoto, 1988). Expected oil and gas flows at a representative wellhead for each of four different fields were generated by reservoir engineers at Sandia National Laboratories, along with a worst-case wellhead flow. Radial mixing of air with combustion products above the flame was also calculated, and an effective stack height was estimated for each case. The average temperature, velocity, and flow rate at the effective stack height were calculated.

These values can be used as inputs to atmospheric-dispersion models. Although the oil droplet sizes used in these calculations were much larger than those expected, (Appendix A), the results indicate that all droplets are consumed in the combustion process (i.e., no droplets fall to the ground to form pools, and CO production is insignificant). Approximately 5% of the oil mass is left as soot during droplet combustion (Urban and Dryer, 1990). Soot production from oil pool fires may be as high as 15% of the mass of the oil, but significantly less soot is observed from oil well fires (Engi, 1990). Because soot production is not modeled in the code, an estimate (<5% of the oil mass) was used.

TRENCH ISSUES

The 80 Iraqi fire trenches across southern Kuwait are roughly 3.7 m wide, 4.6 m deep, and 1 km long. The Iraqi pipeline feeding the trenches can handle 1.5 Mbpd (million barrels per day), and the total trench volume is 1,360,000 m^3. The total flow rate into the trenches is 225,000 m^3/day (1.5 Mbpd). Thus, the trenches can be filled in roughly 145 hours if nothing seeps out or evaporates. Figure III-5 shows the trench array and detail of a single trench from which oil is seeping.

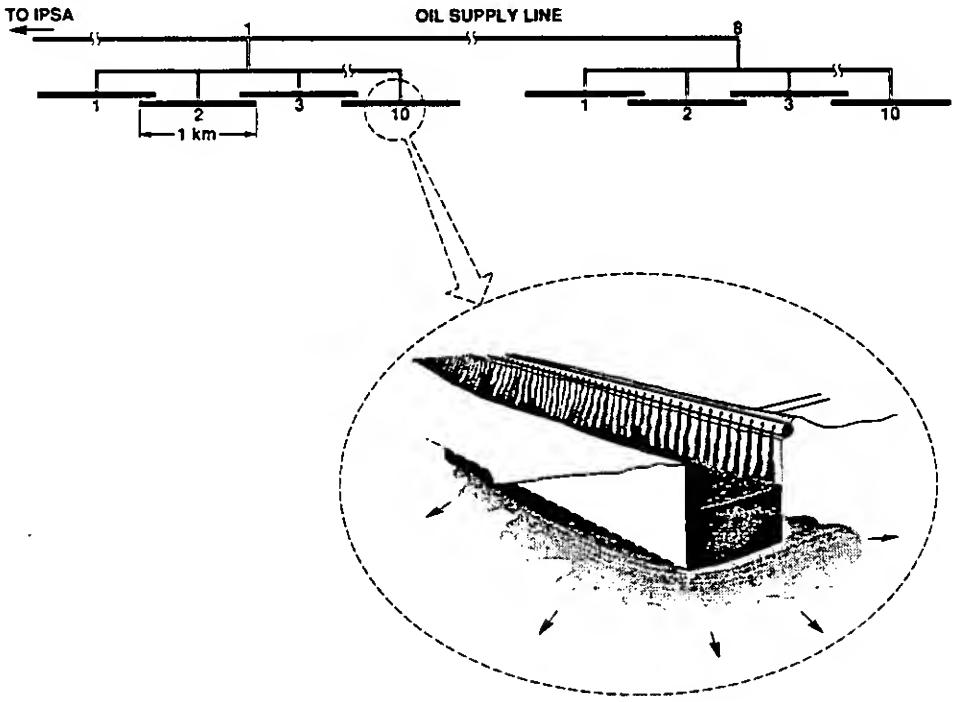

Figure III-5. Trench System.

Approximate analyses tell us that evaporation losses from the trenches will be small and that seepage losses will be 28.7 barrels per day for each meter of (unlined) trench length. The total seepage loss is 340,000 m^3/day. We are not confident in

this seepage rate because soil permeability can vary by orders of magnitude. The permeability we used comes from a Saudi Arabian sand sample taken roughly 100 miles from the trench area, and it may not be representative of trench soil. Seepage rates will be reduced when paraffins, tars, and asphalts from the oil clog the soil. With a seepage rate of 28.7 bbl/m-day, the trenches cannot be filled simultaneously because seepage rate exceeds fill rate. The trenches can probably be preconditioned with oil to allow paraffins, tars, and asphalts to build up and reduce seepage.

Several experts confirm that burning can be started by using a strong enough ignition source even though volatiles have evaporated from the oil surface. They also say that the oil will continue to burn until it is nearly or completely consumed. We believe that a burn rate of 3.5 millimeters per minute (mm/min) is appropriate for crude oil in a trench 3.7 m wide. We also believe that the burning rate will be fairly constant. A burning rate of 3.5 mm/min corresponds to 1.5×10^6 m^3/day (10 Mbpd). The length of time the trenches will burn depends on burning and seepage rates, and whether oil is replenished during burning. Burn times for different assumptions are given in Table III-2.

Table III-2. Burn Times for Various Oil Input, Loss, and Burn Rates

Refill Rate (Mbpd)	Seepage Rate (bbl/m-day)	Burn Rate (mm/min)	Burn Time (h)
1.5	28.7	3.5	20
0.0	28.7	3.5	18
1.5	0	3.5	26
0.0	0	3.5	22

Flame heights are expected to be 15 to 20 m, and flame temperatures are expected to be around 2200 °F (1500 K). The table gives the length of time until the oil in the trench is depleted, but **burning will not stop if the supply of oil continues.** Even if there is no oil in the trench, oil flowing from feeder pipes in the trench bottoms will burn. This oil will be supplied at 15% of the burning rate for trenches that are full of oil. Thus, we expect burning directly from feeder pipes to be 15% as intense as that for a full trench. Burning will continue until the oil supply is stopped. High winds can reduce the expected burning rate by limiting burning to only the downwind side of the trench, and thus increase the burn time. Figure III-6 shows the intensity of trench burn with and without a continued supply of oil after the oil in the filled trench is depleted.

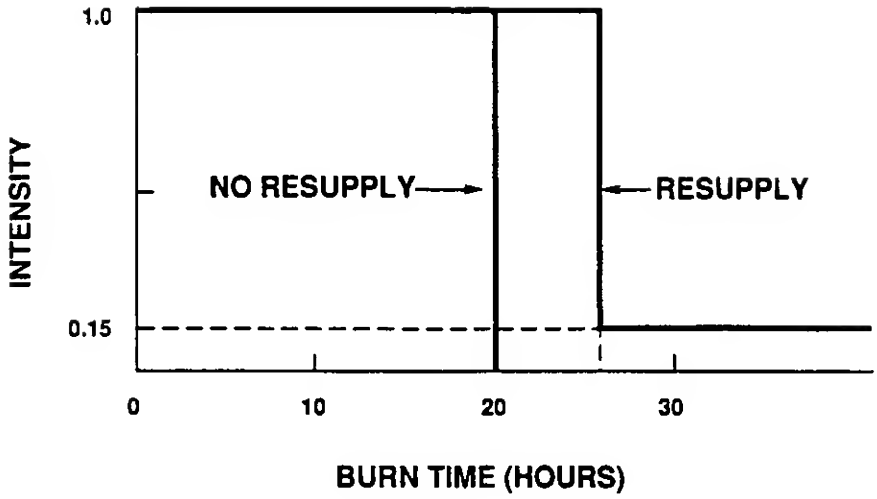

Figure III-6. Intensity of Trench Burn With and Without Continuous Resupply.

OPTICAL EFFECTS

LOCAL EFFECTS

An analysis of smoke emissions from both blown-wellhead fires and oil-pool fires shows that large amounts of particulate carbon in the form of soot would be released into the atmosphere between ground level and 2 km (Figure III-7). For the base-case burn scenario (300 severed wellheads in the Southeast and West Fields with 150 of these on fire), soot concentrations 5 to 30 km downwind of the Southeast Field would be about 0.5 to 1 milligrams per cubic meter (mg/m^3) between ground level and about 2 km above ground. Such soot concentrations would seriously degrade visibility both in the visible and infrared regions of the electromagnetic spectrum. The visual range calculations discussed in Appendix D reveal that the local visual range would be less than 500 m under such conditions. The region of maximum visibility degradation would most likely range from about 5 to 30 km downwind from the Southeast (Burgan) Field at a bearing of about 145 degrees under the most probable wind conditions. Reduced visibility conditions would extend out over the Persian Gulf to a range in excess of 100 km. However, local visibility impairment would diminish with increasing distance. Downwind of burning trenches and under expected wind conditions, soot concentrations would be more than twenty times greater, resulting in a visual range of less than 15 m. Such soot concentrations would impede military maneuvers because of general visibility impairment for aircraft pilots and tank crews, and diminished performance of electro-optical weapons systems designed to acquire enemy targets by optical or infrared means. Heavy concentrations of airborne soot would absorb most of the light incoming from a distant enemy target or outgoing from a weapon platform.

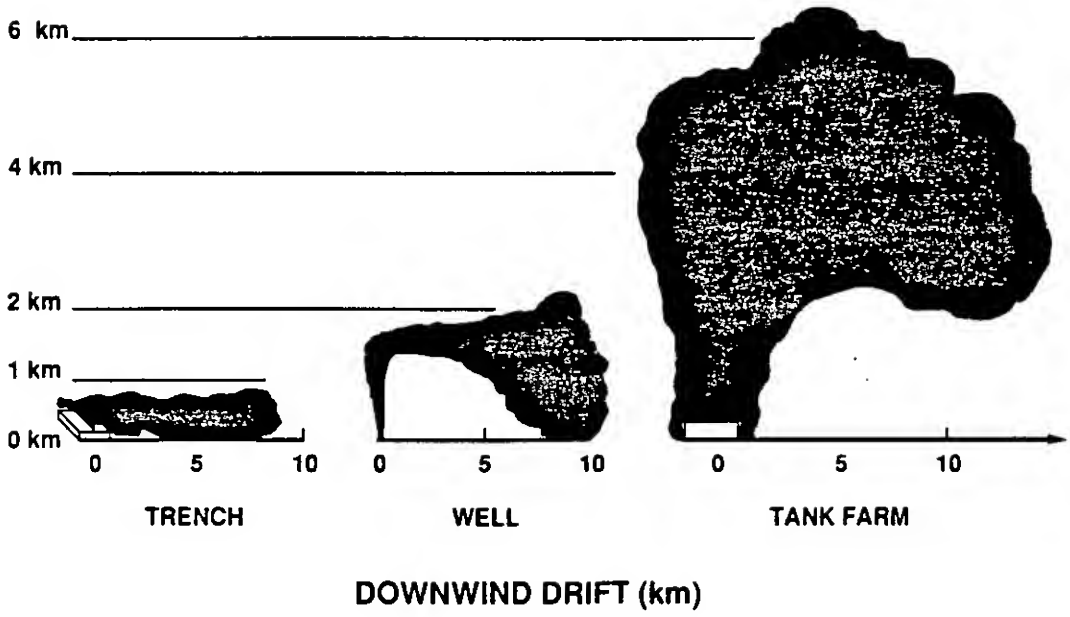

Figure III-7. Smoke Plumes Created at Various Sources (About 30 Minutes after Ignition and with a 10-knot Wind).

A second plume would arise from the vicinity of the West (Manageesh) Field and also extend along an approximate bearing of 145 degrees under typical meteorological conditions. Similar plume heights would be encountered in this region as well. However, visibility impairment would be less than that anticipated for the smoke plume from the Southeast Field.

The worst-case scenario (900 wells at the Southeast, West, and North Fields severed with 720 burning) would result in very high soot concentrations downwind from all three oil field regions. Downwind from the Southeast Field, the levels would be about a factor of two higher than for the base case. Levels would be particularly high downwind of the North Field where the worst-case assumption was that over 500 wells would be on fire. Smoke plumes downwind from the North Field would likely affect visibility in the immediate vicinity of Kuwait City.

Superimposed on the plumes from burning wellheads in the oil fields are additional smoke plumes from burning oil storage facilities along the eastern perimeter of the Southeast Field and from burning trenches along the western portion of the Kuwaiti-Saudi border. Fires in the breached oil storage facilities are likely to be in more concentrated burning pools, in contrast to the individual burning wellheads in the oil fields. These concentrated fires in the vicinity of storage tanks would have extremely high energy release rates, perhaps in excess of 100 gigawatts (10^{11} watts). As a result, the atmospheric smoke injection height would likely be as high as 7 to 10 km (Figure III-7). At this height, the plumes from the tanks would have little

effect on visual range at the lower altitudes where the plumes from the burning wells of the Southeast Field would be found. The duration of fires at the oil storage facilities would depend very much on how the facilities were breached. A cursory analysis, which assumes that all of the 15 million barrels of oil in storage are quickly released into berms surrounding the tanks to a depth of 2 to 4 m, suggests that intense fires would persist for 12 to 24 hours. The extent of burning and smoke production is of course very much dependent on how the oil is released and the degree to which it would be allowed to form pools in the vicinity of the storage tanks.

The burning trenches along the Kuwaiti-Saudi border are yet another major source of visibility-reducing smoke. Visibility downwind of the trench would be particularly poor because the heat release per unit length of the pool (which determines how fast and how far the smoke rises) is considerably less than that encountered for a burning wellhead or oil-filled berm. Plume injection heights along the trench would be highly dependent on surface wind speed; however, for speeds of around 6 knots (3 m/s), plume injection heights would not much exceed 500 m (Figure III-7). As a result, high ground-level soot concentrations would be encountered in the vicinity of the trench. Downwind dispersion estimates for a trench burn are that soot concentrations in excess of 20 mg/m^3 could be encountered at points 5 to 30 km downwind from the trenches. Such soot concentrations would create IFR (Instrument Flight Rules) conditions at lower altitudes and would (as would the soot concentrations downwind of burning oil fields and other burning oil sources) adversely impact the performance of various electro-optical weapons systems. It is possible that the plumes from the burning trenches would superimpose on the downwind plume from the West Field, further reducing visibility downwind from that region.

The most dramatic optical effect expected, however, is not visibility degradation in the horizontal, but sunlight extinction in the vertical. The optical depths of some of the plumes for the base-case scenario may be greater than 20. That corresponds to an attenuation of sunlight by a factor of 4.8×10^8. At noon, light levels under the plumes may be several orders of magnitude lower than on a moonlit night. Even if the optical depth were only half as large, the light levels would still be not much greater than those on a moonlit night. Thus, corridors of darkness tens of kilometers wide can be expected downwind of the Southeast Field in the base-case scenario and downwind of the trench system in all scenarios (see Figure III-8). In scenario #1, the effect would be considerably less severe, with light levels perhaps comparable to twilight. Because of low light levels, artificial light sources (flashlights, etc.) might be used, but even with these, extinction in the horizontal would limit the visual range.

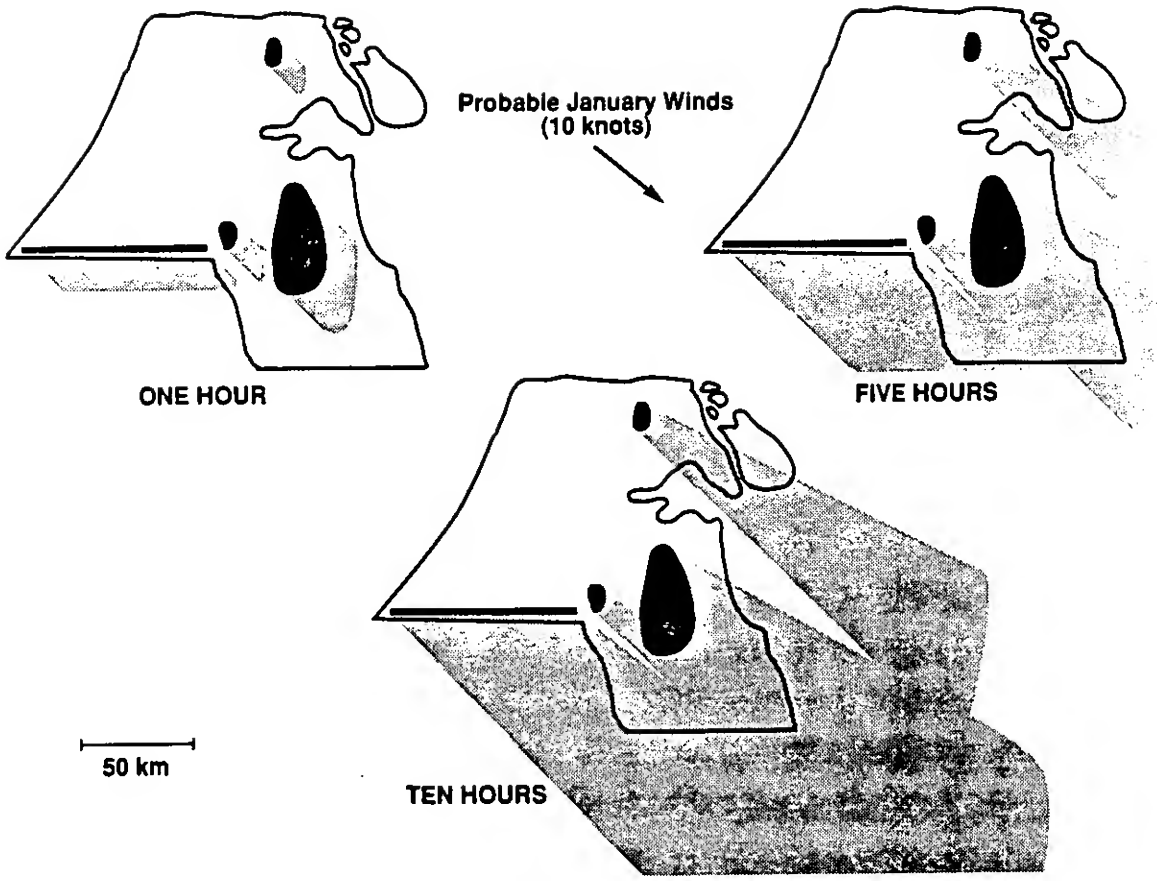

Figure III-8. Development of Low Light Level Corridors of Soot Produced in Worst-case Burning Fields and Trenches.

An additional source of visibility-reducing aerosol could arise from breached, nonburning wellheads in the various oil fields of interest. Analysis of the oil exiting the pipe reveals that oil droplet size would be predominantly under 5 μm for the higher pressure wellheads (Appendix A). As a result, these small particles would remain suspended and would be found in a low-level plume close to the ground because, in the absence of combustion and heat release, no significant plume rise would occur. The light extinction efficiency of oil mist is about three times less than that of an equal mass of soot. Large sources of oil mist, particularly in the vicinity of nonburning, venting high-pressure wells in the Southeast Field, could contribute to a local visibility problem. However, the problem would be localized in the vicinity of the breached nonburning wellheads because of droplet evaporation. The effects of the vaporized organic species on extinction in the infrared region, however, could be widespread.

It is important to note that all optical effects would be reduced by high winds, especially downwind of burning pools or trenches.

LONG-TERM CLIMATIC EFFECTS

An estimate of the total weekly smoke yield from all combined burning oil fields, trenches, and oil storage facilities for the four burn scenarios considered in this analysis is given is Table III-3. The base-case burn scenario results in a weekly release of about 0.34 Tg (10^{12} g) of smoke from the uncontrolled burning wells in the various oil fields. If the assumption is made that the wells burn uncontrolled for

Table III-3. Total Smoke Injection for Burn Scenarios

	Total Smoke Production (Tg)[1]			
Burn Scenario	All Fields (per week)	Trench	Storage	Total Release (8 weeks)[2]
1	0.09	0.21	0.31	1.3
2	0.34	0.21	0.31	3.2
3	0.11	0.21	0.31	1.4
4	0.49	0.21	0.31	4.5

[1] All calculations assume a constant release rate over an 8-week interval with no drop-off in wellhead pressure.

[2] The smoke release from trench and storage burning is added into the final column.

8 weeks, the total smoke yield is about 2.7 Tg. Adding in the smoke release from the trench and storage facility burning (0.5 Tg) results in a total smoke release of about 3.2 Tg over the 8 weeks. This calculation assumes that the oil and gas flow rate at the wellhead remains constant. The result would be less if the well pressure drops during the uncontrolled venting. A similar calculation for the worst-case scenario results in a total release of about 4.5 Tg, which includes emissions from burning trenches and oil storage facilities. Total smoke injection into the atmosphere resulting from all combustion activities on earth is estimated to be about 200 Tg/yr (Seiler and Crutzen, 1980). Thus, as long as the fires burn at the

estimated rates, they would add about 10% to the world's smoke production. The climatic effect of this smoke would be roughly doubled because crude oil smoke absorbs light very efficiently in comparison to most urban, industrial, and agricultural burning smokes.

A recent assessment of the potential for climatic change that would arise from smoke injection into the atmosphere from mass fires following a 1,000 megaton nuclear exchange between the Superpowers established a baseline smoke injection mass of 180 Tg (National Academy of Sciences, 1985). This assessment further assumed that intense urban fires would result in smoke injection heights up to and beyond the tropopause (10 to 15 km above ground), where the smoke would persist and ultimately be dispersed over the northern hemisphere. For an 8-week burn interval at constant well production rates, the worst-case smoke-release scenario examined in this analysis is below the baseline nuclear winter assessment by about a factor of forty. Most of the smoke from the Kuwaiti oil fires would be injected into the lower atmosphere where such atmospheric phenomena as cloud formation and precipitation would facilitate smoke removal. In light of these differences in total mass release and injection height, it is reasonably clear that major long-term climatic effects would not result from Kuwaiti oil fires. Prolonged burning for up to a half year at the rates in Table III-3 would still not inject enough smoke to cause major global climatic changes because atmospheric removal processes in the lower atmosphere would significantly reduce the total mass of smoke injected into the atmosphere over the release interval. Nevertheless, it is quite possible that measurable climatic effects would be created at least regionally, if not globally.

ECOSTRESSES

Oil releases from damaged Kuwaiti oil fields, tank farms, and offshore tankers can potentially disrupt both terrestrial and marine ecology. Unburned oil flowing over and pooling on the ground will have toxic effects on native desert vegetation near the oil fields. It can pollute nearby shallow freshwater aquifers important to Kuwait's limited agriculture, (which is quite limited); and the hydrogen sulfide release can have toxic effects on people and animals near oil fields. If the oil is burning, it can affect vegetation, humans, and animals because of SO_2, CO, soot, and heavy metals in the combustion products. Unburned oil released near the coast can damage salt marshes, the marine ecology, and desalination plants.

TERRESTRIAL EFFECTS

Oil discharged across the desert's surface will kill vegetation by smothering and poisoning. The destruction will be limited to areas immediately around the oil fields. Some recovery is expected over time because seeds will survive the oil and germinate when conditions become favorable. In most places, the oil will not penetrate to deep aquifers because of hard pan (gatch); however, shallow coastal wells fed by percolating rainwater could be polluted by releases from the Burgan oil

field or coastal storage tanks. The huge groundwater field at Rawdhatain (Figure III-9) has a nearby main, shallow, freshwater aquifer at a depth of 30-60 ft, which is partially recharged annually by rainfall and which could become polluted by oil flow from the northern oil field. Also, large areas of beach sand marshes southeast of the Burgan oil fields would be destroyed by an oil covering.

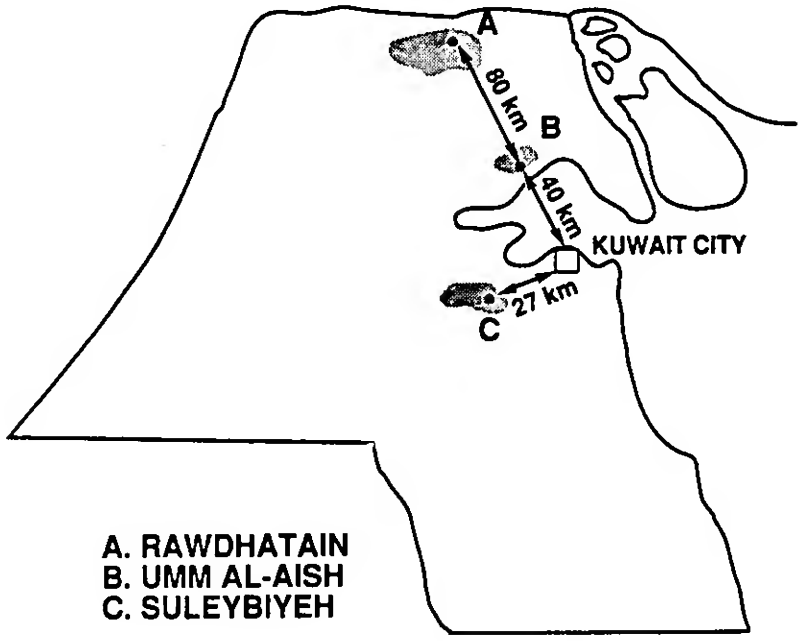

Figure III-9. Map of Kuwait Showing Principal Groundwater Fields. The Rawdhatain Field is the shallowest and most vulnerable.

For short-term exposure (hours or days), SO_2 from burning wells would probably visibly damage vegetation up to 20 km from the source. For long-term exposure (years), SO_2 from as few as 60 burning wells would probably cause some damage up to 100 km. Thresholds for destructive effects are difficult to quantify, but assuming that long-term SO_2 concentrations of 0.5 mg/m^3 and above are destructive, then as few as 100 burning wells would probably produce destructive effects up to at least 20 km. The desert vegetation tends to minimize air pollution damage, and the most sensitive vegetation would be irrigated crops and city landscaping. Little or no effect would be expected from acid rain. Kuwait does have some irrigated agriculture, east of the Burgan oil field and in the north, mostly dates and some vegetables. The agriculture is not extensive, and Kuwait imports most of its food.

Based on concentration analyses and toxicity data, the effects of airborne contaminants on mortality are expected to be small, except possibly downwind or burning trenches where concentrations may be adequate to produce nausea and eye and respiratory irritation. Carbon monoxide, carcinogens and heavy metals are not expected to have a significant effect. The largest effect is expected from SO_2. Some

increased mortality in a small, sensitive population, especially newborns and the elderly, is expected and will be most severe at 10 km from a burning field. The largest effect will occur if the wind is from the south, putting Kuwait City in the path of combustion products from the Burgan oil field. Winds from the south occur infrequently. Even with winds from the south, SO_2 concentrations are probably not large enough to affect nonsensitive people in Kuwait City seriously. Hydrogen sulfide is expected to have a negligible effect except in the immediate vicinity of the oil fields. For personnel in the vicinity of trenches or wells, respiratory protection is recommended because the fumes and toxins may cause debilitating nausea.

MARINE EFFECTS

Based on information we have received, a 20-million-barrel crude oil spill to the Persian Gulf is possible near Kuwait's coast. Ten million barrels could be released in the first 24 hours followed by another 10 million in the next 36 hours. The potential source is a combination of pipelines, tankers, and on-shore storage tanks near the Kuwaiti coast (Figure III-10). The magnitude of this potential oil spill is 77 times that of the Exxon Valdez. A comparison of the equivalent of the slick created by the Exxon Valdez spill and the slick created by the 20-million-barrel spill is shown in Figure III-11. Such an oil spill could disrupt the important fishing industry in the Gulf, shut down water desalination plants in Kuwait, Saudi Arabia, Bahrain, and Qatar that supply a large share of the area's water, and cause long term damage to the Gulf's ecology.

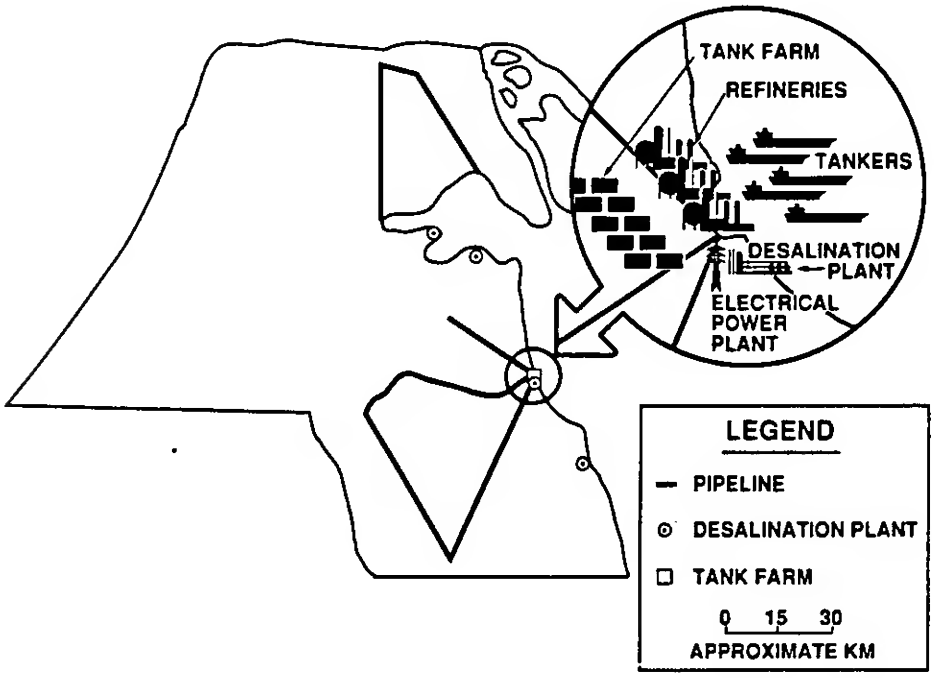

Figure III-10. Slick Source Terms.

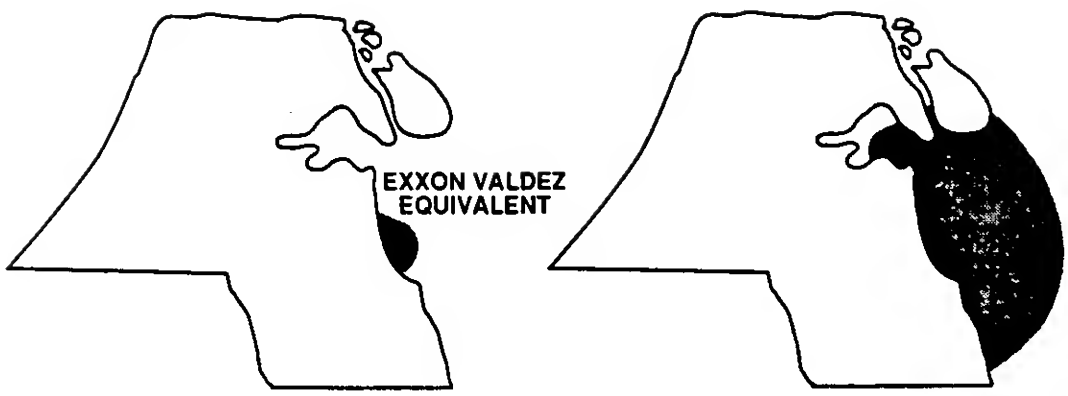

Figure III-11. Comparison of Exxon Valdez and 20-Mbbl Slicks.

The Nowruz spill, tied for the world's largest, put 4 million barrels into the Persian Gulf over several months in 1983. We have been unable in the short term of this project to obtain accounts of scientifically determined quantitative effects from this spill, but news articles reported a paralyzed shrimp industry and suspended operation of two Saudi desalination plants. Damage from this spill was probably minimized because it was in the northeastern part of the Gulf and a combination of northwesterly wind and currents carried the oil down the Iranian coast away from the Saudi coast.

We estimate that a 20-million-barrel spill off Kuwait can spread to cover an area about 90 kilometers wide and will probably travel south along the Saudi coast due to natural Gulf circulation patterns. It will probably interfere with the operation of several desalination plants along the coasts of Kuwait, Saudi Arabia, Bahrain, and Qatar. These areas are dependent on desalinated water. The locations of various desalination facilities and the expected locations of the slick at various times are shown in Figure III-12.

An oil spill in the Persian Gulf will have relatively serious effects on marine life because the Gulf is small and shallow, has slow circulation, and is very biologically productive. The Arabian Sea, which includes the Gulf, is the area with the highest marine life productivity in the world. Much of the oil will degrade by biodegradation or photochemical reactions relatively quickly (over a few days) because of warm temperatures. Oil sediments, on the other hand, will persist for a long time and will enter the food chain through species such as shrimp, which feed on the Gulf bottom. Thus, there is the potential for long-term fishing industry disruption as well as general ecological disruption.

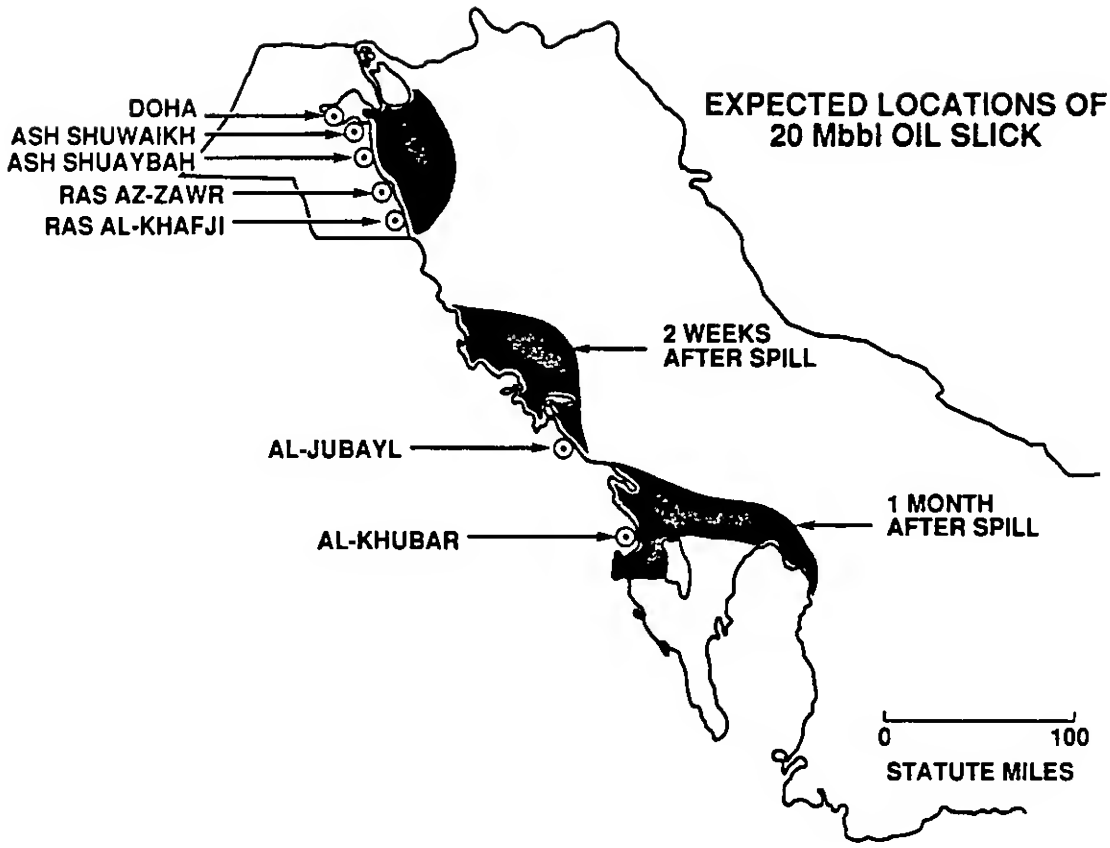

Figure III-12. Desalination Plants and Expected Migration of 20-Mbbl Oil Slick.

Consideration should be given to igniting the oil spill. Burning the oil, even at the cost of creating more atmospheric pollutants, is probably better for the marine ecology and desalination plants than not burning it because burning helps to remove the most volatile oil compounds that are the most soluble in water and hence the most toxic. Dispersants, while effective in deep water, cannot be used in the shallows of the Gulf or over reefs because they are more toxic than the oil.

This page intentionally left blank

IV. SUMMARY AND RECOMMENDATIONS

SUMMARY

RESERVOIR DAMAGE

In any of the scenarios, damage from uncontrolled venting will lead to loss of oil and gas reserves, loss of drive energy, and loss of productivity. The effects of the damage will not be severe. On average, damage will reduce uncontrolled gas and oil production by only about 20 percent. Furthermore, most of this decrease in productivity is remediable; the damage can be reversed or overcome, although some of the costs may be high. In addition, during the course of the blowout, the damage will limit the loss of reserves.

Most of the uncertainty is in regard to the temporal behavior of the production from the blown wells. Of particular interest is how rapidly and to what extent the deposition of asphaltenes and paraffins will affect the oil and gas production rates.

BLOWOUT EFFLUENT CHARACTERISTICS

For most wells, production flow rates are very high, and the type of flow that is expected will lead to the formation of an oil mist in which the droplets are mostly quite small (maximum diameter ≤ 14 μm). If not burned, this oil mist will behave like a heavy gas. Droplet evaporation will limit the major effects of the oil mist to within a kilometer or so of breached nonburning wellheads. In this regime, no pools of oil are created around the well.

Droplet size is sensitive to flow conditions; small variations in conditions lead to large variations in size distributions. Flow conditions are likely to vary greatly during the initial phase (perhaps several days) of the blowout, and pool rather than mist formation may prevail during this time.

COMBUSTION ISSUES

Combustion code calculations, using an oil droplet size much larger than the expected size, indicate that all the droplets will be consumed in the flame zone and that the production of carbon monoxide will be insignificant. At an ignited wellhead, pool burning, if it occurs, will be of little importance. These conclusions are also valid for the expected size distributions.

Because of the inherent difficulties and uncertainties in modeling the combustion process, outputs from the code should be regarded only as reasonable estimates.

TRENCH ISSUES

Without seepage, trenches can be filled in 145 hours. Seepage will increase the fill time. Depending on seepage and fill rates, the burn time ranges from 20 to 26 hours. The greatest uncertainty is in the input data for the seepage calculations. Data on the soil properties in the vicinity of the trenches are needed to generate better estimates of the seepage.

OPTICAL EFFECTS

Long-term global effects will be minor, but regional effects will be substantial as long as the fires burn. Plume heights are expected to be 1 to 2 km except for the storage tank farm east of the Burgan oil field where plume height is expected to be up to 7 km.

For not only the worst-case scenario but also for the base-case scenario, smoke plumes created by trench and wellhead fires will include soot in concentrations sufficient to degrade visibility seriously in both the visible and the infrared regions of the spectrum and to reduce sunlight to nighttime light levels over very large downwind areas. Darkness coupled with widespread obscuration would likely have a profound effect on military operations. In the base case, the worst optical effects are expected downwind from trenches.

However, use here of a relatively simple one-dimensional dispersion model to estimate downwind pollutant concentrations entails two- or three-fold uncertainties in optical depth. Replacing the line source used in these calculations with a source based on the actual pattern of wells in the fields and using a more sophisticated model that more accurately accounts for meteorology are needed refinements.

The treatment of extinction in the infrared and the potential impact on electro-optical (EO) systems has been very limited. To be more useful, the optical properties of similar crude oil soots need to be measured in the infrared, and the data applied to EO systems with specified characteristics. A similar approach is needed to evaluate effects in the infrared of the organic vapors produced in the vicinity of burning and nonburning pools and trenches.

ECOSTRESSES

Airborne pollutants created by burning wells and pools (trenches and breached storage tanks) are not expected to affect major population centers, except for possible increased mortality in a small population of sensitive individuals. Downwind of trenches, however, the concentration of pollutants is expected to be sufficient to cause incapacitation of unprotected personnel. Most affected vegetation is expected to recover within a year. Unburned oil spilled over the ground will kill vegetation and is a threat to shallow aquifers. Large quantities of oil

(20 million barrels) discharged from tankers or on-shore storage facilities into the Gulf will cause major damage to the marine ecology, to the fishing industry, and to desalination facilities in four countries.

Much uncertainty exists regarding the thresholds for plant and animal responses to the estimated levels of pollutants. Better data in these areas would help to quantify the effects of the pollutants.

RECOMMENDATIONS

RESERVOIR ISSUES

Reservoir Damage

Reservoir damage will occur, and there is little that can be done to either predict it quantitatively or control it. The only known way human intervention can minimize damage is to control the blown wells as quickly as possible. This is an obvious solution, and steps have been taken by the Kuwaitis to involve all the wild well control companies. One step to consider, however, is for these companies to train selected military personnel to increase manpower and use military equipment when needed. There are clearly complications related to liability and public involvement with a private company's operation, but the benefit of such a cooperative effort could be substantial.

Phase II of this project, if needed, will require better information about Kuwaiti crude oil and reservoir geology. Pressure-dependent volume and temperature data for the crude are essential for accurate prediction of the temporal behavior of the production from the blown wells. In addition, a study of the rate of deposition and effect on permeability of asphaltene and paraffin is needed. Any information on observed asphaltene or paraffin problems is also needed.

Blowout Effluent Characteristics

The actual flow conditions expected at the wellheads are probably quite uncertain, and these conclusions are highly sensitive to those conditions. Droplet size scales inversely as the gas velocity to the 4/3 power.

Even more uncertain than the flow conditions at "steady state" are the flow conditions as a function of time for the first several days. Bowden (1990) has pointed out that when a producing well that has been shut-in suffers a blowout, initially the production tubing and the casing below it are filled with liquid oil. Hence, the initial effluent flow velocities are much lower, and the effluent is much "wetter" (probably higher oil content; much larger oil droplet size) than it is some period of time after the blowout occurs. What has been modeled here is the steady-state behavior after the well "clears its throat." The time required to reach this

quasi-steady state is not known and is probably a complex function of the well and perhaps reservoir parameters. Bowden suggests that it may take days.

Similarly uncertain is the long-term behavior (weeks, months) of the flow conditions. In both cases, much greater insight could probably be obtained by more detailed modeling of the two-phase flow in both the well and the reservoir.

COMBUSTION CALCULATIONS

Oil well fires involve a large number of complex processes. The type of fires considered in this work are fed by turbulent two-phase flow (crude oil driven by natural gas under high pressure). Flow velocities in the well casings may approach the speed of sound in the gas, in which case some system of shock and rarefaction waves must exist as the jet expands into the atmosphere. This high-speed flow leads to fluid-dynamic processes that break up the liquid stream into droplets of various sizes. Some of these droplets then evaporate, and the resulting gaseous mixture burns. Other droplets, if sufficiently large, fall back to the ground. Air adjacent to the flame is entrained into it and provides oxygen for combustion of the fuel. The burning process involves dozens of chemical species undergoing hundreds of chemical reactions. The small carbon particles known as soot are formed because of incomplete reaction of the hydrocarbon fuel with oxygen. The soot provides an efficient source of thermal radiation that can be an important mechanism for transfer of heat away from the flame (and, for example, for heat transfer into the liquid fuel, which increases the evaporation rate). The hot combustion products are driven upward by buoyancy into a plume above the fire and then dispersed into the atmosphere.

This description of the intricacies of turbulent reacting flows is to caution the reader against the expectation of great accuracy in these combustion calculations. It typically requires a considerable amount of research to achieve good agreement between a computer model and a well-controlled laboratory experiment. Fires in oil wells provide a much more severe test of modeling capabilities; hence, results from the well-fire model in this study should be regarded only as good engineering estimates.

The combustion modeling was performed with a modified version of the PCGC-2 (Pulverized Coal Gasification and Combustion in 2 dimensions) computer code. The code, which is normally used for modeling coal combustion, was modified to treat an evaporating oil spray. Given more time, the following issues should be addressed in future work:

- Grid resolution near the wellhead,
- Droplet size,

- Boundary conditions for air entrainment,
- Multicomponent droplet evaporation,
- Formation, combustion, and thermal radiation from soot and cenospheres,
- Refinement of the solution of the gas-phase energy equation and buoyancy effects,
- Additional means of interfacing combustion calculations with atmospheric dispersion calculations.

These recommendations are discussed in greater detail in Appendix B. Some, if not all, of the questions implied in the list above might be answered by sensitivity studies using the existing models. Such studies could identify which assumptions and models most strongly affect critical results.

TRENCH ISSUES

We estimate that the fire trenches can be filled in 145 hours, depending on the seepage rate. Burn times range from 20 to 26 hours depending on fill rate and seepage rate. The largest uncertainty in these figures comes from seepage-rate calculations. The use of a triangular rather than a rectangular trench geometry introduces probably a factor of two uncertainty, at most, in the estimate of the seepage rate, but the uncertainty in the soil permeability introduces at least a factor of five uncertainty in the same estimate. We recommend obtaining and characterizing soil samples from the trench area and using more detailed seepage analyses in a follow-up project. We also recommend doing a more rigorous evaporation loss analysis to assure that we have not neglected an important loss mechanism.

Prevention of continuous trench refill by destruction of the pipelines feeding the trench system at a location likely to cause fewer problems than the trench itself should be considered at an early time.

OPTICAL EFFECTS

A variety of assumptions with associated uncertainties were made to carry out the source term and plume dispersion estimates outlined in this report. The assumptions and their associated uncertainties include oil burning rates, pollutant emission factors in burning jets and pools, dispersion model selection, meteorological conditions, and source configuration. **Of these, the source configuration and the meteorology are the most ill-defined parameters in the downwind dispersion estimates.** The actual configuration may consist of clusters of wells that have no particular directional bias but are distributed around the oil field

in almost random fashion. This would alter the corridor-of-darkness picture considerably. Instead of a large plume of uniform composition (except for the vertical gradient), the corridors would contain a patchwork of plumes providing areas of darkness and light. However, in the absence of better siting data for the various oil fields considered, a line source through the oil field normal to the prevailing wind direction was selected as a first-order estimate. Clearly more detail on well location would allow a better definition of the smoke sources. Use of models capable of handling actual wind profiles (wind shear) would also produce a greater degree of confidence.

In the interest of timeliness, a simple Gaussian diffusion model was selected that employs standard atmospheric stability classes to estimate downwind plume dispersion. Results from dispersion models such as employed in this analysis can have two- or three-fold uncertainties in the downwind estimates of pollutant concentrations, and hence in the calculation of optical depth.

Although meteorological data from Kuwait City were used in this analysis, time constraints did not permit their complete characterization. Although the prevailing wind direction is clearly from the northwest at this time of year, some probability exists that in a given period the winds could originate from any sector. This would of course send the plume in an entirely different direction and could have greater impact on population centers such as Kuwait City.

Although the estimates of oil droplet size and burning characteristics at a venting wellhead have been reasonably well addressed in the available time, a considerable uncertainty is associated with the 0.05 estimate of soot production in a burning oil jet. What is known is that the emission factor is greater than 0.005 and less than 0.15 and that one study indicates that the estimate of 0.05 may be reasonable. We have chosen to use this value, which is probably conservative (high). The soot production level could be a factor of two lower. In our analysis, we have estimated that 10 percent of the oil exiting a severed wellhead will burn as a pool, while the balance is completely consumed in the flame zone of the jet. This accounts for the likelihood that not all wells would develop optimal jets. The uncertainty associated with this estimate could easily be in the range of two or three and could change the final source term because with our current estimates the soot production from burning oil pools is three times that estimated for burning oil jets for the same mass of oil burned.

Estimates of smoke injection height and pollutant emission factors from burning pools have the least uncertainty because much of relevant experimental work has been carried out and was reviewed prior to selection of emission factors for use in this analysis.

A more realistic treatment of the pollutant dispersion and optical effects would entail

- More complete analysis of Kuwait City meteorological data (which is in our possession) so that a probability distribution of wind direction and speed can be determined. This would allow better estimates of the plume ground track and concentration as a function of time of day and season.

- Better definition of the oil fields of interest with particular interest in the positions of wellheads with respect to each other. This would enable the oil field source to be input to dispersion models as a two-dimensional array and would result in better downwind plume dispersion estimates.

- Use of a more sophisticated dispersion model to predict downwind pollutant concentrations. Such models are available and would provide such desirable features as concentration isopleths with altitude above ground. The model would also take local meteorological data as input in arriving at downwind pollutant concentrations.

- More detailed modeling of two-phase flow in the well and reservoir to better define the time-dependent behavior of the flows.

- More detailed modeling of oil mist size distributions and evaporation in the absence of burning.

- More detailed modeling of infrared optical extinction effects.

- Additional contact with well fire fighting crews, and viewing and analysis of video tapes of burning oil and gas jets to better define their characteristics.

ECOSTRESSES

Terrestrial Effects

The most serious ecological damage is expected from polluting shallow aquifers with oil released by damaged oil fields and storage tanks, and from damage to the Gulf caused by ruptured storage tanks along the coast and by oil tankers in the Gulf.

Shallow aquifers are near enough to oil fields to become polluted and unusable for agricultural irrigation. Effects from combustion products are expected to be small and limited to sensitive people roughly 10 km from the largest oil field, except perhaps downwind of the burning trenches. Our study of combustion product effects did not include lethality concentration data for desert and agricultural plants. Such lethality data were not found but may exist. We recommend seeking these

data and performing more rigorous studies to quantify lethality effects in a follow-up.

Based on our study, the potential effects of combustion products appear to be less hazardous than those of unburned oil and hydrogen sulfide. The mean size of the oil droplets that are generated during blowout is probably less than 3 μm, and thus many of these particles will not only be inhalable, but also respirable. The toxic effects of both H_2S and oil mist would be localized near nonburning breached wellheads.

At the cost of additional optical impact, we recommend igniting the oil if it is not already burning. Based on our analyses, the worst environmental damage results from unburned oil.

Marine Effects

Our studies draw us to the conclusion that a 20-million-barrel oil spill off the coast of Kuwait will be very damaging to the Gulf's ecology and fishing industry, and to desalination plants in Kuwait, Saudi Arabia, Qatar, and Bahrain. However, we have not quantified these effects. We believe that quantification may be possible. There are sources of information outside the U.S. that we were not able to tap during this brief project who have studied the Gulf since the Iran-Iraq war and may have estimates for damage caused by the Nowruz spill. A detailed treatment of oil-slick migration should be obtained from the Naval Oceanographic and Atmospheric Research Laboratory, which is doing modeling of the Gulf. Also, Applied Science Associates in Rhode Island has a model that projects the fate of an oil spill and predicts effects on marine life. Such a model may help quantify effects. We have not investigated specific effects of dissolved or suspended oil on desalination plants. Quantifying reduction in their performance should be possible. We believe that quantifying effects will be very useful, and we recommend a follow-up effort to do that.

At the cost of additional optical impact, we recommend burning as much oil as is possible to reduce damage to marine life and desalination plants. Dispersants should not be used because they are more toxic than oil.

V. REFERENCES

Abriola, L. M. 1988. "Multiphase Flow and Transport Models for Organic Chemicals: A Review and Assessment," EPRI EA-5976, Project 2377-5, Electric Power Research Institute, Palo Alto, CA.

Air Force Geophysics Laboratories. 1989. Users Modeling Workshop (LOWTRAN/MODTRAN/FASCODE-HITRAN), Kirtland AFB, Albuquerque, NM.

Amdur, M. O., A. F. Sarofim, M. Neville, R. J. Quann, J. F. McCarthy, A. E. Rogers, M. W. Conner. 1986. Coal Combustion Aerosols and SO_2; an Interdisciplinary Analysis, *Environ. Sci. Tech.* 20, pp. 139-45.

Arnold, I. M., R. M. Dufresne, B. C. Allegne, P. J. Stuart. 1985. "Health Implications of Occupational Exposure to Hydrogen Sulfide," *J. Occup. Med.* 27, pp. 373-76.

Aviation Week and Space Technology. 1983. "Oil Spill in the Gulf Hinders Fishing, Desalination," 44, May 23.

Beauchamps, R. O., Jr., J. S. Bus, J. A. Popp, C. J. Boreiko, A. Dragano, A. Kovich. 1984. "A Critical Review of the Literature on Hydrogen Sulfide," *CRC Crit. Rev. Toxicol.* 13, pp. 25-57.

Berechly, R. W., W. B. Riggan, V. Hassel. 1973. "Hasselblod Sulfur Dioxide Levels & Perturbations in Mortality; A Study of New York-New Jersey Metropolis," *Arch. Environ. Health* 27, pp. 134-37.

Bethe, H. A. 1981. "Energy Supply," in the *AIP 50th Anniversary Physics Vade Mecum,* ed. H. L. Andersen, American Institute of Physics, New York, NY.

Bohren, G. F., D. R. Huffman. 1983. *Absorption and Scattering of Light by Small Particles*, Wiley, New York, NY.

Bowden, J. 1990. Personal Communication, Wild Well Control, Houston, TX.

Briggs, G. A. 1975. "Plume Rise Predictions," in Chapter 3 *Lectures on Air Pollution and Environmental Impact Analyses*, American Meteorological Society, Boston, MA, pp. 54-111.

Burns, K. 1990. Personal Communication, Bermuda Biological Station for Research, December 13.

Casarelt, L. J., J. Doulls. 1986. *Toxicology: The Basic Science of Poisoning*. 3d ed., Macmillan Publishing Co., New York, NY.

Chapman, R. J., J. L. Mumford, D. B. Harris, Hezz, W. Z. Jiang, R. D. Yang. 1988. "The Epidemiology of Lung Cancer in Xuan, Wei, China, Current Progress, Issues & Research Strategies," *Arch. Environ. Health* 43(2), pp. 180-85.

Chen, J. Y. 1990. Personal Communication, Sandia National Laboratories, Albuquerque, NM, December.

Chevone, B. I., D. E. Herzfeld, S. V. Krupa, A. H. Chappelka. 1986. "Direct Effects of Atmospheric Sulfate Deposition on Vegetation," *J. of Air Pollution Control Assoc.* 36, pp. 813-15.

Crowe, C. T., M. P. Sharma, D. E. Stock. 1977. In *Journal of Fluids Engineering, Transactions of the ASME,* American Society of Mechanical Engineers, p. 325.

Dalzell, W. H., A. F. Sarofim. 1964. "Optical Constraints of Soot and Their Application to Heat-Flux Calculations," *J. Heat Transfer* 91, pp. 100-104.

Darley, E. F. 1971. "Vegetation Damage from Air Pollution," in Starkman, E. S. (ed), *Combusion-Generated Air Pollution*, Plenum Press, New York, NY, pp. 245-55.

Daubert, T. E., R. P. Danner. 1985. "Data Compilation Tables of Properties of Pure Components," AICHE, New York, NY.

Day, T., D. Mackay, S. Nadeau, R. Thurier. 1979. "Emissions from In Situ Burning of Crude Oil in the Arctic," *Water Air and Soil Pollution* 11, pp. 139-52.

Doviak, R. J., D. S. Zrnic. 1984. *Doppler Radar and Weather Observations*, Academic Press, New York, NY.

Dracos, T. 1978. "Theoretical Considerations and Practical Implications on the Infiltration of Hydrocarbons in Aquifers," *Proceedings IAH Intern. Symposium on Ground Water Pollution by Oil Hydrocarbons*, Prague, Czechoslovakia, pp. 127-37.

Einfeld, W., B. V. Mokler, D. J. Morrison, B. D. Zak. 1990. "Scale Effects for Smoke Emissions in Hydrocarbon Pool Fires," submitted for publication in *J. Geophysical Research.*

Eisler, R. 1975. "Acute Toxicities of Crude Oils and Oil-Dispersant Mixtures to Red Sea Fishes and Invertebrates," *Israel Journal of Zoology* 24, November.

Ellenhorn, M. J., D. G. Barceloux. 1988. *Medical Toxicology*. Elsevier, New York, NY.

Emmel, T. E., B. B. Lee. "Control Technology Assessment of Petroleum Refinery Operations." NIOSH/00130208.

Encyclopaedia Britannica, 1982.

Engi, D. 1990. Personal Communication of conversation with Joe Bowden, Wild Well Control, Houston, TX, December.

Fay, J. A. 1971. "Physical Processes in the Spread of Oil on a Water Surface," Conf. on Prevention and Control of Oil Spills, Washington, DC.

Fiveland, W. A. 1984. *ASME Journal of Heat Transfer* 106, p. 699.

Fletcher, M. 1990. Personal Communication.

Fletcher, T. H. 1980. "Theoretical Model of Reacting Coal Particles in Pulverized Coal Combustion and Gasification," M.S. Thesis, Chemical Engineering Department, Brigham Young University, Provo, Utah.

Fletcher, T. H. 1983. "A Two-Dimensional Model for Coal Gasification and Combustion," Ph.D. Dissertation, Chemical Engineering Department, Brigham Young University, Provo, Utah.

Fletcher, T. H., D. R. Hardesty. 1990. "Coal Combustion Science: Task 1, Coal Devolatilization," DOE/PETC Quarterly Progress Report for January to March, 1990, ed. D. R. Hardesty, Sandia Report No. SAND90-8223.

Gajewski, K. 1983. "Response of Some Weeds to Pollution from Copper Smelting Plants," Bioindyk. Skazen Pryem. Roln., Mater. Pokonf., Meeting 1980, pp. 201-209, ed. J. Fabiszewski. Ossolineum, Wroclaw, Poland.

Gifford, F. A. 1961. Uses of Routine Meteorological Observations for Estimating Atmospheric Dispersion, *Nuclear Safety* 2(4), pp. 47-51.

Gosman, A. D., W. M. Pun, A. K. Ruchal, D. B. Spalding, R. Wolfstein. 1969. *Heat and Mass Transfer in Recirculating Flows,* Academic Press, London, England.

Govier, G. W., K. Aziz. 1972. *The Flow of Complex Mixtures in Pipes*, Van Nostrand Reinhold Company, New York, NY.

Green, W. H., G. A. Ampt. 1911. Studies on Soil Physics: I. Flow of Air and Water Through Soils, *Journal of Agr. Sci.* 4, pp. 1-24.

Harr, M. E. 1962. *Groundwater and Seepage*, Section 9.3, McGraw-Hill Book Co., New York, NY.

Hayduk, W., B. S. Minhas. 1982. *Can. J. Chem. Eng.* 60, p. 295.

Hedman, P. O., L. D. Smoot, T. H. Fletcher, P. J. Smith, A. U. Blackham. 1983. "Prediction and Measurement of Entrained Flow Coal Gasification Processes," Interim Report Volume I prepared for U.S. DOE/METC, Contract No. DE-AC21-81MC16518, Combustion Laboratory, Brigham Young University, Provo, Utah.

Hertzberg, M. 1990. Personal Communication, Bureau of Mines, Pittsburgh Research Center, December 7.

Heyer, N., W. S. Weiss, P. Demers, L. Rosenstock. 1990. "Cohort Mortality Study of Seattle Fire Fighters; 1945-1983," *Am J. Ind. Med.* 1714, pp. 493-504.

Hill, A. D. 1985. *Production Logging*, Society of Petroleum Engineers.

Hinds, W. C. 1982. *Aerosol Technology*, Wiley, New York, NY.

Hompesch, H. 1989. "Fatalities and Danger to Health Caused by Smog," *Off Gesundheitswesen* 51(4), pp. 178-81.

Hottel, H. C. 1954. *Heat Transmission*, 3d ed., McGraw-Hill, New York, NY.

Hudson, F. L. 1991. Personal Communication, Sandia National Laboratories, January 9.

Jamaluddin, A. S., P. J. Smith. 1988. *Combustion Science and Technology* 59, p. 321.

Janzen, J. 1980. "Extinction of Light by Highly Non-Spherical Strongly Absorbing Colloidal Particles: Spectrophotometric Determination of Volume Distributions for Carbon Blacks," *Applied Optics* 19, pp. 2977-2985.

Jennings, S. G., R. G. Pinnick. 1980. "Relationships Between Visible Extinction, Absorption, and Mass Concentration of Carbonaceous Aerosols," *Atmospheric Environment* 14, p. 1123.

Jennings, S. G., R. G. Pinnick, J. B. Gillespie. 1979. "Relation Between Absorbtion Coefficient and Imaginary Index of Atmospheric Aerosol Constituents," *Applied Optics* 18, p. 1368.

Kaluarchchi, J. J., J. C. Parker. 1989. An Efficient Finite Element Method for Modeling Multiphase Flow, *Water Resources Research* 25(1), pp. 43-54.

Kataoka, I., M. Ishii, K. Mishima. 1983. "Generation and Size Distribution of Droplet in Annular Two-Phase Flow," *Transactions of the ASME* 105, p. 230.

Keltner, N. 1990. Personal Communication, Sandia National Laboratories, Albuquerque, New Mexico, December 11.

Kendall, D. N. 1966. *Applied Infrared Spectroscopy*, Reinhold, New York, NY.

Kobayashi, H., J. B. Howard, A. F. Sarofim. 1976. *Sixteenth Symposium (International) on Combustion*, Combustion Institute, Pittsburgh, PA, p. 411.

Koseki, H. 1989. "Combustion Properties of Large Pool Fires," *Fire Technology*, August.

Koseki, H., T. Yumoto. 1988. *Fire Technology* 33, February.

Lahre, T. 1977. "Compilation of Air Pollutant Emission Factors," 3d ed., Publication No. AP-42, U.S. Environmental Protection Agency, Research Triangle Park, NC, pp. 1.3-1 - 1.3-5.

Launder, B. E., D. B. Spalding. 1972. *Mathematical Models of Turbulence*, Academic Press, London, England.

Li-shi, Y., S. P. Levine, C. R. Straseg, W. F. Herget. 1989. "FTIR Spectroscopy for Monitoring Gases and Vapors of Industrial Hygiene Concern," Amer. Ind. Hyg. Assoc. J. 50, p. 354.

Liang, C. K., N. Y. Quamn, S. R. Cao, X. Z. He, F. Ma. 1988. "Natural Inhalation Exposure to Coal Smoke and Wood Smoke Induces Lung Cancer in Mice and Rats," *Bromed. Environ. Sci.* 1(1), pp. 42-50.

Markey, W. 1990. Personal Communication, Ft. Belvoir Night Vision Lab, December 6.

Marx, K. D., T. H. Fletcher. 1991. "Estimate of Droplet Lifetimes," Memo to B. D. Zak, Jan. 7.

Melville, E. K., N. C. Bray. 1979. *International Journal of Heat and Mass Transfer* 22, p. 647.

Mercer, T. T. 1973. *Aerosal Technology in Hazard Evaluation*, Academic Press, New York, NY.

Middle East and North Africa. 1989. 36th ed., Europa Publications Ltd., Australia and New Zealand.

Mulholland, G. 1990. Telephone Communication.

Nash, J. H., R. P. Traver. 1989. "Field Studies of In Situ Soil Washing," in Kosecki, P. T., E. J. Calabrese, *Petroleum Contaminated Soils. Vol. 1. Remediation Techniques, Environmental Fate, and Risk Assessment*. Lewis Publ., Chelsea, MI, pp. 157-161.

National Academy of Sciences. 1985. *The Effects on the Atmosphere of a Major Nuclear Exchange*, National Academy Press, Washington, DC.

National Research Council (NRC), Ocean Sciences Board. 1985. *Oil in the Sea*, National Academy Press, Washington, DC.

Navara, J., I. Horvath, M. Kaleta. 1978. "Contribution to the Determination of Limiting Values of Sulfur Dioxide for Vegetation in the Region of Bratislavia," *Environ. Pollut.* 16(4), pp. 263-75.

Newsweek. 1983. "Death of the Persian Gulf," July 25, p. 79.

Orkiszewski, J. 1967. "Predicting Two-Phase Pressure Drops in Vertical Pipe," *J. Petroleum Technology* 19, p. 829.

Ottesen, D. K. 1991. Personal Communication with B. D. Zak.

Pagni, P. 1990. Personal Communication, U. of California, Berkeley, CA, December 11.

Pasquill, F. 1961. "The Estimation of the Dispersion of Windborne Material," *Meteorological Magazine* 90 (1063), pp. 33-49.

Patankar, S. V. 1980. *Numerical Heat Transfer and Fluid Flow,* Hemisphere Publishing Corporation, New York, NY.

Pickett, R. L., R. M. Partridge, R. A. Arnone, J. A. Galt. 1984. "The Persian Gulf, Oil and Natural Circulation," *Sea Technology*, September.

Pilch, M., C. A. Erdman, A. B. Reynolds. 1981. *Acceleration Induced Fragmentation of Liquid Drops,* U.S. Nuclear Regulatory Commission Report NUREG/CR-2247.

Pilson, M. 1990. Personal Communication, Marine Ecosystem Research Lab, University of Rhode Island, November 28.

Plotts, W. 1991. Personal Communication, American Spill Control Company, January 10.

Pogson, J. T., J. H. Roberts, P. J. Waibler. 1970. "An Investigation of the Liquid Distribution in Annular-Mist Flow," *J. Heat Transfer* 92, p. 651.

Pueschel, R. F., J. M. Livingston, P. B. Russell, D. A. Colburn, T. P. Ackerman, D. A. Allen, B. D. Zak, W. Einfeld. 1988. "Smoke Optical Depths: Magnitude, Variability, and Wave Length Dependence," *J. Geophysical Research* 93, p. 8388.

Reed, M. 1990. Personal Communication, Applied Science Associates, RI, November 27.

Reliable Source. 1990. "Review on the Fields and Reservoirs of Kuwait."

Roessler, D. M., F. R. Faxvog. 1980. "Optical Properties of Agglomerated Acetylene Smoke Particles at 0.5156 μm and 10.6 μm Wavelengths," *J. Opt. Soc. Am.* 70, p. 230.

Schwartz, J., A. Marcus. 1990. "Mortality and Air Pollution in London; a Time Series Analysis," *Am. J. Epidemiology* 131(1), pp. 185-94.

Seiler, W., P. J. Crutzen. 1980. "Estimates of Gross and Net Fluxes of Carbon Between the Biosphere and the Atmosphere from Biomass Burning," *Climatic Change* 2, pp. 207-47.

Sheppard, D. A., A. J. Shusho, A. Nadel, H. A. Boushey. 1981. "Exercise Increases Sulfur Dioxide Induced Broncho Constriction in Asthmatic Subjects," *Am. Rev. Resp. Dis.* 123, pp. 486-91.

Smith, P. J., T. H. Fletcher, L. D. Smoot. 1980. "Model for Coal-Fired Reactors," in *Eighteenth Symposium (International) on Combustion,* Combustion Institute, Pittsburgh, PA, p. 1285.

Smith, P. J., L. D. Smoot, T. H. Fletcher. 1983. "User's Manual for a Computer Program for 2-Dimensional Coal Gasification or Combustion (PCGC-2)," Interim Report Volume II prepared for U.S. DOE/METC, Contract No. DE-AC21-81MC16518, Combustion Laboratory, Brigham Young University, Provo, Utah.

Smith, P. J., T. H. Fletcher, L. L. Baxter, L. D. Smoot. 1984. "Coal-Water Mixtures Combustion Modeling," Final Report for U.S. DOE/METC Contract No. DE-AC21-83MC20182, Combustion Laboratory, Brigham Young University, Provo, Utah.

Smith, P. J., T. H. Fletcher. 1988. *Combustion Science and Technology* 58, p. 59.

Smoot, L. D., L. D. Pratt (eds.). 1979. *Pulverized Coal Combustion and Gasification,* Plenum Press, New York, NY.

Smoot, L. D., P. O. Hedman, P. J. Smith, A. U. Blackham. 1982. *Combustion Processes in a Pulverized Coal Combustor*, Final Report for Project 364-2, Brigham Young University; EPRI, Report No. CS-2490 Volume 1, Palo Alto, California.

Smoot, L. D. 1984. *Progress in Energy and Combustion Science* 10, p. 229.

Smoot, L. D., T. H. Fletcher, K. R. Christensen. 1984. "Data Book: For Evaluation of Pulverized Coal Reaction Models," Interim Report Volume III prepared for U.S. DOE/METC, Contract No. DE-AC21-81MC16518, Combustion Laboratory, Brigham Young University, Provo, Utah.

Soo, S. L. 1987. *Fundamentals of Multiphase Fluid Dynamics*, S. L. Soo Associates, Urbana, IL.

Sowers, G. F. 1979. *Soil Mechanics and Foundations: Geotechnical Engineering,* 4th ed., MacMillan Publishing Co., New York, NY, p. 621.

Spalding, D. B. 1971. *Chemical Engineering Science* 26, p. 95.

Taylor, J. 1991. Personal Communication, 1/3/91, University of Central Florida.

Turner, D. B. 1970. *Workbook of Atmospheric Dispersion Estimates*, U.S. Public Health Service Publication No. 999-AP-26, Cincinnati, OH.

Ubhayakar, S. K., B. D. Stickler, C. W. von Rosenberg, R. E. Gannon. 1976. *Sixteenth Symposium (International) on Combustion,* Combustion Institute, Pittsburgh, PA, p. 427.

Unwin. 1989. *Middle East and North Africa, 1990*, Europa Publications, London, England.

Urban, D. L., F. L. Dyer. 1990. "Measurement of the Coke Formation Index," Presented at the 1990 EPRI Fuel Oil Utilization Workshop, Arlington, VA.

Varma, S. A. 1979. "Radiative Heat Transfer in a Pulverized-Coal Flame," in *Pulverized Coal Combustion and Gasification,* ed. L. D. Smoot and D. T. Pratt, Plenum Press, New York, NY.

Volz, F. E. 1972. "Infrared Absorption by Atmospheric Aerosol Substances," *J. Geophysical Research* 77, p. 1017.

Westerman et al. 1975. "Toxicity of Hydrogen Sulfide in Animal Feeding," *Landiovitsch Forsch.* 28, pp. 70-80.

Wichmann, H. E., W. Mueller, P. Allhoff, M. Beckmann, N. Boctes, M. Z. Asicsaky, M. Jung, B. Molik, G. Schoeneberg. 1989. "Health Effects During a Smog Episode in West Germany in 1985," *Environ. Health Perspect.* 79, pp. 89-99.

Wichmann, H. E., D. Sugeri, G. Heroldy, E. Rnulle. 1988. "Measurement of Respirator Resistance in Healthy Persons in Winter of 1985/86 and in Jan.-Feb./1987," 2 *Gesamteldy* 34(1), pp. 57-9.

World Almanac. 1990. Pharos Books, New York, NY.

APPENDIX A

BLOWOUT EFFLUENT ISSUES

This page intentionally left blank

OIL WELL BLOWOUT EFFLUENT CHARACTERISTICS

Blowout effluent is typically a mixture of natural gas (predominantly methane) and liquid crude oil. Depending upon the velocities of the flows and the gas-to-oil ratio, the two-phase flow in a vertical pipe venting to the atmosphere can be very different (Soo, 1987; Hill, 1985; Govier and Aziz, 1972; Orkiszewski, 1967). At a low gas-to-oil ratio and low flow rates, the effluent is a flowing liquid containing gas bubbles. At a higher gas-to-oil ratio and higher flow rates, a transition occurs to slug flow in which the gas bubbles mostly coalesce and span the diameter of the pipe. This type of flow produces alternating bursts of liquid and gaseous effluent, not unlike those that occur in violent volcanic eruptions. At even higher flow rates, the slugs of gas and liquid become a froth. Finally, as the flow rate increases further, an annular-mist flow pattern is established in which an unbroken core of gas flows up the center of the pipe and an annular film of liquid flows up the pipe wall. The gaseous core also contains liquid mist droplets. As the gas flow increases within the annular-mist flow regime, the proportion of the liquid carried as a mist embedded in the gaseous core also increases until the annular liquid film no longer exists.

The ecostresses, atmospheric conditions, and safety hazards created by blowouts depend critically upon the flow regime at the wellheads as venting occurs. At low flow rates and low gas-to-oil ratios, a crude oil fountain simply spills oil onto the ground surface. The oil droplets are so large that very little oil mist is generated. The natural gas separates from the oil in the fountain and rapidly rises (because pure methane is less than two thirds as dense as air at the same temperature and pressure). Should such a low pressure blowout ignite, a natural gas flame would occur above the wellhead with a crude oil pool fire around it.

At the opposite extreme of high gas-to-oil ratio and high flow rates, a mixed gas/oil mist jet deposits very little oil on the surface in the immediate vicinity of the wellhead. The impacts depend strongly upon the oil droplet size distribution emerging from the wellhead. The gravitational settling velocity of particles and droplets above 1 μm diameter varies approximately as the square of the particle or droplet diameter, and directly as the material density. (Note that in aerosol science and in this text, the term *particle* includes droplets.) The settling velocity as a function of droplet diameter over the range of interest is given in Table A-1 for unit density spheres. The *aerodynamic diameter* (AD) of a particle is defined as the physical diameter of a unit density sphere having the same gravitational settling velocity. For oil droplets, the physical and the aerodynamic diameters are within about 10% of each other.

Table A-1. Terminal Settling Velocity of Unit Density Spheres at One Atmosphere Pressure and 20 Degrees Celsius*

Particle Diameter (μm)	Settling Velocity (m/s)
$1x10^{-2}$	$7.0x10^{-8}$
$1x10^{-1}$	$8.8x10^{-7}$
1	$3.5x10^{-5}$
10	$3.1x10^{-3}$
100	$2.5x10^{-1}$
1000	$2.0x10^{1}$

*From Hinds, 1982.

This table reveals that particles significantly larger than 100 μm AD (0.1 mm) do not stay suspended for very long. Hence, droplets of this size or larger deposit on the surface near the well. In contrast, particles below 1 μm AD essentially follow the air flow, and stay suspended for days or weeks. They are removed from the atmosphere principally by precipitation rather than gravitational settling.

Particle size also strongly influences the effective toxicity of airborne particles (Mercer, 1973). Particles much larger than 10 μm AD are not normally inhalable. Particles between 10 and 2.5 μm AD are deposited in the respiratory track between the nose and the bronchial tubes. If it is not overwhelmed by high concentrations, the human body rids itself of such particles in a day or two. Particles smaller than about 2.5 μm AD, however, are deposited in the lungs. Typical residence time in the lungs is about a year. Fluids in the lung dissolve soluble materials and carry them into the bloodstream.

The effects of airborne particles on light transmission through the atmosphere are also strongly dependent on particle size. For visible light (500-nm wavelength), light scattering per unit mass for particles larger than the wavelength varies approximately inversely as the particle diameter. Hence, oil droplets around 1 μm in diameter degrade visibility ten times as effectively per unit mass as 10 μm particles (Hinds, 1982).

Application to predicted Blowout Conditions

Using typical blowout oil flow rates and gas-to-oil volumetric ratios for an *average* well in each of the oil fields of interest, Marx and Fletcher (1991) calculated (Table B-3) gas exit velocities as follows:

SE	486 m/s
MW	454 m/s
W	207 m/s
N	396 m/s

Note that the velocity for the SE field is 486 m/s, rather than the 644 m/s initially calculated by Marx and Fletcher. They commented that 644 m/s exceeds the speed of sound in methane, which is not reasonable. They remarked that the actual velocity is probably close to the speed of sound in methane, 486 m/s. The Southeast Field has so-called *choked flow.*

A number of authors (Soo, 1987; Hill, 1985; Govier and Aziz, 1972; Orkiszewski, 1967) give similar criteria for the existence of the annular-mist flow regime. The predicted blowout conditions for each of the average wells for all four fields satisfy these criteria. Hence, oil mist production will probably be important, and droplet size of the oil mist will have a strong effect on the impacts of interest. If, however, the estimated gas flow rates are in error, and annular mist flow does not in fact occur, then the following analysis of droplet size the oil mist not pertinent.

Model Predictions for Droplet Size

Kataoka et al. (1983) presented a model for the droplet size distribution generated in annular mist flow that predicts both the droplet mass median diameter (MMD) and the droplet size distribution. The model was verified using large quantities of data acquired by other researchers in air-water systems. If reasonable estimated values for crude oil surface tension and viscosity are assumed, Kataoka's model gives the following results for the cases of interest:

Field	MMD (μm)
SE	1.40
NW	1.54
W	4.39
N	1.85

If V is taken to be the volume fraction contained in droplets of diameter larger than d, then Kataoka asserts that the volume distribution vs droplet size is lognormal and is given by

$$dV/dy = -0.50 \exp(-0.781\, y^2),$$

where $$y = \ln(d/MMD).$$

Kataoka's model does not apply to droplets produced at the pipe exit from the annular liquid film traveling up the pipe wall. As noted earlier, if the gas flow rate and the gas-to-oil ratio are sufficiently high, the film does not exist. Pogson et al. (1970) gives an expression for film thickness verified by experiment, and Bowdon (1990) has called attention to the Venturi effect at the wellhead for high gas-to-oil blowouts. The high velocity flow emerging from the wellhead entrains ambient air, producing a radially converging flow field. To complete the droplet size model, the annular film (if it exists under the flow conditions of interest) is assumed to come off the pipe exit as a sheet that is thrust into the turbulent flow by the Venturi effect described above. The sheet is broken up by the turbulent flow according to the aerodynamic breakup model presented by Pilch et al. (1981). Under these assumptions, the film gives rise to droplets of MMD within a factor of two of the mist droplets predicted by Kataoka in the core flow.

As the droplets emerge from the wellhead, dilution of the jet by ambient air reduces the partial pressures of the droplet organics in the gas phase to below their respective saturation vapor pressures and the droplets begin to evaporate. If the wellhead is on fire, the evaporation occurs in the flame zone and is extremely rapid. If the wellhead is not on fire, evaporation is much slower. Calculations using the evaporation model presented by Hinds (1982) and the data on Kuwaiti crude oil composition from the National Research Council (1985) indicate that all but a few percent of the oil droplet mass will evaporate within minutes. Marx and Fletcher (1991) reach a similar conclusion using a somewhat different evaporation model. Hence, the high concentrations of oil mist will be localized within about a kilometer of the nonburning wellheads. The droplets remaining will consist mostly of nonvolatile chemical species. These droplets will contribute to visual obscuration, but are expected to be much less important to visibility than the soot generated by burning wells.

APPENDIX B

COMBUSTION ISSUES

This page intentionally left blank

1. OIL WELL CALCULATIONS

A number of models for dispersion of smoke plumes in the atmosphere use stack height as one of the input parameters. If the velocity and/or stack temperature of the plume are very high, an *effective* stack height is used that accounts for the momentum and buoyancy of the plume. In an oil well fire from a moderate- or high-pressure reservoir, enormous pipe exit velocities (as high as Mach 1) are encountered because of the volume of natural gas expelled with the oil. The high pipe exit velocity and towering flame from an ignited blowout well need to be translated into an effective stack height for use in these dispersion models.

Simple empirical jet mixing correlations are not applicable to oil well fires because of (a) the two-phase flow and (b) the combustion processes involved. A two-dimensional, steady-state fluid dynamics and combustion model was therefore used to describe the combustion of the natural gas and oil from wells typical of the Kuwaiti area of concern. The model (PCGC-2) was originally developed for treatment of pulverized coal combustion in boilers (Smith et al., 1980; Fletcher, 1983), but was modified for this project to treat oil droplets instead of coal particles. The side walls were replaced with an air inlet along the vertical sides of the computational domain, and the air flow rate was set to five times the amount required for stoichiometric combustion of the oil and natural gas. Expected oil and gas flows from four different regions were generated by reservoir engineers at Sandia National Laboratories (J. Waggoner, 6253), along with a worst-case scenario. Radial mixing of air with combustion products above the flame was also calculated, and an effective stack height was estimated for each case. The average temperature, velocity, and flow rate at the effective stack height were calculated and were available for use as input parameters in the atmospheric dispersion models.

This appendix briefly describes the combustion model (PCGC-2) used in the oil well fire calculations, along with a summary of the modifications and assumptions made to change the model from coal combustion to oil well fires. A summary of the input conditions provided by the reservoir engineers is listed for five different scenarios. Sample calculations of the oil well fire are also shown. Finally, the method of reducing the calculations to a form compatible with the atmospheric dispersion model is discussed, and results are presented.

General Description of PCGC-2

A steady-state, two-dimensional computer model called Pulverized Coal Gasification and Combustion in 2 dimensions (PCGC-2) was developed by Fletcher, Smith, and Smoot (Fletcher, 1983; Smith et al., 1980), partially through the support of the Department of Energy (Hedman et al., 1983; Smith et al., 1983; Smith et al., 1984) and the Electric Power Research Institute (Smoot et al., 1982). The code has been extensively evaluated by comparison with experimental data (e.g., Fletcher 1983; Smith et al., 1980; Smoot et al., 1982; Smoot 1984; Smoot et al., 1984),

showing many areas of agreement. The code can be used to describe pulverized coal combustors and gasifiers, and the typical geometry modeled is two-dimensional and axisymmetric. A brief description of the code is provided here.

Gaseous fluid mechanics are solved using steady-state finite difference techniques (Gosman et al., 1969; Patankar, 1980) and the k-ϵ turbulence model for closure (Launder and Spalding, 1972). Particle mechanics are solved along Lagrangian trajectories using the PSI-CELL technique (Crowe et al., 1977). Gas phase turbulence is adjusted for the presence of particles, and the effect of turbulence on particle motion is modeled semi-empirically (Fletcher, 1980; Melville and Bray, 1979). In the axisymmetric formulation, the effect of gravity on particle motion allows either a downward-fired or upward-fired reactor.

Gas phase chemistry assumes that reactions are micromixing limited, with transport equations governing the mixture fractions of inlet gas and coal "off-gas", as well as their mean square fluctuations (Spalding, 1971). The coal off-gas includes volatiles liberated during the rapid devolatilization process, as well as the subsequent gaseous products of char oxidation. Instantaneous gas properties, such as temperature and species concentrations, are calculated by chemical equilibrium from local elemental composition as a function of the mixture fractions. Time-mean gas properties are calculated by convoluting the instantaneous properties over a clipped-Gaussian probability density function (PDF) based on the turbulence statistics of the mixture fractions. The importance of treating the interactions between turbulence and chemistry is discussed by Smith and Fletcher (1988).

Changes in the material properties of each coal particle are assumed to be slow with respect to the time scale of turbulence, so coal particle reactions are based on time-mean gas properties. Coal devolatilization is commonly modeled using a simple two-step kinetic scheme (Kobayashi et al., 1976; Ubhayakar et al., 1976), with kinetic coefficients and yields dependent on the particular coal type. Char oxidation rates based on external surface area are used, with rate coefficients also based upon the coal type (Smoot and Pratt, 1979).

Gas and particle radiation are solved using either a relatively simple six-flux model (Varma, 1979) or a discrete ordinates method (Fiveland, 1984; Jamaluddin and Smith, 1988) that includes anisotropic and multiple scattering. Gas phase emissivities are calculated for emitting species (H_2O and CO_2) based on recommendations of Hottel (1954). Optical properties of coal particles are based on recommendations of Varma (1979).

Two approaches have been developed to solve the gas phase energy equation in PCGC-2 when turbulence affects chemical reactions. In the simple approach, the enthalpy is assumed to be a conserved scalar and is calculated as a function of the mixture fraction variables. Gas species concentrations, density, and temperature are calculated from a two-dimensional PDF based on the two mixture fraction variables.

In a more sophisticated approach, the time-mean enthalpy is calculated directly from the energy equation, and the gas species concentrations and density are calculated from a three-dimensional PDF based on the two mixture fractions and the enthalpy. Experience has shown that the simple approach provides meaningful solutions if the overall heat loss by convection and radiation to reactor walls is specified. In the calculations presented here, the simple approach is used (enthalpy as a function of the mixture fraction variables), with 0% heat loss. The more sophisticated approach is significantly more time consuming, and will be considered if this project is continued in a follow-on effort.

Modifications to PCGC-2 for Oil Well Fire Predictions

The version of PCGC-2 used in these calculations originally allowed for coal particles or coal-water slurries (fine coal particles in water droplets). In previous calculations of coal-oil slurries, oil was substituted for the water in the slurry droplet, with air as the entrainment gas. In the oil well fire calculations, natural gas (assumed to be methane, CH_4) is the entrainment gas for the oil droplets, and it is not possible simply to replace the water droplet with an oil droplet because of the way the mixture fractions are defined. To model oil droplet vaporization, the coal particles are thus replaced with oil droplets. The vaporization of the oil droplet is modeled using a one-step devolatilization rate:

$$dm_d/dt = - k\, m_d,$$

where the rate constant, k, is given by the familiar Arrhenius expression. The pre-exponential factor and the activation energy are taken from an empirical vapor pressure expression developed by Fletcher and Grant (Fletcher and Hardesty, 1990), assuming that a representative molecular weight for crude oil is 150 AMU. The resulting expression for the rate constant is

$$k = 8.7 \times 10^4 \exp(-11\ \text{kcal/mole/RT}).$$

The low activation energy is typical of vaporization. The devolatilization rate is first order in the mass of the droplet m_d, whereas a more standard approach to vaporization is not dependent on the mass of the droplet. However, the use of a devolatilization rate allows for a range of vaporization temperatures, which works better for crude oil than an approximation using a single vaporization temperature.

To model oil droplets with PCGC-2, it is also necessary to change the calculations of particle diameter as a function of devolatilization. Oil droplets maintain a constant density, so the diameter changes as mass is vaporized from the droplet. To save computational time, particle trajectories of the droplets are stopped whenever 99.9% of the droplet mass vaporizes. Cenosphere formation, combustion, and radiation are not treated in these calculations. Trace mineral particles (e.g.,

vanadium oxide) and soot are assumed to disperse at the same rate as the gas and are therefore not modeled with the Lagrangian particle scheme.

The high flow rate of natural gas expected from some of the wells results in superficial pipe exit velocities (calculated only from the flow of gas) greater than the speed of sound in CH_4 (486 m/s), and PCGC-2 does not treat the compressible effects of gas density at sonic or supersonic conditions. These calculations limit the pipe exit velocity to Mach 1 (in CH_4). When the mass flow rate of gas indicates supersonic exit velocities from a 3.5-inch-diameter pipe, the pipe diameter is changed in the calculations to yield a superficial exit velocity of Mach 1 with the prescribed mass flow rate.

The flow domain previously used in typical PCGC-2 coal combustion calculations is shown in Figure B-1, with the primary fuel jet surrounded by a concentric secondary stream of oxidizing gas (typically air). Wall boundary conditions are used for all variables; previous attempts at changing the wall boundaries to free flow conditions (allowing the code to calculate the air entrainment rate) have been unsuccessful. However, additional inlet streams are permitted anywhere along the wall boundary, recognizing that these are two-dimensional, axisymmetric calculations. Inlets in the side wall are actually slits around the circumference of a cylinder.

In the oil well fire calculations, the entire vertical side wall is changed to a large air flow inlet. The mass flow rate of air is specified as an input parameter, and uniform radial velocities are assumed along the vertical boundary. The stoichiometric amount of air required to burn the natural gas and oil is calculated based on the composition of the natural gas (assumed to be CH_4) and oil. In these calculations, five times the stoichiometric amount of air is used, in accordance with observations of oil pool fires by Koseki and Yumoto (1988).

Input Conditions

The heat of combustion of crude oil is estimated at 6.1 GJ/barrel (Bethe, 1981). Heats of formation and vaporization for several long-chain hydrocarbons (decane, dodecane, hexadecane) on a mass basis (kcal/g) exhibit asymptotic behavior as a function of molecular weight (Table B-1). The estimated properties of crude oil from the area of concern are given in Table B-2. The expected droplet size distribution from an oil well is not known; the mass mean droplet size of 175 μm used here is between that expected for fine nozzles (20-μm droplets) and raindrops (1 to 10 mm in diameter). Note that much smaller droplets are predicted in Appendix A.

The maximum number of finite difference grids in the current version of PCGC-2 is 40 x 40. Grids are spaced unevenly: small grid spacing is used near the pipe exit and large grid spacing is used near the vertical inlet boundary and the top boundary.

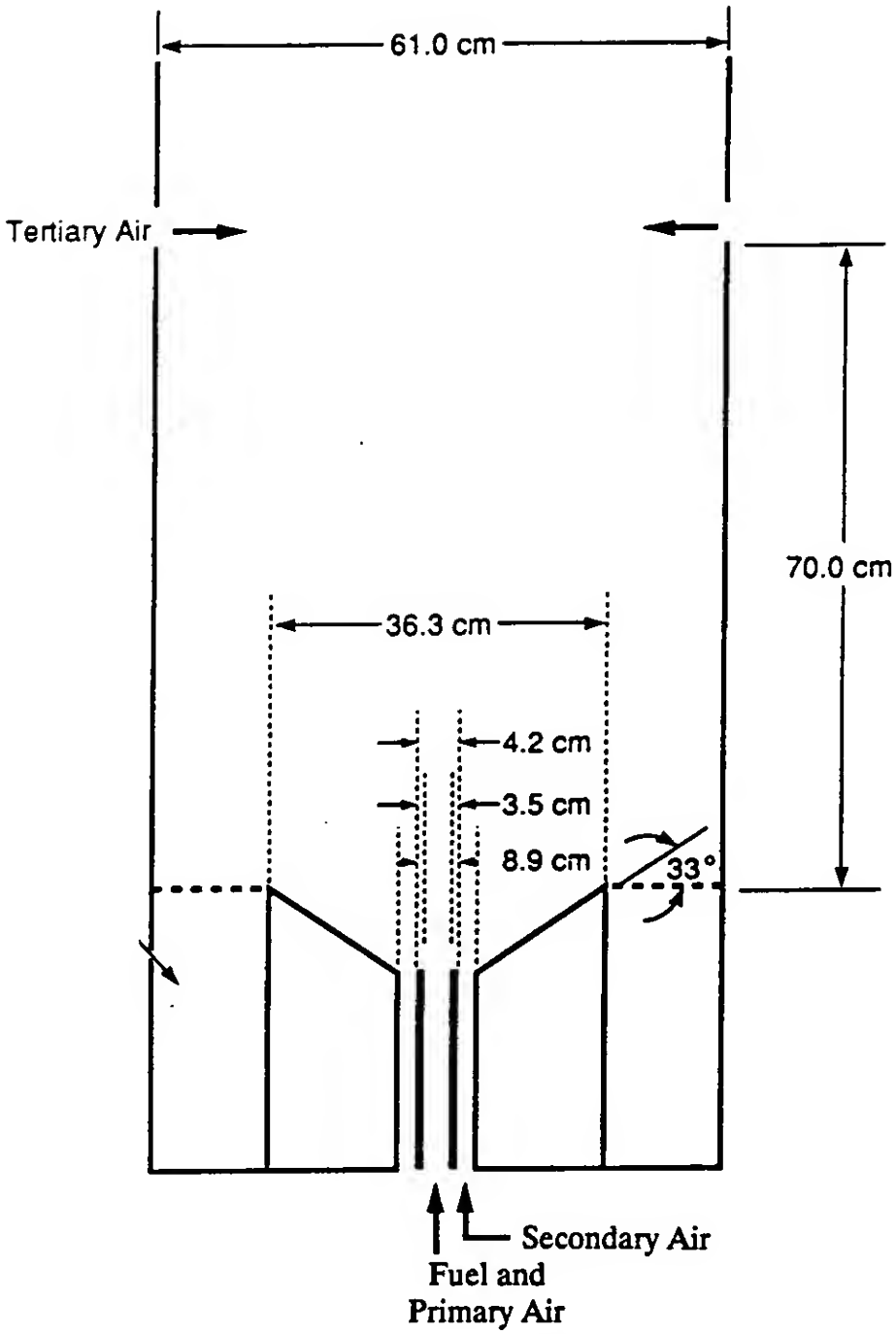

Figure B-1. Schematic of the Burner Used in a Typical PCGC-2 Combustion Calculation.

Table B-1. Heats of Formation and Combustion of Hydrocarbon Compounds

Compound	Molecular Weight	ΔH_f^o (kcal/mole)	ΔH_{vap} (kcal/mole)	Boiling Point (K)	ΔH_f^o (kcal/g)	ΔH_{vap} (kcal/g)
methane	16	-16	1.96	112	-1.00	0.122
propane	44	-19.5	4.49	231	-0.44	0.102
n-heptane	100	-34.6	7.58	372	-0.35	0.076
n-hexane	114	-38.2	9.22	399	-0.34	0.081
dodecane	170	-52.8	11.9	489	-0.31	0.070
n-tridecane	184	-56.4	13.0	508	-0.31	0.070
n-tetradecane	198	-61.1	13.8	527	-0.31	0.069
n-hexadecane	226	-67.4	15.4	560	-0.30	0.068
acetylene	26	54.3	4.2	192	2.09	0.16
ethylene	28	14.5	3.2	170	0.52	0.12
benzene	78	24.0	7.4	353	0.31	0.09
diesel #2	170	-52.8	*	*	-0.31	*

*Not applicable

Table B-2. Properties of Oil Used in PCGC-2 Calculations

Estimated Droplet Sizes

Initial Size (μm)	Distribution (wt. %)
30	18
75	25
150	30
300	15
500	12

ΔH_{vap} = 70 cal/g
ΔH_f = -300 cal/g

Vaporization Rate = $8.7 \times 10^4 \exp(-11 \text{ kcal/mole}/RT)$
(from the Fletcher-Grant vapor pressure correlation with molecular weight = 150)

Composition

Element	Wt. %
C	84.0
H	12.0
O	1.0
N	0.5
S	2.5

A large domain (50-m radius, 500-m vertical height) is used to provide residence time for the ambient air to cool the hot combustion gases to typical stack exit temperatures (200 to 300 °F, or 360 to 420 K). One radial grid point describes the pipe exit, which determines the grid spacing factor ($\Delta r_1 = d_{pipe}/2$, 40 grid points, $r_{boundary}$ = 50 m). A grid spacing factor of 1.2 ($\Delta r_2/\Delta r_1 = 1.2$) is used in the vertical direction.

The temperature of the CH_4 at the pipe exit is set at 350 K, while the temperature of the ambient air is set at 293 K. The ambient air calculation may be too low for desert conditions, but this temperature is not expected to affect calculations significantly. The droplet velocity at the pipe exit is set to 50% of the gas velocity at the pipe exit, but this would not be accurate for the small droplets predicted in Appendix A. A 2-degree cone angle for the initial droplet dispersion is used in these calculations. Many of these variables are unknown, and parametric calculations should be performed in the future to determine which variables most affect the results.

Sample Calculations

Sample calculations are shown for combustion at a wellhead in the Southeast Field in Figure B-2; the plots show the plume height and air entrainment, rather than the flame height. This figure illustrates the spatial scaling problems in these calculations: fine time and spatial scales are required near the wellhead, while large scales are necessary to model the air entrainment and plume rise. The pipe exit is located at the centerline (r = 0) at a vertical distance of 0. The flame is located where the temperature is high and at the interface between the regions of high O_2 and CO concentrations. The flame is just under 50 m high, and more than 300 m are required to cool the plume to 400 K. The methane is consumed first, followed by the oil. The high axial velocity at the pipe exit decreases rapidly from near sonic conditions to a few meters per second within the first 5 m along the centerline. No droplets recirculate and hit the ground in these calculations because of the droplet sizes used and the high gas velocities at the pipe exit. The streamlines show the predominant flow direction as air flows toward the centerline and is carried upward with the flame.

Results

The PCGC-2 results (Figure B-2) were condensed into a few simple parameters to be used as input parameters for the atmospheric dispersion code. The data needed for the atmospheric calculations are the effective stack height, the mass flow rate of gas, the heat release rate, and the velocity at the effective stack height (the height at which the centerline gas temperature reaches 400 K). Gas velocity and temperature profiles at the effective stack height are not uniform across the cross section defined

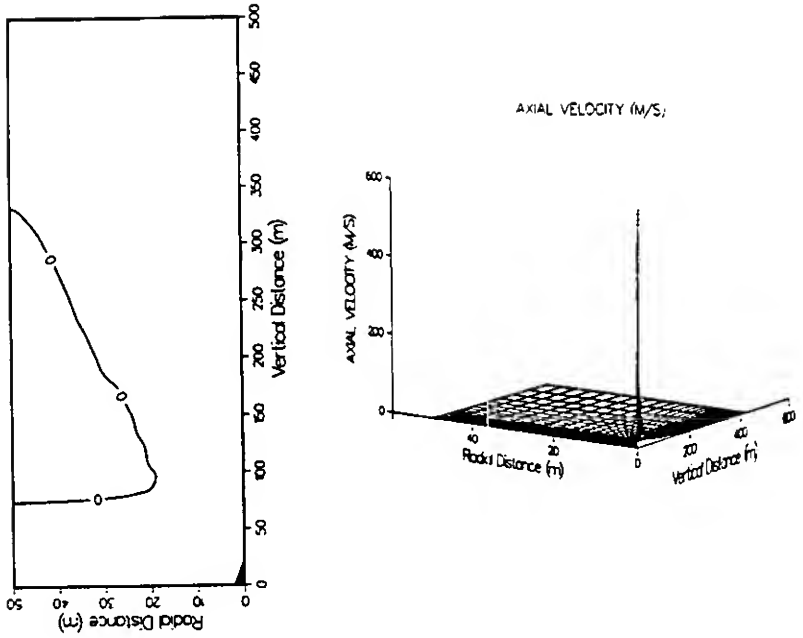

Figure B-2a. Axial Velocity Contours Predicted by PCGC-2 for an Oil Well Fire in the Southeast Field (m/s).

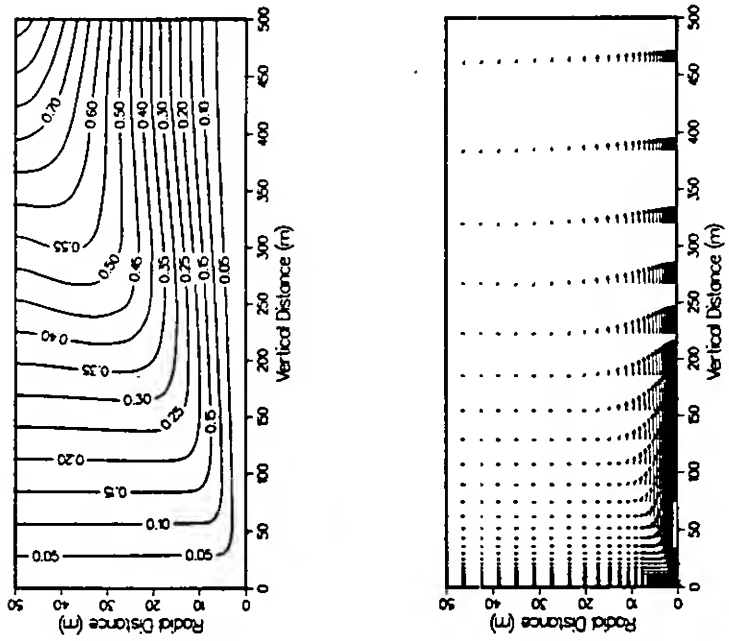

Figure B-2b. Gas Streamlines and Velocity Vectors Predicted by PCGC-2 for an Oil Well Fire in the Southeast Field. For clarity, high velocities near the pipe exit are not plotted. Units on streamlines are values for the stream function normalized by the total input mass flow rate.

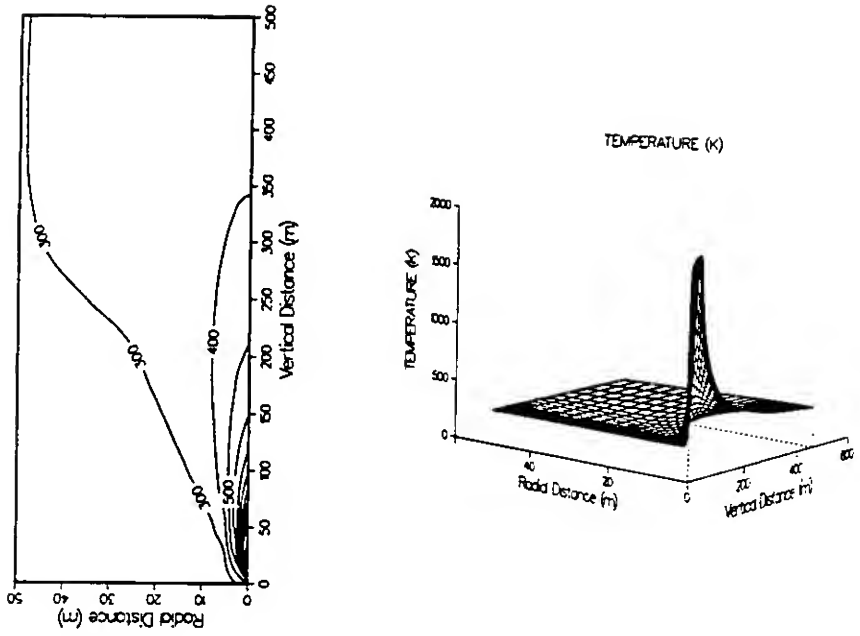

Figure B-2c. Gas Phase Temperature Contours Predicted by PCGC-2 for an Oil Well Fire in the Southeast Field (K).

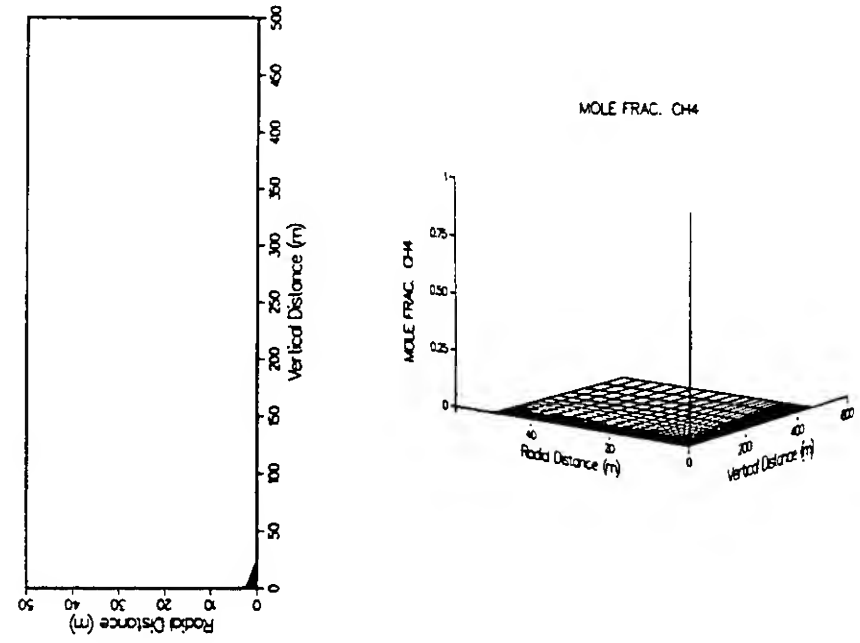

Figure B-2d. Mole Fractions of CH_4 Predicted by PCGC-2 for an Oil Well Fire in the Southeast Field.

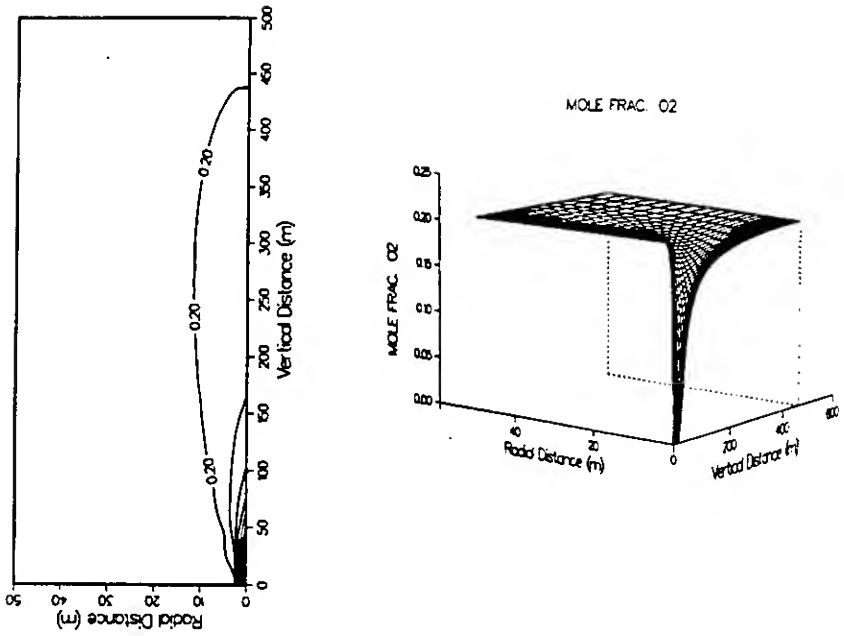

Figure B-2e. Mole Fractions of O_2 Predicted by PCGC-2 for an Oil Well Fire in the Southeast Field.

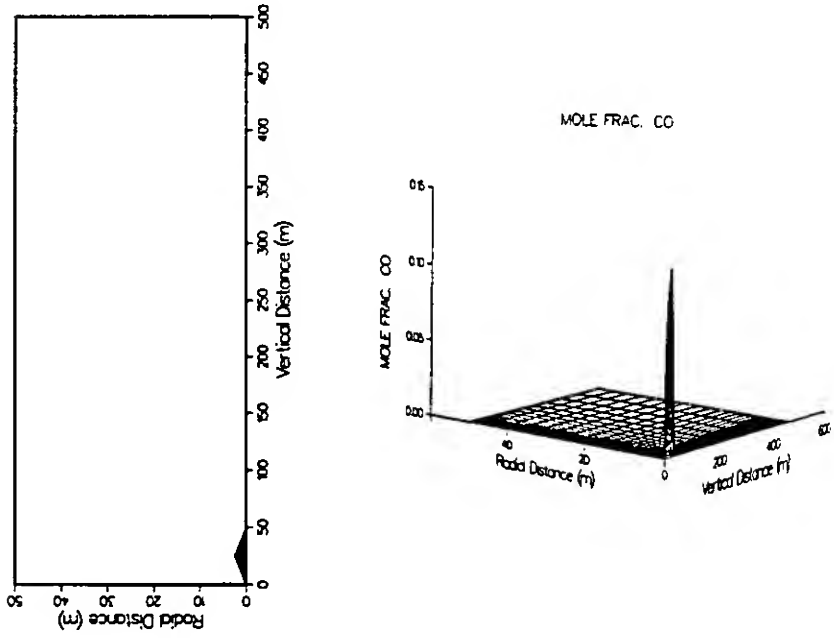

Figure B-2f. Mole Fractions of CO Predicted by PCGC-2 for an Oil Well Fire in the Southeast Field.

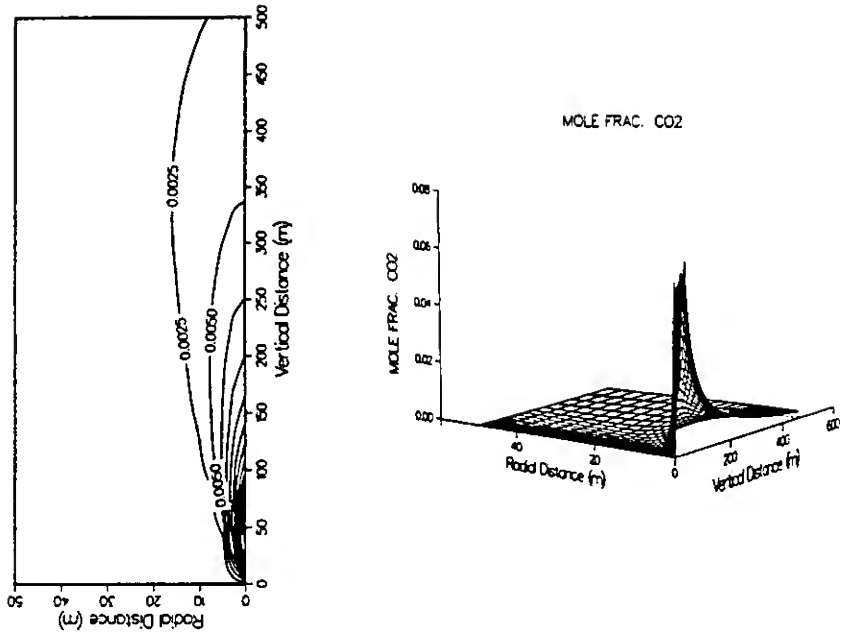

Figure B-2g. Mole Fractions of CO_2 Predicted by PCGC-2 for an Oil Well Fire in the Southeast Field.

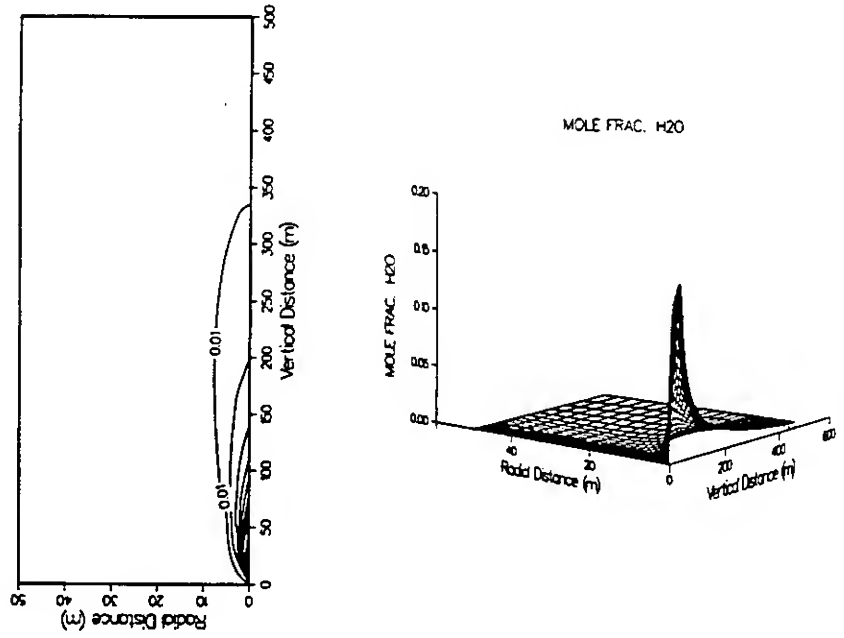

Figure B-2h. Mole Fractions of H_2O Predicted by PCGC-2 for an Oil Well Fire in the Southeast Field.

by the effective stack radius. Consequently, some integrations were performed to obtain average values for the mass flow rate and gas temperature. The effective stack radius was defined as the radial distance at which the axial velocity was 10% of the centerline gas velocity.

The effective gas density was calculated at the average gas temperature using the ideal gas law. The average stack velocity was then calculated from the mass flow rate, the effective stack radius, and the effective stack density. The volumetric flow rate at the effective stack height was obtained by dividing the effective mass flow rate by the effective density.

The results of the PCGC-2 calculations for the five cases in Table B-3 are summarized in Table B-4. As expected, the highest mass flow rates at the effective stack height are for the highest oil flow rate. The effective stack heights range from 275 m for the Midwest, West, and North cases to 340 m for the Worst Case. The stack height for the Worst Case is highest because the mass flow rates of oil and gas in this case are higher than in the other cases. In addition, the computational grid used for the Worst Case was 600 m high instead of 500 m high, which decreased the flux (mass flow per unit area) of air at the boundary (r = 50 m). Because less air and combustion products mix at the lower heights, the effective stack height is raised. The effective stack radius for the Worst Case is also much larger than in the other cases, which explains why the effective stack temperature and the effective stack velocity are lower for the Worst Case. In the future, it may be necessary to specify a given height for all cases and then compare effective stack temperatures and velocities.

Recommendations

If it is decided to refine and/or extend the combustion calculations, the following specific recommendations are proposed:

1. Computations should be performed in which the region near the wellhead is better resolved (i.e., the finite-difference grid should be refined there). Modeling of shock and rarefaction waves is not suggested, although additional thought should be given to the influence of the assumptions regarding the exit of the flow from the wellhead. The principal question requiring resolution concerns the accuracy of the calculation in the region where the oil is evaporating and the gas mixture is starting to burn.

2. The process by which the oil breaks up into droplets should be studied in more detail. This will require knowledge of the flow conditions as a function of time after blowout. Droplets falling from oil well blowout plumes generally range in size from pinhead to quarters. Sufficiently small droplets would not fall near the wellbore. The distribution of droplet sizes has a crucial influence on the amount of oil that is burned versus that which falls to the ground (and then perhaps burns in a pool fire).

Table B-3. Estimated Input Flow Rates for Different Oil Wells

Input Parameters	Southeast	Midwest	West	North	Worst Case
Mass Flow Rate of Oil (kg/s)	42.3	18.4	12.9	23.0	55.2
Mass Flow Rate of Gas (kg/s)	2.66	1.88	0.86	1.64	3.27
% Gas (by volume)	99.0	99.4	99.0	99.1	98.9
Theoretical Pipe Exit Velocity (m/s)*	644	454	207	396	792
Heat Release from Oil (GW)	1.62	0.71	0.49	0.88	2.12
Heat Release from Gas (GW)	0.15	0.10	0.05	0.09	0.18
Stoichiometric Combustion Air Req'd (kg/s)†	635	289	194	348	825

* Speed of sound in CH_4 = 486 m/s; the velocity in this table assumes a pipe diameter of 3.5 inches with the given gas flow rate.
† PCGC-2 calculations used five times this value.

Table B-3. Summary of PCGC-2 Calculations

Results	Southeast	Midwest	West	North	Worst Case
Effective Stack Height (m)	300	275	275	275	340†
Mass Flow Rate (kg/s)	1202	859	431	714	1835
Effective Stack Radius (m)	23.4	23.6	23.6	20.3	39.4†
Average Stack Temperature (K)	354	359	353	357	321†
Average Stack Velocity (m/s)	0.57	0.48	0.24	0.43	0.29†
Volumetric Flow Rate (m^3/s)	1203	872	431	721	1668

† The centerline temperature in this case is high for longer distances. This causes a higher effective stack height, greater radial dispersion, and consequently lower average stack temperatures and velocities. The mass flow rate, however, is higher for this case.

3. The computational domain should be extended radially to ensure that the boundary conditions at the outer radius of the domain do not influence the results significantly. Furthermore, the following assumptions should be tested to determine whether (a) the flame entrains an amount of air equal to five times the stoichiometric requirement and (b) the source of this combustion air can be modeled with a uniform influx of air from the outer radius.

4. The models that describe the evaporation of the oil and the burning of the resulting gaseous mixture should be investigated. As noted above, the chemical processes in the burning of hydrocarbon fuels are very complex, and the turbulence of the flow field further complicates the combustion process. The PCGC-2 code has proven useful in the past for modeling the burning of coal particles, but it is relatively untested in the area of spray fuel combustion.

5. The processes by which soot is formed should be studied, and appropriate models should be incorporated into the computer code. The effects of soot on the radiative properties of the flame should also be more carefully investigated.

6. Two approaches have been developed to solve the gas-phase energy equation in PCGC-2 when turbulence affects chemical reactions. In the simple approach, the enthalpy is assumed to be a conserved scalar and is calculated as a function of the mixture fraction variables. Gas species concentrations, density, and temperature are calculated from a two-dimensional PDF based on the two mixture fraction variables. In a more sophisticated approach, the time-mean enthalpy is calculated directly from the energy equation, and the gas species concentrations and density are calculated from a three-dimensional PDF based on the two mixture fractions and the enthalpy. The simple approach has provided meaningful solutions if the overall heat loss by convection and radiation to reactor walls is specified. In the calculations performed under Phase I, the simple approach was used (enthalpy as a function of the mixture fraction variables), with 0% heat loss. The more sophisticated approach is significantly more time consuming, yet more accurate, and should be considered if this project is continued under Phase II.

7. Buoyancy is not treated in the gas phase in PCGS-2 calculations. This is a seemingly minor correction (adding ρg terms to the equations), but corrections must be made to the turbulence expression and may be needed to adjust the postflame mixing rate between combustion gases and ambient air (Chen, 1990).

Some questions implied above might be answered by parametric studies using existing models to identify which assumptions and/or models strongly influence critical code results and would require research in greater depth.

APPENDIX C

TRENCH ISSUES

This page intentionally left blank

1. TRENCH DESCRIPTION AND OIL FLOW RATE

The 80 Iraqi fire trenches across southern Kuwait were described as roughly 3.7 m wide, 4.6 m deep, and 1 km long. The Iraqi pipeline feeding the trenches can handle 1.5 Mbpd (million barrels per day). The total trench volume is 1,360,000 m^3. The total flow rate into the trenches is (1.5 Mbpd) 225,000 m^3/d. Thus, the trenches can be filled in roughly 145 hours if nothing seeps out or evaporates.

2. SEEPAGE AND EVAPORATION LOSSES

Approximate analyses were performed to estimate the importance of seepage and evaporation losses. The evaporation analysis assumed that there is no convection of oil in the trench, and it considered only methane, the most volatile constituent of oil, and pentanes. The losses of methane and pentanes from diffusion through the oil and evaporation at the surface are negligible over a few days. Convection speeds up the loss of volatiles but, in our judgement, not enough to make evaporation losses significant. We neglected evaporation losses but can revisit them in a more rigorous follow-up. Seepage losses can be significant and depend very strongly on soil permeability. Our seepage analysis assumed that the trench was triangular (we do not have a simple seepage model for rectangular trenches) but had the same depth and volume per unit length as the rectangular trench. The triangular trench had an 11.8-m wetted perimeter compared to 12.9 m for the rectangular trench. The analysis also assumed that the ground surrounding the trench was already saturated with oil.

Soil permeability was based on two soil samples from Saudi Arabia given to us by Ft. Belvoir's Night Vision Lab (Markey, 1990). Unfortunately, the samples were from an area about 100 miles southeast (N 28.00.00, E 49.25.00) of the trench area. One sample was dune sand taken from the dune top, and the other was soil at the dune base. Seepage for the dune-top sand is twenty times faster than that for the dune-base sand because the particles are larger and have less resistance to oil flow. We suspect that the soil in the trench area is more like the dune-base sand because the trenches were excavated into the subsurface soil.

Although we used the dune-base permeability in our analysis, we cannot be confident in our results without data on soil from the trench area. Permeability can change by orders of magnitude depending on soil characteristics. For dune-base sand, the seepage rate for a full trench is roughly 28.7 barrels per day per meter of trench length, and this is the value we used in the analysis. We believe that slower seepage rates are very possible due to lower soil permeability in the trench area or because of clogging by paraffins, tars, and asphalts in the oil (no quantitative estimate is available for these effects). Because of the uncertainty in seepage rate, getting more relevant soil data and using a more detailed seepage model are recommended for a follow-up project. The use of a triangular rather than a rectangular trench geometry introduces probably a factor of two uncertainty, at

most, in the estimate of the seepage rate, but the uncertainty in the soil permeability introduces at least a factor of five uncertainty in the same estimate.

3. FILLING RATE AND REPLENISHMENT REQUIREMENTS

With a trench volume of 1,360,000 m^3, a filling capacity of 225,000 m^3/d (1.5 Mbpd), if there is no seepage, the trenches can be filled in 145 hours. With our assumed seepage rate of 340,000 m^3/d, trenches cannot be filled simultaneously and maintained full because the assumed seepage rate is greater than the filling capacity. We do not recommend assuming that seepage will keep the trenches from being filled or kept full because of the uncertainty in seepage rate. Indeed, the trenches can be preconditioned to reduce seepage by repeated filling with oil, allowing deposition of the paraffins, tars, and asphaltenes that decrease soil permeability.

4. IGNITION AND BURNING

As the more volatile components of oil evaporate from the surface of the trench, the oil becomes more difficult to ignite; however, our contacts (Hertzberg, 1990; Keltner, 1990; Evans, 1991; Fingas, 1991), who have experience with burning oil pools, say that burning can always be started by using a strong enough ignition source. These experts also say that the oil will continue to burn until it is nearly or completely consumed. In fact, the saturated soil can continue to burn very weakly for a short time (quantitative estimates for saturated soil burning are not available) after the oil is gone.

Oil burning rates depend on the type of oil, the size of the pool, and the atmospheric conditions. We believe that a burn rate of 3.5 mm/min (.21 m/h) is appropriate for crude oil in a 3.7-m-wide trench based on studies done by Koseki (1989). A reasonable range of burning rates might be from 2.5 to 5 mm/min. We also believe that the burning rate will be fairly constant (Pagni, 1990). A little wind should increase the rate slightly, but a strong wind should decrease it slightly by blowing the flame plume to an angle with the oil surface. High plume angles may decrease burning rate because the rate depends on radiation transferred from the plume to the oil surface. Keltner (1990) observed a 45 degree plume angle caused by a 2 to 2.5 m/s wind, which had little effect on burning rate.

A burning rate of 3.5 mm/min corresponds to 1.5×10^6 m^3/d (10 Mbpd). The time the trenches will burn depends on burning rate, seepage rate, and whether oil is replenished during burning. Burn times for different assumptions are given in Table C-1 below.

Table C-1. Burn Times for Various Oil Input, Loss, and Burn Rates

Refill Rate (Mbpd)	Seepage Rate (bbl/m-day)	Burn Rate (mm/min)	Burn Time (h)
1.5	28.7	3.5	20
0.0	28.7	3.5	18
1.5	0	3.5	26
0.0	0	3.5	19
0.0	28.7	5.0	13

Flame heights are expected to be 15 to 20 m (Pagni, 1990), and flame temperatures are expected to be around 1500 K (Hertzberg, 1990). The table assumes that burning will stop when there is no oil left in the trench. **Burning will not stop if the supply of oil continues.**

5. SEEPAGE ANALYSIS

To estimate the rate at which oil would seep out of the trenches, a variety of mathematical modeling approaches could be taken. The physics of flow and transport of nonaqueous petroleum liquids through porous media is relatively well developed (Abriola, 1988). Models available range in sophistication from simplified "sharp interface" models that neglect the effects of capillarity between the oil and water phases, to "black oil" simulators that account for capillary effects but neglect interphase mass transfer between the fluids (air, oil, and water), to "compositional" models that attempt to account rigorously for both capillarity and interphase partitioning of the fluids. The data needs, as well as computing power required, for the models increase significantly with the level of sophistication. For the problem at hand, interphase mass transfer would probably minimally impact the flow rates out of the trenches; however, capillary effects may be important. Therefore, a black-oil model would be the most rigorous approach.

A model conceptualized and coded by Dr. Jack Parker and his colleagues at the Center for Environmental and Hazardous Materials at Virginia Tech would be perhaps the most appropriate black-oil simulator for this problem (Kaluarachchi and Parker, 1989). To implement this simulation would require data on capillary pressure-saturation relationships and unsaturated permeability-saturation relations. It would require two to three weeks to obtain these data through laboratory measurements and some additional time to complete the simulation, so a simpler modeling approach has been used.

Two simple sharp-interface models were employed to investigate this problem. The first was a simple one-dimensional (1D) analysis (Green and Ampt, 1911), which has been widely applied in agricultural soil physics for many years and has been applied recently to oil infiltration problems (Dracos, 1978). The second was a two-dimensional (2D) profile simulation of steady seepage from a triangular shaped trench (Harr, 1962). This 2D model was modified to allow for oil as the wetting fluid and to allow for analysis of transient drainage behavior. In both cases, the conceptual model investigated examines drainage from an oil-filled trench cut off from its oil supply. In both cases, a finite-difference time-marching algorithm was used to simulate the transient drainage behavior:

1. The initial volume (17 m^3 per meter of trench length) and depth (4.6 m) of oil in the trench was specified at time t=0.

2. The flow rate of oil out of the trench, Q, for time step t_i was computed using either the 1D or the 2D analytical equation.

3. The volume of oil seeping out of the trench for time step t_i was computed as $V_{out} = Qdt$, where dt is the length of time between time step t_i and time step t_{i+1}.

4. This volume of oil, V_{out}, was subtracted from the volume of oil at the beginning of the time step to obtain the volume and depth of oil in the trench at the end of the time step.

5. Repeat steps 2 through 4.

To use these models the principal input needed was the permeability of the soils from the site. Soils from a nearby site in Saudi Arabia were provided for testing. A particle size analysis was performed, and these results were used to estimate the permeability using the empirical relation developed by Hazen (Sowers, 1979, pp. 95-96) for clean sands:

$$k = C(D_{10})^2,$$

where k is the permeability to water in mm/s, D_{10} is the 10% passing grain size in mm, and C is an empirical coefficient ranging between 10 and 15. The results of the grain size analysis are shown in Figure C-1. From this information, and by correcting permeability to account for oil as the wetting fluid, media permeabilities to oil are estimated to range between 0.25 and 5.1 m/d. It should be emphasized that these are merely estimates and that the amount of variability between the two samples is not unusual. **To perform a more rigorous analysis that accounts for variability in the soil properties, one should obtain a statistically significant number of soil samples from the actual site(s) of interest.**

Using these estimated properties in the 1D and 2D seepage models, we obtained the time series predictions of oil remaining in the trench (per meter length of trench) shown in Figure C-2. As seen in Figure C-2, the 2D analyses predicted quicker drainage than the corresponding 1D models. This is not surprising because the 2D model allows for some horizontal spreading and thus larger cross-sectional area for the oil seepage. Also notable is the large difference in predicted drainage times, depending on whether the high permeability or the low permeability value is used. Because of spatial variability in soil properties, some portions of the trench would probably drain at the rate reflected by the higher permeability curves, while other sections would drain at lower rates. Given the opportunity for oil to flow along the ground surface through the trench, a process not accounted for in the models, it is likely that the true overall drainage behavior would represent some *average* value between the extremes. Whether the actual extremes are even captured in Figure C-2 is unknown because of the relative paucity of permeability data.

6. EVAPORATION ANALYSIS

To estimate the potential loss rate of light ends from the crude oil, the diffusion rates of methane and pentanes, representing the light and heavier light-end components, were investigated. Thermal convection, caused by density fluctuations from temperature changes, and evaporative effects are likely to affect the loss rate. However, for computational simplicity, convection contributions to the loss rate were neglected. In addition, it was assumed that once the light ends left the liquid phase, they were immediately blown away by wind.

For this geometry, the appropriate form of Fick's second law is

$$\frac{\partial C_i}{\partial t} = D_i \frac{\partial^2 C_i}{\partial z^2}, \qquad (1)$$

where C_i is the concentration of the i^{th} component, t is time, D_i is the diffusion coefficient of the i^{th} component, and z is the vertical axis, taken to be 0 at the bottom of the pool of oil and L at the top. The two boundary conditions were

$$C_i(t,\ z = L) = 0 \qquad (2)$$

or no light ends in the gas phase, and

$$\frac{\partial C_i(t,\ z = 0)}{\partial z} = 0 \qquad (3)$$

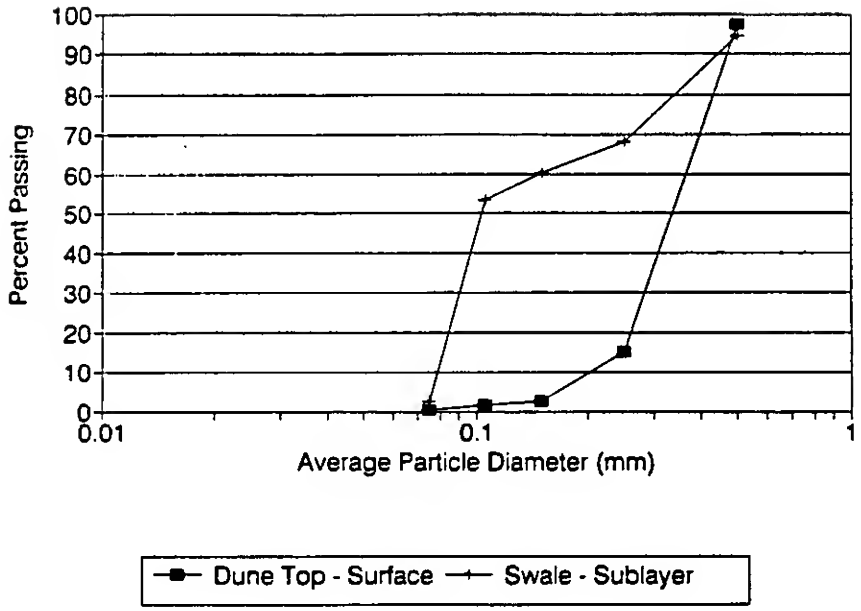

Figure C-1. Particle Size Analysis for Two Soil Samples Obtained Near Trench Sites.

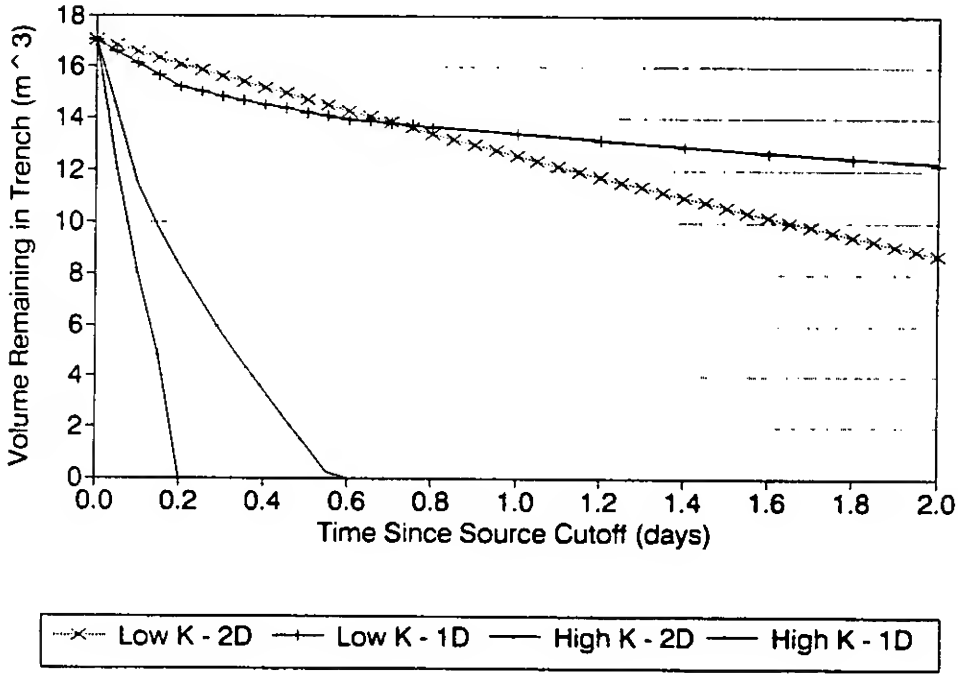

Figure C-2. Volume of Oil Remaining in the Trench (per Meter Length of Trench) Versus Time as Predicted by Both 1D and 2D Models for High Permeability and Low Permeability (High k and Low k, Respectively) Soils.

or no transfer of material across the bottom boundary of the pool. The initial condition was taken to be

$$\frac{\partial C_i(t = 0,\ z)}{\partial z} = 0. \qquad (4)$$

That is, the pool is initially well mixed.

Solving Equation (1) subject to the conditions in Equations (2), (3), and (4) yields an expression for the concentration of the i^{th} component as a function of t and z,

$$\hat{C}_i(\hat{t},\ \hat{z}) = \sum_{n\ odd}^{\infty} \frac{4}{n\pi}\ e^{-\left(\frac{n\pi}{2}\right)^2 \hat{D}_i \hat{t}}\ \sin\left(\frac{n\pi}{2}\right) \cos\left(\frac{n\pi\hat{z}}{2}\right). \qquad (5)$$

In this equation, normalized quantities are denoted by the carets (^); C_i has been normalized by $C_i(t = 0, z)$, D_i by D_{CH4}, t by L^2/D_{CH4}, and z by L. Once the diffusion coefficients are known, this equation can be used to calculate concentration profiles at various times.

To determine the diffusion coefficients of the light ends in crude oil, a thorough literature search was conducted. When neither measured values nor adequate correlations were found in the literature, a correlation for normal paraffin solutions (Hayduk and Minhas, 1982) was used to obtain the diffusion coefficients for methane (C_1) and the isomeric pentanes (C_5):

$$D_i = 13.3 \times 10^{-8} \left[\frac{T^{1.47}\varepsilon}{\eta\ V_m^{0.71}} \right]. \qquad (6)$$

In this equation, D_i is the diffusion coefficient in cm^2/s, T is the temperature on the Kelvin scale, η is the viscosity of the solvent in centipoise, and V_m is the molar volume at the normal boiling point in cm^3/mole. The parameter ε is calculated from the other parameters according to the equation

$$\varepsilon = \frac{10.2}{V_m} - 0.791. \qquad (7)$$

The temperature was taken to be 373 K (100 °F), and the molar volumes at the normal boiling points, V_m, were obtained from Daubert and Danner (1985). The viscosity of the oil was taken to be 5.3 centipoise, an approximate value for crude oil at 100 °F. The parameters for the isomeric pentanes were averaged, yielding a lumped diffusion coefficient for the C_5 fraction. The calculated diffusion coefficients are listed in Table C-2.

Table C-2. Calculated Diffusion Coefficients for Methane and the Pentanes

Component	Diffusion Coefficient cm^2/s
Methane (C_1)	1.95E-05
Pentanes (C_5) (lumped isomerically)	6.43E-06

These diffusion coefficients were implemented in Equation (5), which was then used in a FORTRAN program to calculate the concentration profiles in Figures C-3 to C-6. Figure C-3 provides normalized methane concentration, $C_1/C_{1(t = 0)}$ ($C_{1(t = 0)}$ is the initial uniform concentration of methane at t = 0) as a function of depth (z = L at the top of the trench) for six different times from 0 to 2.85 days. Figure C-4 shows similar methane concentration profiles for six times ranging from 0 to 285 days. Similar results for the lumped isomeric pentanes are shown in Figures C-5 and C-6. Because C_5 diffuses more slowly than C_1, its concentration profile changes more slowly.

From these figures, it can be seen that loss of the light end components from the crude oil is a slow process, even for the most volatile component, CH_4. If convection does play an appreciable role in moving oil containing light ends to the surface, the diffusion rate might be much faster. If the resulting *effective* diffusivity were 100 times greater from convection, the time scales of all figures would drop by a factor of 100. The results presented in Figures C-2 and C-3 for up to 285 days would apply to a time scale of 2.85 days. Consequently, unless the contribution of convection to the overall mass transfer rate is two orders of magnitude, it is unlikely that the loss of light-end components from a pool of crude exposed to the atmosphere would be significant.

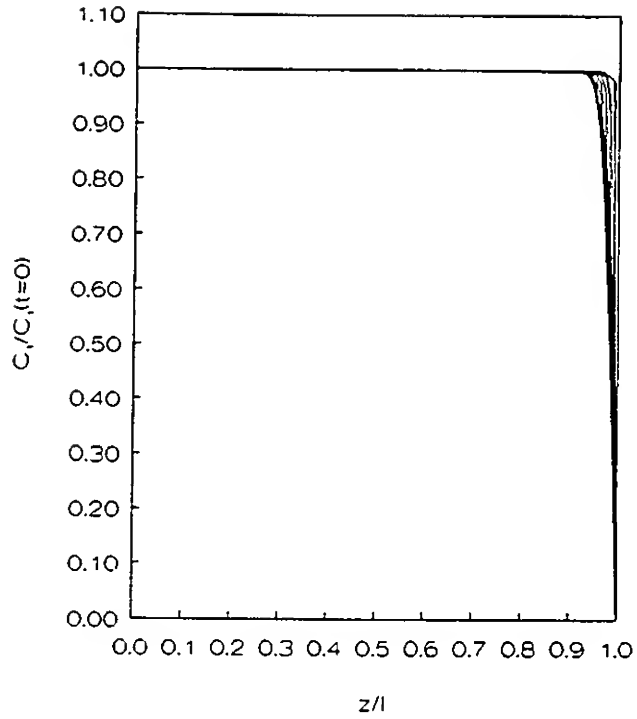

Figure C-3. Diffusion for Methane (C_1). Six Time Profiles: 0 to 2.85 Days.

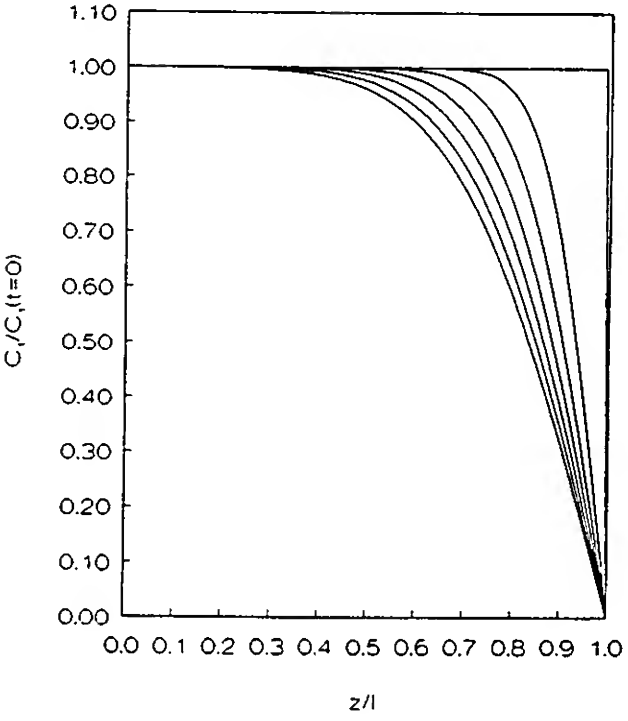

Figure C-4. Diffusion for Methane (C_1). Six Time Profiles: 0 to 285 Days.

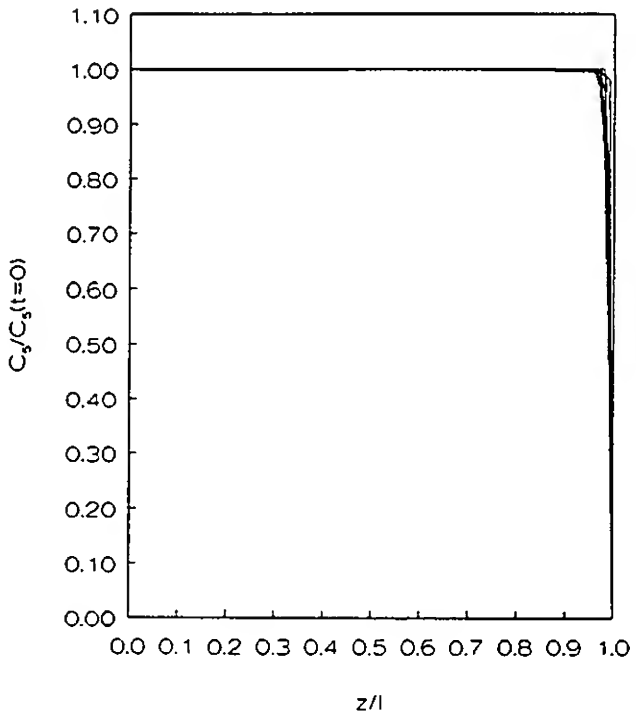

Figure C-5. Diffusion for Isomeric Pentanes (C_5). Six Time Profiles: 0 to 2.85 Days.

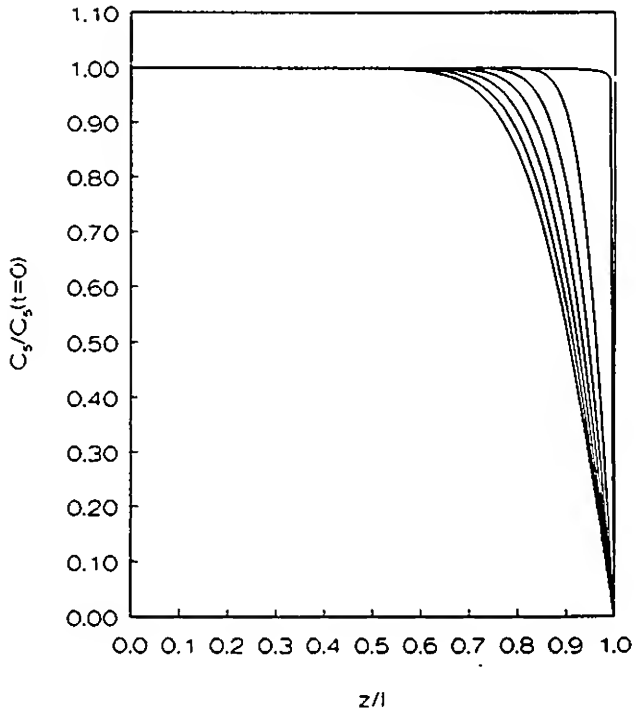

Figure C-6. Diffusion for Isomeric Pentanes (C_5). Six Time Profiles: 0 to 285 Days.

APPENDIX D

ATMOSPHERIC ISSUES

This page intentionally left blank

1. POLLUTANT PRODUCTION

Analysis of pollutant production from large-scale regional fires requires that the two combustion processes likely to be encountered (burning oil and gas jets from severed high-pressure wellheads and burning oil pools) be treated separately. This is necessary because the combustion conditions are different and result in different pollutant production rates. The burning oil and gas jet case begins with an estimate of the mass median and maximum oil droplet size in the wellhead jet as a function of the wellhead pressure. These results are then input along with gas and oil flow rates into a combustion code that predicts flame temperatures and combustion efficiency. The combustion code output then allows reasonable estimates of pollutant production rates to be made. Pollutant release rates from burning pools can be addressed directly from published data. Pollutant production rates from burning gas and oil jets and pools are then combined in the various established scenarios to yield a total release rate for input into atmospheric dispersion calculations.

Pollutant Emission Factors from Burning Gas and Oil Jets

Principal gaseous and aerosol pollutants that would result from burning gas and oil jets emanating from a severed wellhead would include soot, sulfur dioxide (SO_2), nitrogen oxides (NO_x), and unburned volatile hydrocarbons. Hydrogen sulfide (H_2S) is another possible pollutant near a severed wellhead that is not burning. Droplet breakup calculations (Appendix A) show that median diameters of oil droplets from severed wellheads in the three regions of interest are mostly under 5 microns in diameter with maximum diameters no larger than 14 microns. Using droplets larger than 14 μm, the PCGC-2 code made two predictions. First, all the droplets will be consumed in the jet flame zone, which implies that gas and oil jet combustion will be the dominant combustion process at an ignited wellhead and that pool burning will be of secondary importance. Second, CO production will be insignificant in the burning oil and gas jet. Both results should also hold for the smaller droplets now expected.

Since the combustion code cannot predict total particulate or soot concentrations, additional information to estimate particle production in the burning jet was taken from the literature. The resulting pollutant emission factors for a burning jet are given in Table D-1.

Pollutant Emission Factors from Burning Pools

Principal gaseous and aerosol pollutants from burning oil pools would include soot, carbon monoxide (CO), sulfur dioxide (SO_2), nitrogen oxides (NO_x), and unburned volatile hydrocarbons.

Table D-1. Pollutant Emission Factors for Crude Oil Pool Fires

Pollutant	Jet Emission Factor (kg/kg)	Pool Emission Factor (kg/kg)
Total Particulate	0.05 ± 0.01[a]	0.15 ± 0.03[b]
SO_2	0.05 ± 0.02[c]	0.05 ± 0.02[c]
CO	0[d]	0.15 ± 0.03[e]
NO_x	0.01 ± 0.01[f]	0.01 ± 0.01[f]

[a] The soot production rates in a gas and oil jet are taken from Urban and Dryer (1990). In this work, the soot formation was measured during combustion of burning oil droplets. Although the work used larger droplets than would be encountered here, we conservatively use their values of 0.05.

[b] Taken from the work of Mullholland (1990) in which measurements were made of smoke emission from burning crude oil in intermediate (3 m diameter) pool fires. The total particulate category can be broken into elemental carbon and volatile carbon estimates based on the work by Einfeld et al. (1990) on kerosene pool fires and Mullholland (1990) on crude oil pool fires. The mass ratio of soot to volatile carbon is approximately 4:1.

[c] Kuwaiti crude oil typically contains 2.5% sulfur by weight. Here we conservatively assume that all sulfur in the oil is converted to SO_2 during burning in both jet and pool fires. Since the molecular weight of SO_2 is twice that of S, the emission factor is accordingly doubled.

[d] The results of the PCGC-2 code show no production of CO in the jet fire.

[e] The CO emission factor is taken from Day et al. (1979), which reports CO emission factors from small arctic crude oil pool fires that are about two to three times those of SO_2 emissions. Mullholland (1990) and Einfeld et al. (1990) report much lower (<0.5 - 3%) CO emission factors from crude oil and kerosene fires. For this work, we conservatively use the higher values from Day et al.

[f] NO_x emission factors are taken from experimental work measuring NO_x from oil fired burners using residual (heavy) fuel oil as summarized by Lahre (1977).

Pollutant production rates from burning pools can be estimated by considering three parameters that control the rate of release. The first is the pollutant emission factor, which is defined here as the mass of a given pollutant released per unit mass of crude oil consumed in a fire. The second is the fuel surface regression rate or burning rate of oil, which is expressed in units of length per unit time. The third parameter is simply the area of the burning pool. Taken together, these three variables can express the pollutant production rate in units of mass per unit time as shown in the following expression:

$$M_p = EFRAD,'$$

where M_p is the pollutant production rate in kg/s, EF is the pollutant emission factor in kg/kg, R is the burning rate in m/s, A is the pool area in m^2, and D is a density correction factor to convert cubic meters of oil to kilograms of oil.

Estimates of pollutant emission factors in this analysis are given in Table D-1 along with appropriate references from the literature. A crude oil burning rate estimate of 3.5 mm/min (5.8×10^{-5} m/s) is taken from the work of Koseki (1989). As a part of this work, carried out at the Fire Research Institute in Japan, burning rates of various crude oils in large (>7 m^2) pools were measured and were found to be in the range of 3 to 4 mm/min.

2. PLUME CHARACTERISTICS

Atmospheric properties downwind from mass crude oil fires were examined by using a total pollutant production rate from both burning jets and pools for each of the oil fields of interest in the various event scenarios. This combined pollutant production rate or source term was then input into simple plume rise and dispersion models that predict ground-level concentration as a function of downwind distance. Data input and assumptions for the various steps in the process are outlined in the following sections.

Source Configuration

In the absence of detailed information on specific oil well locations at the three principal oil fields of interest (Southeast, West, and North), each field was modeled as a line source oriented normal to the expected surface wind direction during January as shown in Figure D-1. Oil field size was estimated from maps showing the approximate geographical extent of each of the oil fields of interest. The Southeast (Burgan) field line source length was set at 35 km, the West (Manageesh) Field at 15 km, and the North (Rawdhatain/Sabriyah) Field also at 15 km.

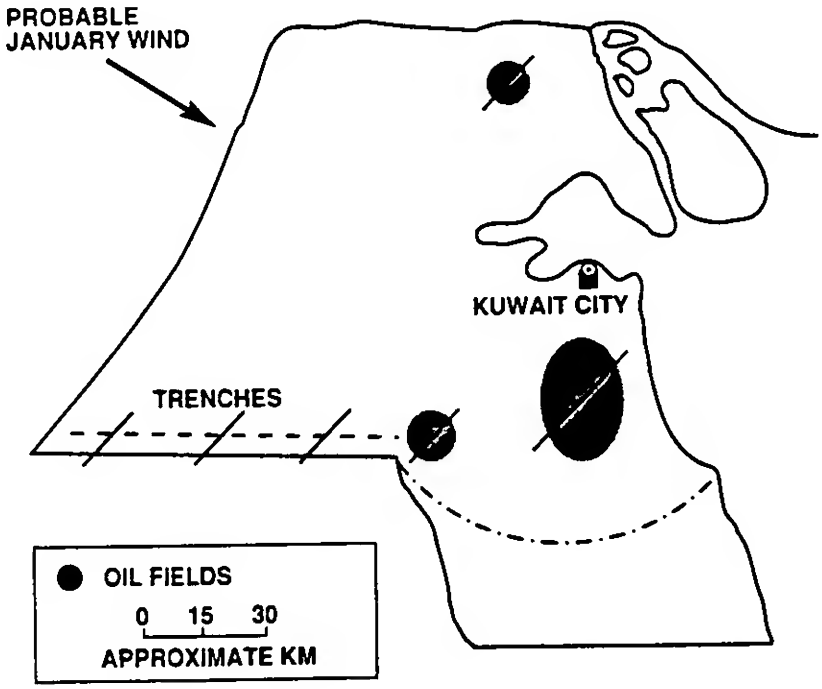

Figure D-1. Map of Kuwait Showing Location of Principal Oil Fields and Trenches of Interest. Modeled line sources are shown superimposed on the smoke sources of interest and oriented normal to the expected wind direction.

Plume Rise Estimates

Estimates of plume rise from a burning oil and gas jet were calculated on a per well basis, since no detailed information on the spatial arrangement of wells in a given field was available. Plume rises were calculated by calculating the heat production rates of an average well in each of the three principal fields of interest. The thermal release of the well fire was calculated using the assumption that all oil and gas are consumed as they exit the wellhead, or in other words, no pooling or accumulation of oil at the source occurs. An expression that relates plume rise to heat release from a fire is

$$Z_c = 1/9\,(Q_h^{1/3})\,(U^{-1/3}),$$

where Z_c is the centerline plume height in km, Q_h is the heat output of the fire in MW, and U is the surface wind speed in m/s (Briggs, 1975). The heat release term can be estimated by combining the heat release from oil and natural gas, which can be estimated by the wellhead release rate of both oil and gas and their associated heats of combustion. The expected plume rise for a burning well jet at each oil field site is given in Table D-2 along with the assumptions used in the calculation. In all cases, plume rise is in the range of 0.5 to 1 km above the ground. The existence of a ground-based temperature inversion at night is not expected to alter the plume height estimate because these fires are of such high intensity that the plume would easily penetrate the inversion layer.

Table D-2. Plume Rise Estimates for Southeast, West, and North Kuwait Single Well Fires

Parameter	Southeast	West	North
Wellhead Oil Flow (bbl/day)	23,000	10,000	12,500
Wellhead Oil Flow (kg/s)	36.7	11.2	20.0
Wellhead Gas Flow (scf/s)	141	45	87
Heat Release - Oil (GW)[a]	1.62	0.49	0.88
Heat Release - Gas (GW)[b]	0.03	0.01	0.02
Heat Release - Total (GW)	1.66	0.51	0.90
Wind Speed (m/s)	3	3	3
Centerline Plume Height (km)	0.9	0.6	0.7

[a] Oil Heat of Combustion is 44 MJ/kg (Fletcher, 1990)
[b] Gas Heat of Combustion is 1 MJ/scf @ STP (Fletcher, 1990). A mean surface level wind speed of 3 m/s is assumed.

Meteorological Conditions

The various burn scenarios were evaluated for typical January day and night conditions using summary surface winds, winds aloft, and temperature data from Kuwait City Airport. The data obtained comprised over 10 years of daily January observations. Summary data are given for wind speed and direction as a function of altitude for night (3 AM) and day (3 PM) conditions in Figures D-2 through D-7. At the expected plume height of 1 km above sea level (3,000 ft) for most burning scenarios, the average wind direction is from the northwest at about 325 degrees for both night and day cases. Surface wind speeds are about 6 knots (3 m/s) at night and 10 knots (5 m/s) during the day. Increases in wind speed with altitude are as expected under normal atmospheric conditions. Temperature structure shows ground-based inversions extending to about 300 m during the night and normal temperature decreases with altitude during the day.

Pollutant Dispersion Calculations

Burning Wells. Estimates of downwind ground-level pollutant concentrations were determined by application of a Gaussian plume model (Pasquill, 1961; Gifford, 1961; and Turner, 1970). The model assumes the following:

- The pollutant is released at a constant rate.
- The released material is modeled as a stable gas or particles with no reaction or deposition loss with downwind travel.
- The plume constituents are normally distributed in the vertical direction.
- Complete reflection of plume constituents is assumed at the ground.

For a continuous line source, the ground-level concentration at a specified downwind distance is given by

$$C_p = \{2q/[(2\pi)^{1/2}\sigma_z U]\} \exp[-(H/\sigma_z)^2/2],$$

where q is the source release rate in g/m-s, H is height in m, σ_z is the vertical dispersion parameter as a function of downwind distance in m, and U is the mean surface wind speed in m/s.

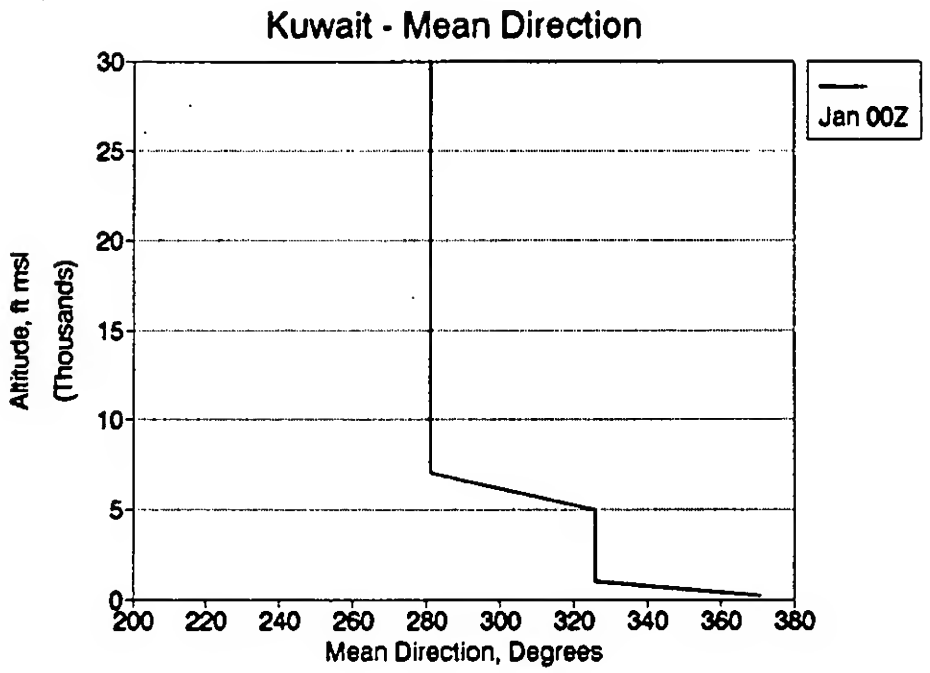

Figure D-2. Summary Nighttime (3 AM) Data for Wind Direction with Altitude from Kuwait City Airport.

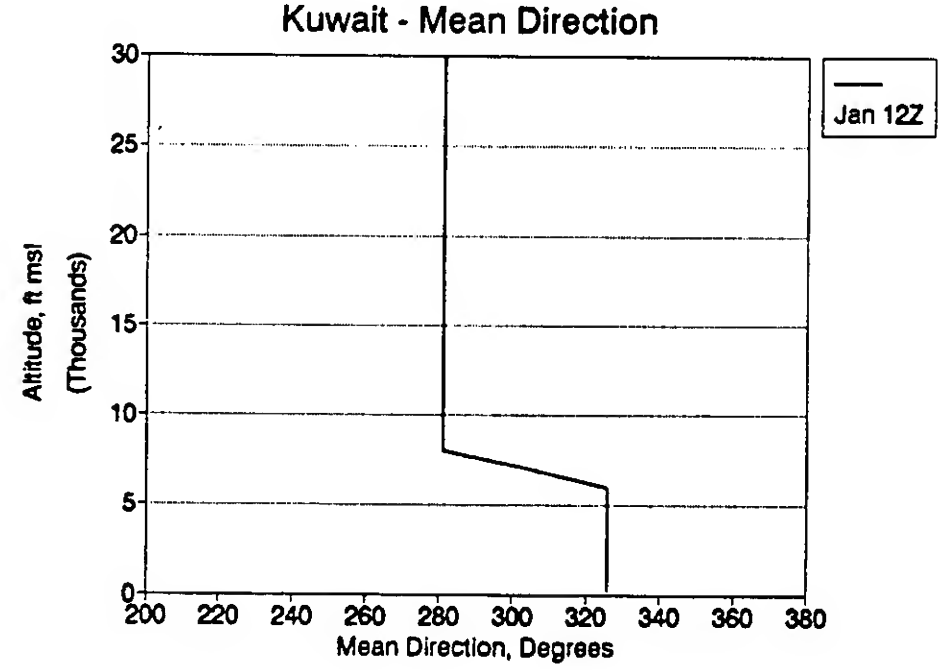

Figure D-3. Summary Daytime (3 PM) Data for Wind Direction with Altitude from Kuwait City Airport.

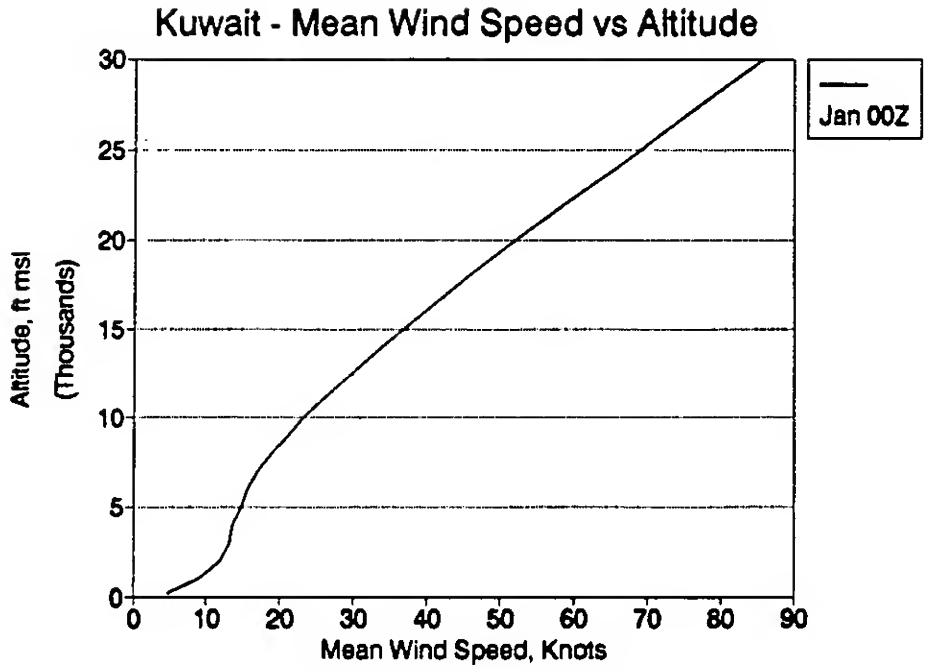

Figure D-4. Summary Nighttime (3 AM) Data for Wind Speed with Altitude from Kuwait City Airport.

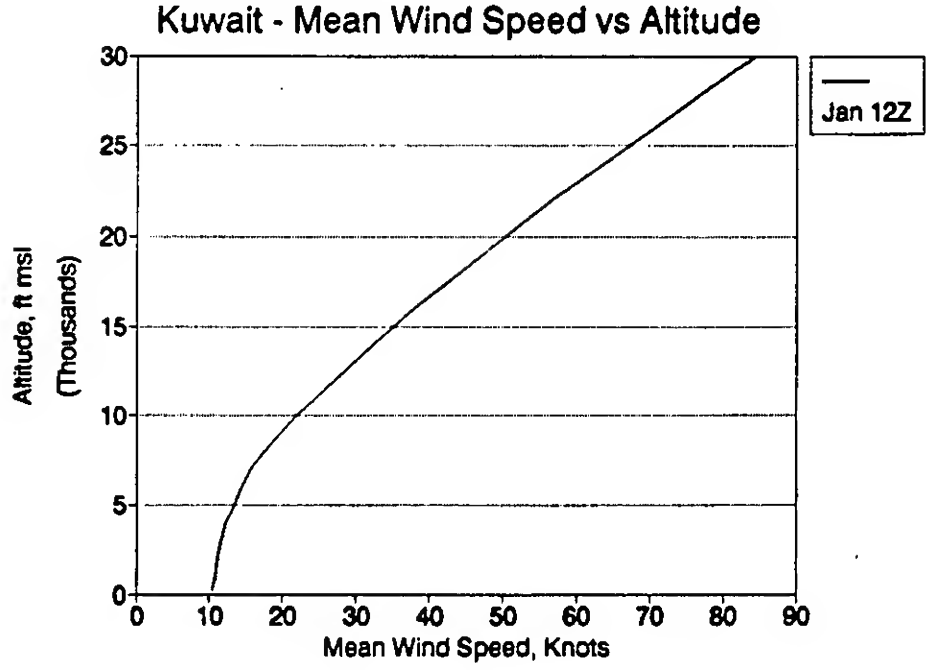

Figure D-5. Summary Daytime (3 PM) Data for Wind Speed with Altitude from Kuwait City Airport.

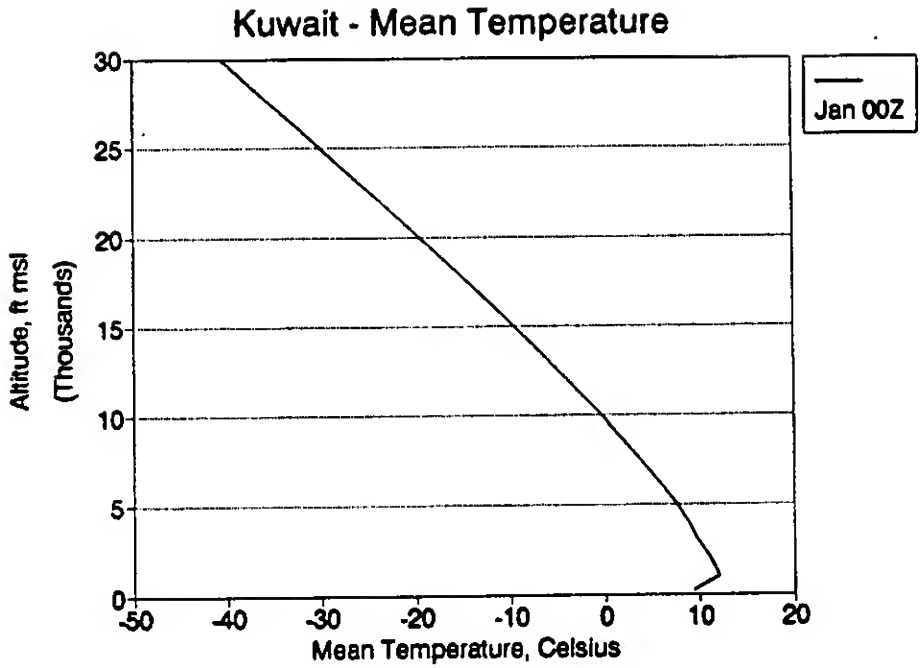

Figure D-6. Summary Nighttime (3 AM) Data for Temperature with Altitude from Kuwait City Airport.

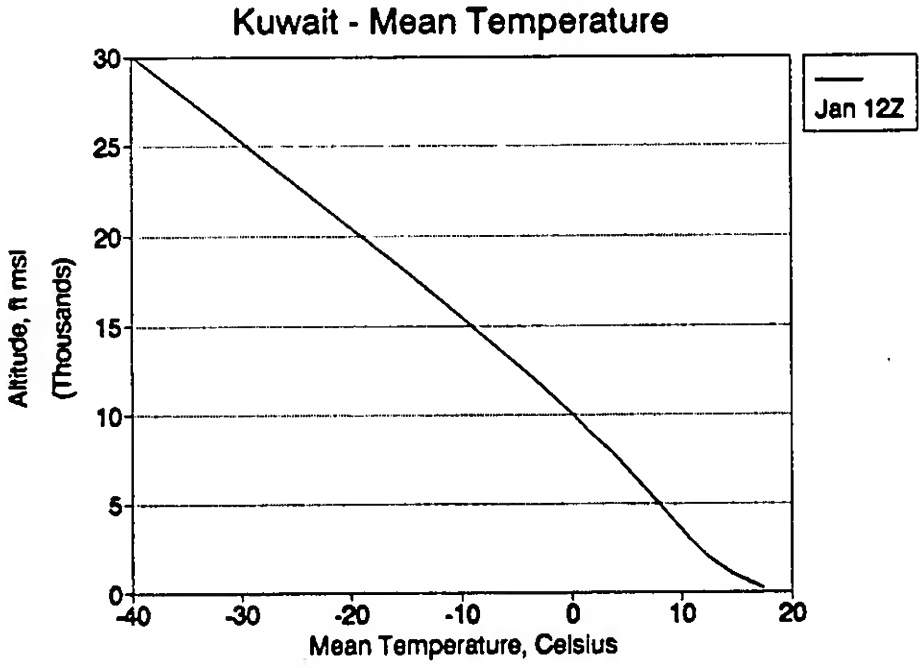

Figure D-7. Summary Daytime (3 PM) Data for Temperature with Altitude from Kuwait City Airport.

The vertical dispersion parameter can be estimated for various atmospheric conditions or stability categories that take both wind speed and temperature structure of the atmosphere into account (Turner, 1970). For this analysis, two stability categories were considered. Stability category B was selected for daytime and assumes strong insolation (clear sunny skies) and surface wind speed in the range of 3 m/s. For the night case, stability category F was selected and assumes clear nighttime skies and less than 3 m/s surface wind speeds. Tabulated values of σ_z as a function of downwind distance were used for each of the selected stability categories to calculate downwind concentrations. Since a continuous line source is considered here, lateral pollutant dispersion within the plume is considered negligible. For this preliminary analysis, downwind pollutant diffusion at the the ends of the line sources are ignored. Figure D-1 is a map of Kuwait showing the three principal source locations and the expected wind direction. Figures D-8 and D-9 show typical daytime downwind ground-level concentrations for the base-case mass fire scenario (#2) at the Southeast (Burgan) Field and the West (Minageesh) Field.

Similar dispersion calculations for the nighttime case show that the plume remains aloft in an approximate 600-m layer centered at about 1 km above ground. For distances ranging from close-in to 100 km, the plume does not mix down to the ground.

Nonburning Wells. Wells in the West Field contain appreciable amounts of hydrogen sulfide that must be treated as a separate case in the analysis. Although in a burning gas and oil jet H_2S would be fully consumed, it would be released in appreciable quantities in a nonburning jet. To estimate downwind H_2S concentrations in these circumstances, a separate dispersion calculation was performed. In this calculation, a worst-case (West Field) point source with no plume rise is considered instead of a line source with elevated plume for the multiple burning well scenarios. Hydrogen sulfide concentrations as a function of downwind distance are shown in Figure D-10.

Downwind Dispersion Estimates for Burning Wells

Downwind concentrations for each of the four well-fire scenarios were calculated and are given in Table D-3 to a distance of 100 km. For the base-case case (#2) at the Southeast Field (Figure D-8), the maximum downwind ground-level concentrations occur at about 10 km for each of the pollutant species modeled. Soot and SO_2 concentrations at 10 km are slightly less than 1 mg/m^3 and drop to about 0.2 mg/m^3 at 100 km. Carbon monoxide concentration levels are about a factor of four lower than those calculated for soot and SO_2. Although calculations are not shown for NO_x species, values can be easily derived by dividing the SO_2 results by 5, since the NO_x emission factor is one-fifth that of SO_2. Maximum NO_x concentrations 10 km downwind from the base-case fire event at the Southeast Field would be about 0.1 mg/m^3. Downwind H_2S concentrations modeled from the same

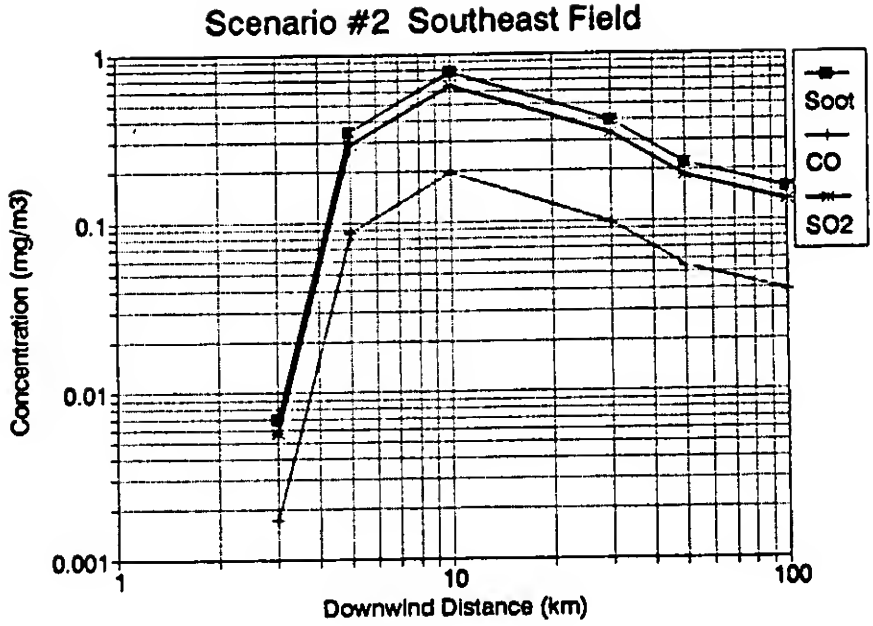

Figure D-8. Soot, SO_2, and CO Daytime Ground-level Concentrations as a Function of Downwind Distance from a 35-km Line Source through the Southeast (Burgan) Field for the Base-case (#2) Burn Scenario. NO_x concentrations are five-fold less than the SO_2 concentrations.

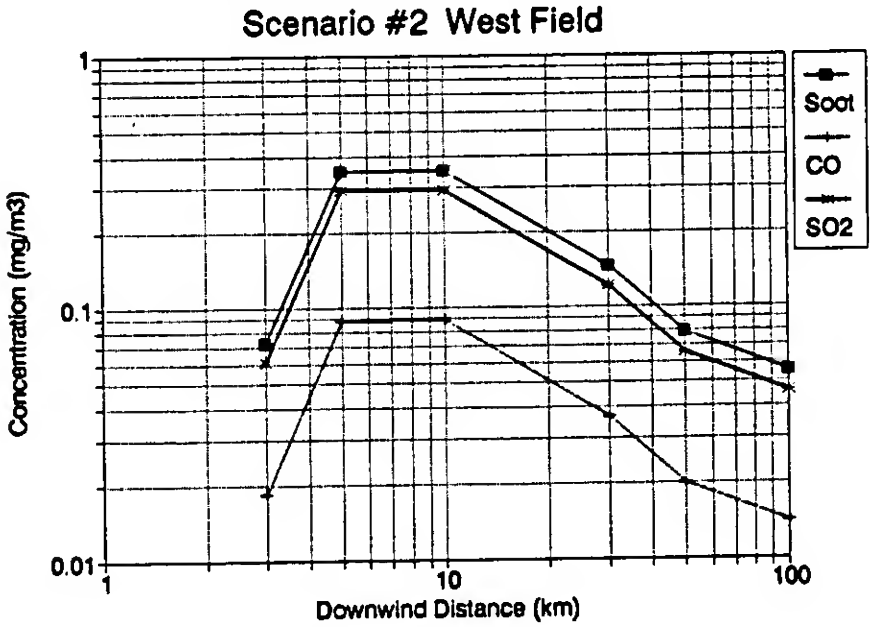

Figure D-9. Soot, SO_2, and CO Daytime Ground-level Concentrations as a Function of Downwind Distance from a 15-km Line Source through the West (Manageesh) Field for the Base-case (#2) Burn Scenario. NO_x concentrations are five-fold less than the SO_2 concentrations.

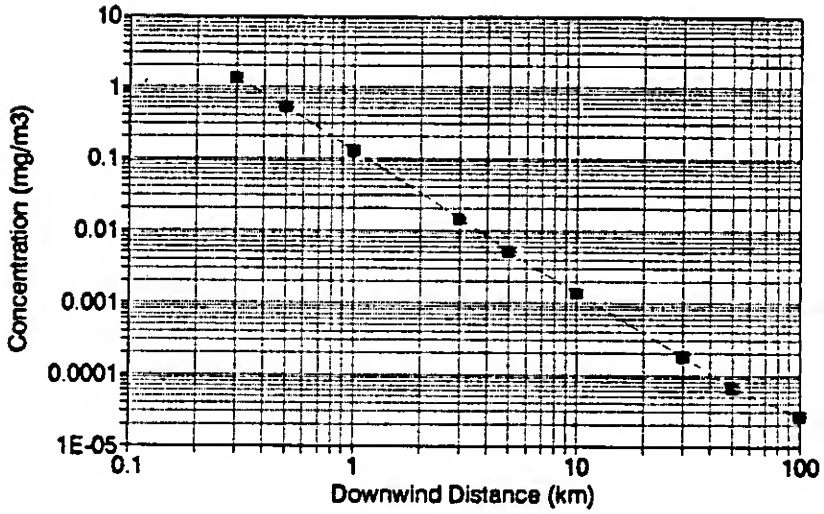

Figure D-10. Hydrogen Sulfide Ground-level Concentrations in the Vicinity of a Single Nonburning Venting Wellhead (West Field).

Table D-3. Ground-Level Pollutant Concentration with Downwind Distance for Selected Oil Fire Scenarios

Pollutant Concentration	Downwind Distance (km) 1	3	5	10	30	50	100
Scenario #1 Southeast Field							
Soot (mg/m^3)	4.6E-30	4.4E-03	2.2E-01	5.0E-01	2.5E-01	1.4E-01	9.9E-02
CO (mg/m^3)	1.1E-30	1.1E-03	5.6E-02	1.2E-01	6.3E-02	3.5E-02	2.5E-02
SO_2 (mg/m^3)	3.8E-30	3.7E-03	1.9E-01	4.2E-01	2.1E-01	1.2E-01	8.3E-02
H_2S (mg/m^3)	6.9E-04	2.1E-04	1.2E-04	5.6E-05	1.9E-05	1.0E-05	7.0E-06
Scenario #1 West Field							
Soot (mg/m^3)	5.0E-15	2.3E-02	1.1E-01	1.1E-01	4.6E-02	2.5E-02	1.8E-02
CO (mg/m^3)	1.3E-15	5.9E-03	2.8E-02	2.9E-02	1.2E-02	6.4E-03	4.5E-03
SO_2 (mg/m^3)	4.2E-15	1.9E-02	9.4E-02	9.4E-02	3.9E-02	2.1E-02	1.5E-02
H_2S (mg/m^3)	1.4E-02	4.1E-03	2.3E-03	1.1E-03	3.7E-04	2.0E-04	1.4E-04
Scenario #2 Southeast Field							
Soot (mg/m^3)	7.1E-30	6.8E-03	3.5E-01	7.8E-01	4.0E-01	2.2E-01	1.6E-01
CO (mg/m^3)	1.8E-30	1.7E-03	8.7E-02	1.9E-01	9.9E-02	5.5E-02	3.9E-02
SO_2 (mg/m^3)	6.0E-30	5.7E-03	2.9E-01	6.5E-01	3.3E-01	1.8E-01	1.3E-01
H_2S (mg/m^3)	6.4E-03	2.0E-03	1.1E-03	5.2E-04	1.8E-04	9.4E-05	6.6E-05
Scenario #2 West Field							
Soot (mg/m^3)	1.6E-14	7.2E-02	3.5E-01	3.5E-01	1.4E-01	7.9E-02	5.5E-02
CO (mg/m^3)	4.0E-15	1.8E-02	8.9E-02	8.9E-02	3.7E-02	2.0E-02	1.4E-02
SO_2 (mg/m^3)	1.3E-14	6.1E-02	2.9E-01	2.9E-01	1.2E-01	6.6E-02	4.6E-02
H_2S (mg/m^3)	0.0E+00	0.0E+00	0.0E+00	0.0E+00	0.0E+00	0.0E+00	0.0E+00

Table D-3. Ground-Level Pollutant Concentration with Downwind Distance for Selected Oil Fire Scenarios (Concluded)

Pollutant Concentration	Downwind Distance (km) 1	3	5	10	30	50	100
Scenario #3 Southeast Field							
Soot (mg/m^3)	4.1E-30	4.0E-03	2.0E-01	4.5E-01	2.3E-01	1.3E-01	9.0E-02
CO (mg/m^3)	1.0E-30	9.9E-04	5.0E-02	1.1E-01	5.7E-02	3.2E-02	2.2E-02
SO_2 (mg/m^3)	3.5E-30	3.3E-03	1.7E-01	3.8E-01	1.9E-01	1.1E-01	7.5E-02
H_2S (mg/m^3)	1.0E-02	3.1E-03	1.7E-03	8.2E-04	2.8E-04	1.5E-04	1.0E-04
Scenario #3 West Field							
Soot (mg/m^3)	4.4E-15	2.0E-02	9.8E-02	9.9E-02	4.1E-02	2.2E-02	1.5E-02
CO (mg/m^3)	1.1E-15	5.2E-03	2.5E-02	2.5E-02	1.0E-02	5.6E-03	3.9E-03
SO_2 (mg/m^3)	3.7E-15	1.7E-02	8.2E-02	8.2E-02	3.4E-02	1.8E-02	1.3E-02
H_2S (mg/m^3)	1.9E-01	5.9E-02	3.3E-02	1.6E-02	5.3E-03	2.8E-03	2.0E-03
Scenario #3 North Field							
Soot (mg/m^3)	2.5E-14	1.1E-01	5.5E-01	5.5E-01	2.3E-01	1.2E-01	8.7E-02
CO (mg/m^3)	6.5E-15	3.0E-02	1.5E-01	1.5E-01	6.0E-02	3.3E-02	2.3E-02
SO_2 (mg/m^3)	2.1E-14	9.5E-02	4.6E-01	4.6E-01	1.9E-01	1.0E-01	7.2E-02
H_2S (mg/m^3)	0.0E+00	0.0E+00	0.0E+00	0.0E+00	0.0E+00	0.0E+00	0.0E+00
Scenario #4 Southeast Field							
Soot (mg/m^3)	1.7E-29	1.6E-02	8.1E-01	1.8E+00	9.3E-01	5.1E-01	3.6E-01
CO (mg/m^3)	4.2E-30	4.0E-03	2.0E-01	4.6E-01	2.3E-01	1.3E-01	9.1E-02
SO_2 (mg/m^3)	1.4E-29	1.3E-02	6.8E-01	1.5E+00	7.8E-01	4.3E-01	3.0E-01
H_2S (mg/m^3)	2.5E-03	7.6E-04	4.2E-04	2.0E-04	6.8E-05	3.6E-05	2.6E-05
Scenario #4 West Field							
Soot (mg/m^3)	1.8E-14	8.3E-02	4.0E-01	4.0E-01	1.7E-01	9.0E-02	6.3E-02
CO (mg/m^3)	4.5E-15	2.1E-02	1.0E-01	1.0E-01	4.2E-02	2.3E-02	1.6E-02
SO_2 (mg/m^3)	1.5E-14	6.9E-02	3.3E-01	3.4E-01	1.4E-01	7.5E-02	5.3E-02
H_2S (mg/m^3)	4.7E-02	1.4E-02	8.0E-03	3.9E-03	1.3E-03	7.0E-04	4.9E-04
Scenario #4 North Field							
Soot (mg/m^3)	1.2E-13	5.7E-01	2.8E+00	2.8E+00	1.1E+00	6.2E-01	4.3E-01
CO (mg/m^3)	3.3E-14	1.5E-01	7.3E-01	7.3E-01	3.0E-01	1.6E-01	1.2E-01
SO_2 (mg/m^3)	1.0E-13	4.8E-01	2.3E+00	2.3E+00	9.5E-01	5.2E-01	3.6E-01
H_2S (mg/m^3)	0.0E+00	0.0E+00	0.0E+00	0.0E+00	0.0E+00	0.0E+00	0.0E+00
Trench Burn Scenario -- 30 km segment (10-km "effective" length)							
Soot (mg/m^3)	5.9E-03	2.0E+01	2.2E+01	1.4E+01	4.9E+00	2.6E+00	1.8E+00
CO (mg/m^3)	5.9E-03	2.0E+01	2.2E+01	1.4E+01	4.9E+00	2.6E+00	1.8E+00
SO_2 (mg/m^3)	2.0E-03	7.0E+00	7.5E+00	4.6E+00	1.6E+00	8.8E-01	6.2E-01
H_2S (mg/m^3)	0.0E+00	0.0E+00	0.0E+00	0.0E+00	0.0E+00	0.0E+00	0.0E+00

Note that 1.7E-29 = 1.7×10^{-29}; 0.0E+00 = 0; 2.2E+01 = 2.2×10^{1} = 22.

Because toxicity limits are normally quoted in ppm rather than mg/m^3, it is useful to have the following conversion factors: 1 mg/m^3 of CO = 0.87 ppm, 1 mg/m^3 of SO_2 = 0.38 ppm, and 1 mg/m^3 of H_2S = 0.72 ppm.

line source as the other pollutant for the nonburning wells show maximum H_2S levels of about 0.006 mg/m^3 very near the line.

For the West Field base-case scenario (#2), downwind concentrations for all modeled species are lower by about a factor of two at the point of maximum ground-level concentration (Figure D-9). As one approaches the line source, the ground-level concentrations fall rapidly from their maximum values at 10 km because the plume is still aloft and not mixed down to ground level.

For the worst-case (#4) scenario, downwind soot concentrations are higher than in the base-case scenario (#2) by about a factor of two. For the worst case, H_2S release from a nonburning well, the H_2S concentrations are about 1 mg/m^3 near the wellhead and drop by about a factor of ten at 1 km.

Smoke Release from Oil Burning in Trenches

A trench-burning smoke-production scenario was modeled using a trench 3 m deep by 3.7 m wide by 80 km long, oriented along the Kuwaiti-Saudi border. Since the trench is not normal to the expected wind direction, the trench was broken up into three trenches with an "effective" trench length of 10 km normal to the wind direction. These three trenches were considered as line sources in the downwind dispersion model. Downwind pollutant concentrations for a daytime case for each of these trenches are given in Table D-3. Maximum downwind soot concentrations are estimated to be about 22 mg/m^3 at a distance of about 3 to 5 km downwind from the trench. Similar CO concentrations are expected with SO_2 concentrations lower by a factor of three.

Calculations for a typical nighttime case (clear sky) reveal that the plume remains aloft with no measurable concentrations of plume constituents at the ground out to 50 km.

Smoke Release from Oil Storage Facilities Leakage

A final smoke release scenario involves the release and ignition of 15 million barrels of crude oil stored along the eastern edge of the Southeast (Burgan) Field. In the absence of detailed data concerning the specific geographical location and capacity of the storage facilities, we have assumed that all the oil is stored at four facilities. If all oil were consumed in large pools of about 800 m^2 near the storage tanks at each of the four locations, we estimate that the fires would burn with extraordinary intensity (128 GW) for 6 hours, and smoke plumes would rise at least 7 km above the ground. This source term would add a short-term increase to the plume from the burning oil wells at the Southeast Field. However, since the plume would be injected so high, little contribution would be expected in the atmospheric region from ground level to 2 km.

2. OPTICAL EFFECTS

The principal optical effect that would result from well-fire plumes would be extinction of light as a result of large airborne soot concentrations. Possible additional visibility degradation might result from reaction of volatile hydrocarbons in the smoke with oxides of nitrogen to produce aerosol from gas-phase plume constituents far downwind, and from oil mist in the vicinity of nonburning well blowouts. Visibility reduction for soot concentrations can be estimated using known extinction cross sections of soot and assuming some optical path length. An estimate of light extinction with distance is given by Beer's Law:

$$I/I_0 = \exp(-\tau),$$

where I_0 is the incident light intensity and I is the intensity after transit through some path length. The exponent value τ (the optical depth) is given by

$$\tau = B_{ext}\, M\, L,$$

where B_{ext} is the specific extinction coefficient for soot, M is the mass concentration of soot in the path length of interest, and L is the path length. The transmittance of light through a path length to an observer can be roughly related to visual range or the maximum distance that a distant white object can be discerned from a black object through use of the Koschmeider equation:

$$R_v = 3.912/(B_{ext}\, M),$$

where R_v is the visual range.

We have taken soot concentrations of 0.01, 0.1, and 1 mg/m^3 and calculated light transmittance (I/I_0) and visual range for optical path lengths of 0.5, 1, 5, 10, and 50 km. For these estimates, we use a soot extinction cross section of 12 m^2/g (Janzen, 1980). The results are given in Table D-4. As can be noted, light extinction and corresponding visual range at high (1 mg/m^3) soot concentrations will result in significant visibility degradation at path lengths less than 500 m. The visual range at this soot concentration level is about 0.3 km, and for the less concentrated case of 0.01, the visual range is about 33 km. These estimates of visual range would compare to an estimate of ambient (no smoke) visual range that would probably be in the range of 30 to 40 km. Together, Tables D-3 and D-4 can be used to ascertain how transmittance and visual range vary downwind of each source. Note, in particular, that the trenches are very effective in producing obscuration; the calculated visual range at 5 km is 13.6 m!

Table D-4. Light Transmission and Visual Range for Expected Soot Concentrations and Optical Path Lengths

Concentration of Soot	Transmittance* at Range (km)					Visual Range
(mg/m³)	0.5	1	5	10	50	(km)
10.0	0.000	0.000	0.000	0.000	0.000	0.033
1.0	0.002	0.000	0.000	0.000	0.000	0.33
0.1	0.549	0.301	0.002	0.000	0.000	3.3
0.01	0.994	0.988	0.942	0.887	0.549	33

*Fraction of original intensity of light that is encountered at range

The most dramatic optical effect expected, however, is not visibility degradation in the horizontal, but sunlight extinction in the vertical. For the line sources assumed here, it is easy to put sunlight attenuation on a quantitative basis. The downwind optical depth is given approximately by

$$\tau = B_{ext} M_c / \sin\phi ,$$

where B_{ext}, the specific extinction coefficient for soot, is assumed to be 12 m²/g (Janzen, 1980) in the middle of the visible spectrum; ϕ is the elevation angle of the sun; and M_c is the column density of soot (the total mass of soot over each square meter of surface area integrated vertically from the ground to infinity) in g/m². Assuming constant wind speed over the plume depth and a line source (ignoring end effects and wind shear), M_c does not vary as a function of downwind distance. Further downwind, the mass is spread over a greater depth, but the same amount of mass covers each square meter of surface area. Thus, M_c is a function only of wind speed, wind direction, and source characteristics. It can be shown that M_c is just the mass of soot put into the air per meter of line source per meter of air that passes over the line. Assuming the line source is a burning trench, M_c in g/m² is given by

$$M_c = 1000\, R\, W\, D\, EF_p / (U \cos\theta) ,$$

where W is the width of the trench in m, EF_p is the soot emission factor for pool burning, U is the surface wind speed in m/s, θ is the angle between the normal to the line source and the wind direction, and all other symbols are as previously defined.

For oil fields with burning blowouts, M_c is given by

$$M_c = 1000\, n_w\, F_w\, (0.9\, EF_s + 0.1\, EF_p) / (L_s\, U) ,$$

where n_w is the number of wellheads burning in the specified field, F_w is the estimated average blowout flow rate per well for that field in kg/s, EF_s is the soot emission factor for spray burning, and L_s is the equivalent line source length normal to the wind direction in m. The weighted sum of emission factors results from the assumption that 10% of the oil undergoes pool burning.

Table D-5 gives the optical depth and the sunlight attenuation factors inferred from these expressions downwind of the trench and each oil field for each scenario.

Table D-5. Optical Depths and Sunlight Attenuation[a] for Plumes from Each Source for Each Scenario at Noon[b] in Late January[c]

	Scenario			
	#1	#2	#3	#4
Trench				
OD	125.1	125.1	125.1	125.1
Atten.	2.1E+54	2.1E+54	2.1E+54	2.10E+54
Southeast				
OD	15.1	29.5	13.8	55.2
Atten.	3.6E+06	6.5E+12	9.8E+05	9.4E+23
West				
OD	2.69	4.20	2.39	9.54
Atten.	14.7	66.7	10.9	1.4E+4
North				
OD	-	-	13.2	52.7
Atten.	-	-	5.4E0+05	7.7E+22

[a] The sunlight attenuation factor is defined as the light level in full sunlight divided by the actual light level. Attenuation factors can be put into perspective by noting that the light level in sunlight divided by the light level from the full moon with the moon in the same position in the sky as the sun is 6.40E+05 (6.4×10^5).

[b] Wind is assumed to be from 325° at 5m/s (10 knots), and the trenches are assumed to run east and west; the wind speed used here is appropriate for conditions at noon.

[c] Sun elevation angle at noon in late January in Kuwait is about 40°.

Thus, corridors of darkness up to tens of kilometers wide can be expected under the smoke plumes, shown in Figure D-11. In fact, wind shear and diffusive spread in the horizontal would increase the affected area downwind, but would decrease the severity of the effect somewhat. A more in-depth and detailed consideration of the darkness-at-noon phenomenon is certainly warranted.

Note that with this level of sunlight extinction, the ground-level air temperature under the plumes would also drop to near nighttime levels under a cloudy sky. In short, most of the same phenomena predicted in a nuclear winter scenario would

occur, but on a local and regional scale. In the nuclear winter scenario, average hemispheric smoke optical depths of less than 5 were predicted.

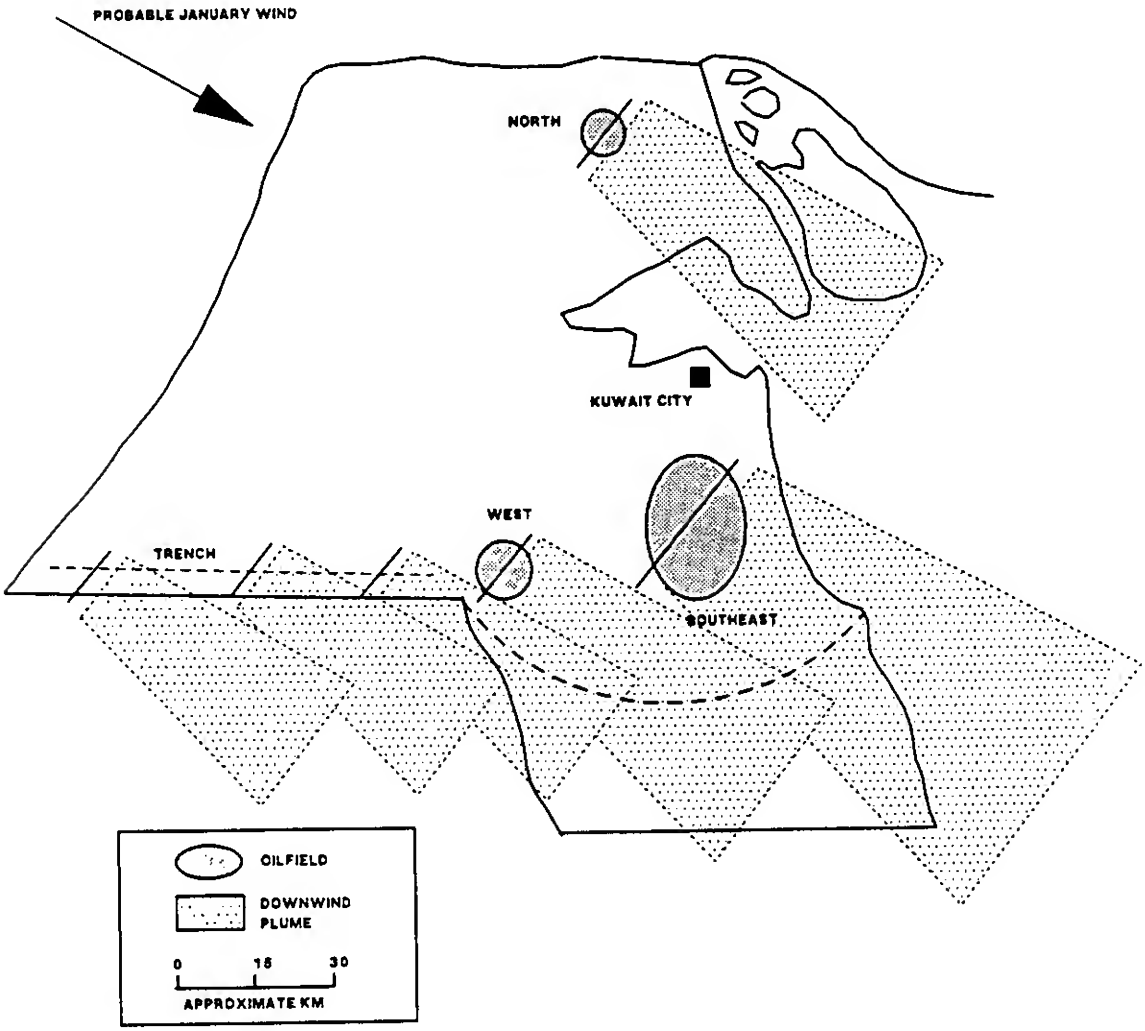

Figure D-11. Map of Kuwait Showing Location of Principal Oil Fields and Trenches of Interest. Modeled line sources are shown superimposed on the smoke sources and oriented normal to the expected wind direction. Expected plume dimensions are shown with dotted lines. Note that the plumes are artificially terminated here, but would actually continue indefinitely. It is important to note that the expected wind direction may not occur on any given day. Hence, the areas affected may be quite different from those shown here.

Both obscuration and darkness would be mitigated by high winds. For the same amount of smoke generated, all downwind concentrations are inversely proportional to wind speed. Downwind of burning oil pools and trenches, the effects of wind may be even more favorable in that only a fraction of the oil surface may burn along the

downwind edge. Reductions can be dramatic because optical effects are exponentially dependent upon concentrations. Use of wind forecasts in planning would seem to be indicated.

A highly relevant question is how extinction and equivalent "visual" range would vary with wavelength. Since many military electro-optical systems operate in the infrared rather than in the visible spectrum, it is important to extend the estimates to cover that region as well. Unfortunately, not all of the information necessary to reach firm conclusions is available to the authors in the time frame of this study. Nevertheless, it is possible to place limits on the effects in the infrared relative to the effects in the visible.

The optical properties of soot from the combustion of Kuwaiti crude oil are not available. To surmount this difficulty, we used optical properties of a well-studied carbon black that are known to be similar to those of liquid hydrocarbon combustion soots in the visible range (Janzen, 1980). The properties of this carbon black are not known in the infrared either, but those of propane soot are known (Dalzell and Sarofim, 1969). Using the optical properties of propane soot and assuming that the wavelength dependence is the same for Kuwaiti crude soot allowed use of the approximation of Bohren and Huffman (1983) relating the optical properties of an aerosol to its specific absorption coefficient and hence, facilitated making the required estimates. Using the procedure sketched above and taking scattering into account in the visible range (but assuming it is negligible relative to absorption in the infrared), one finds that if extinction is normalized to unity in the visible (550 nm), then the extinction at 2.5 μm would be 0.258; at 5 μm it would be 0.132; and at 10 μm it would be 0.046.

This dependence roughly corresponds to extinction being inversely proportional to wavelength as Jennings and Pinnick (1980) calculate (with assumptions) for the near infrared. Volz (1972), however, has presented evidence that while some soots behave as does propane soot, the extinction from others may be a very weak function of wavelength. Jennings et al. (1979) have questioned the techniques used by Volz. Nevertheless, Volz' observations are consistent with the fact that the variation of optical depth with wavelength of smoke from a jet-fuel fire was found to have a relatively weak wavelength dependence (Pueschel et al., 1988). Pueschel's data can be used to estimate that for this soot, from the near UV to the near infrared, extinction was inversely proportional to the wavelength to about the 0.30 power. There is evidence that differences in the wavelength dependence of absorption for different soots is associated with soot particle size distribution (Roessler and Faxvog, 1980; Ottesen, 1991). Since jet fuel and crude oil are chemically and physically more similar than crude oil and propane, it seems more reasonable to use the wavelength dependence found in Pueschel's data than that found in Dalzell and Sarofim's. Using this approach, and extrapolating the wavelength dependence to 10 μm, one finds that if extinction is normalized to unity in the visible (550 nm), then the extinction at 2.5 μm would be 0.635; at 5 μm it

would 0.516; and at 10 μm it would be 0.419. We recommend use of these figures as conservative estimates but cite the wavelength dependence derived from the propane data as a best possible case (least infrared extinction).

Thus, in the plume regions, the effectiveness of many electro-optical systems operating in the infrared region may be severely affected. It is likely, however, that radar would be only slightly affected if at all. Predictions on the basis of extrapolations from the visible region of the spectrum are that there may be some effect at millimeter wavelengths, but not much at longer wavelengths (Doviak and Zrnic, 1984). Crude calculations suggest that at a wavelength of 1 mm, a radar return in the trench plume under anticipated conditions would be attenuated by a factor of ten for a target at 1 km. At a wavelength of 1 cm, it would require a 70-km horizontal path through the trench plume to produce the same attenuation. There would be even less attenuation at longer wavelengths.

So far, extinction only from particles has been considered. However, especially if there are breached wells that are not burning, there will be high concentrations of many gaseous species present that have absorption features in the near to middle infrared (Kendall, 1966). Specific absorption coefficients for organics in the infrared are typically smaller than for soot (Li-shi et al., 1989). In the absence of soot, such as downwind of a blowout that is not burning, absorption could be large enough to cause serious obscuration at selected infrared wavelengths. Broadband electro-optical systems would be less seriously affected because at most wavelengths there is little obscuration. However, narrow band electro-optical systems could be seriously affected if their wavelength corresponds to a strong infrared absorption in one of the organic species present in the oil. A detailed study to assess the absorption by organic vapors would require knowledge of the composition of Kuwaiti crude (National Research Council, 1985), estimates of individual species concentrations, acquisition of available spectroscopic data of the type provided for a limited number of species in the HITRAN data base (Air Force Geophysics Laboratory, 1989), and specification of the electro-optical systems in use.

This page intentionally left blank

APPENDIX E

ECOSTRESSES

This page intentionally left blank

1. TERRESTRIAL ECOSTRESSES - PLANTS

With regard to the effects of oil spills or of pollutants from burning oil wells on the desert environment and vegetation of Kuwait, several fundamental points should be remembered. This region is very arid; in the summer months, all vegetation is dormant. Oases with subterranean or spring water and irrigated areas are of course exceptions because of a continuous moisture supply. Annuals endure the drought as seeds, perhaps for several years; perennials frequently are reduced to very dry, woody stems or well-protected fleshy, stems with a waxy bloom. All the interior areas of Kuwait are very sparsely vegetated with low-growing, spiny, or fleshy-stemmed desert shrubs or half-shrubs that are widely spaced. Some areas on the tops of ridges, frequently with gravel mantles, are barren of vegetation. Vegetation increases with increasing available moisture, as in drainageways. Most of the 2-5 inches of annual rainfall is in the winter months when there may be a short period of vegetative growth, sprouting of perennials, and the rapid completion of the life cycle of winter annuals.

Central and southern Kuwait are quite flat or gently undulating with a slight gradient to the northeast. The country is an extensive pediment covered with loose or poorly consolidated gravels and sands left from debris-laden streams of the past. Many areas are covered with varying thicknesses of wind-drifted sand. There are no permanent or even intermittent streams. Instead, the drainage is poorly developed and consists of short dry stream beds (wadis) that drain into interior basins only when there are occasional severe winter rainstorms.

Crude Oil Release

First, consider the effect of the release of crude oil across the surface of the desert. Where crude oil covers the surface, all vegetation would be killed both from the toxicity and from smothering. Many complex phenomena occur when crude oil enters a soil. These include volatilization, runoff, adherence, hydrophobilizing soil particles, downward and lateral flow, barriers, vapor diffusion, degradation, and effects on groundwater. Some attributes of this desert would lessen the long-term effects. The lack of drainage would prevent contamination of a flowing surface water supply and would result in shortening the distance over which the oil is transported. Each short, temporary wadi would receive any runoff from adjacent slopes, and if the release continued for a long enough time, it would direct the crude into a local depression. Because the Dibdibba formation of the southwestern area is of coarse gravel and sandy strata, often with a pebble surface over sands, the porosity would favor absorption and penetration into the soil thereby reducing runoff. The bottoms of the wadis, which are aggrading, are filled with a deeper, high porosity alluvium of sand, gravel, and even boulders. In this area, there are varying thicknesses of windblown sand that is also porous.

Typical of most of the desert is the hard pan (gatch)—a hard impervious layer at or below the surface cemented together by the concentration of calcium carbonate, gypsum, and salts, the extent of which indicates the depth of penetration of past rainfall. Surface soils may have been removed by wind erosion exposing the gatch at the surface. This impervious layer would stop the infiltration of oil into the subsoil and into the groundwater. This would be important in areas of shallow wells that are used for humans or livestock, or even for irrigation.

Where there are large, flat depressions, playas develop that accumulate a soil surface of fine silts and clays that are relatively impermeable. After winter rains, water stands in these areas until it evaporates or is consumed by livestock or camels. Oil would not penetrate such soils but would accumulate on the surface or float on the surface of the water if present. The principal areas of playas are in the north between the Rawdhatain and Sabriyah oil fields and in the southeast around the Magwa and Burgan oil fields. The areas around the Manageesh oil field farther inland are very flat, but lack playas.

Between the southeastern oil fields and the coast and to the south, there is a zone of former marine deposits with gypsiferous and calcareous hard pans and irregular layers of mixed textures partly cemented under the influence of marine groundwater. In the southeastern corner and into the Neutral Zone are large areas of beach sand marshes that would be seriously affected by a covering of oil.

Because the lack of water is such a serious problem in Kuwait, there should be concern about the effect on groundwater. Coastal wells are 3-15 m deep, and rain water percolates through the sand to the water table. If such areas were flooded with crude oil, soluble products could be carried into the water table and contaminate water used for irrigating vegetables, cereals, and palms, or for mixing with desalinized water. The Sulebybiyeh groundwater field 15 km WSW of the City of Kuwait has been used by the city since 1951. Its water comes from 350 feet and may be safe from contamination. However, the Rawdhatain groundwater field to the north along the Basra Road and northwest of the Rawdhatain oil field provides great quantities of freshwater used by Kuwait City. It is in a large basin into which the winter runoff waters of many wadis converge. Of three main aquifers separated by impermeable layers, the upper main one is in the Dibdibba formation of highly porous sand and gravel, and it is only 30-60 feet deep. Its waters are a mixture of fossil water and recent, annually recharged rainwater. Release of oil into this major depression and transport downward through the soil could have very serious impacts on a valuable resource.

South of Kuwait City, between the coast and the Burgan oil field, the Ahmadi Ridge parallels the coast and gently rises to 385 feet with a crest 5 miles inland. South of Kuwait City are sand dunes that also would not be affected by an oil release.

The long-term course of events involves some speculation. In the upland desert plains and steppes of the interior, the high temperatures of the long, hot summers would favor maximum volatilization of compounds from the oil. Through the porous surface soils of sand and gravel above the hard pan, one would expect some improvement by the washing of the occasional winter rainstorms. Although the results of reclamation field experiments using soil washing to reclaim pits where oil has been burned are not very encouraging (Nash and Traver, 1989), some improvement may be possible in desert soils because of the lack of fine organic matter, colloids, and fine clays that would retain the oil film. Most of the plant species of the desert are winter annuals with highly resistant seeds of great longevity. They may lie in the soil for years before they germinate, and many seeds may not be affected by the oil. Many desert annuals have a material in the seed coat that inhibits germination until there is a supply of water sufficient to leach away the inhibitor. This adaptation may be significant in preventing premature germination until the soils have been well washed and reduced in toxicity.

Atmospheric Pollutants

Secondly, the atmospheric emissions from burning oil released from wells must be considered. There is little or no information about the effect on desert plants or on the concentrations that would kill vegetation. Most studies measure concentrations that result in visible damage to plants as evidenced by leaf spotting, necrosis, or a decrease in chlorophyll concentration. Studies are either of long-time ambient concentrations as annual averages or short-term experimental dosages. Studies in Bratislava using sulfur dioxide as a measure of mixed pollutants (dust, H_2S, Cl, F, and organics) from smelters indicate that annual average concentrations of 0.1 mg/m^3 caused serious damage to vegetation (Navara et al., 1978). On the other hand, concentrations up to 0.1 mg/m^3 have been reported for the Southern California Basin with some visible injury but no destruction of the vegetation (Darley, 1971). Experimental exposures to 0.5 mg/m^3 of sulfate aerosol or 0.3 mg/m^3 of O_3 for a short term (4 hours) showed no visible injury to beans (Chevone et al., 1986). When they were combined at those concentrations some loss of chlorophyll occurred, but not death. Killing of vegetation from smelters in north temperate areas has occurred after several years of exposure within a downwind area of about two miles (Gajewski, 1983).

Figure E-1 shows the results of calculations of the ground-level concentrations of SO_2 in plumes from the Southeast Field. Cases 1, 2, 3, and 4, are computed for 64, 100, 58, and 234 burning wellheads. In general, on a short-term basis (hours or days), one might expect visible injury in cases 2 and 4 at distances to approximately 20 and 50 km and, on a long-term basis (years), some damage for all cases to 100 km and beyond. Assuming that concentrations of 0.5 mg/m^3 have long-term destructive effects on vegetation, cases 2 and 4 would produce such effects to distances of about 20 and 45 km.

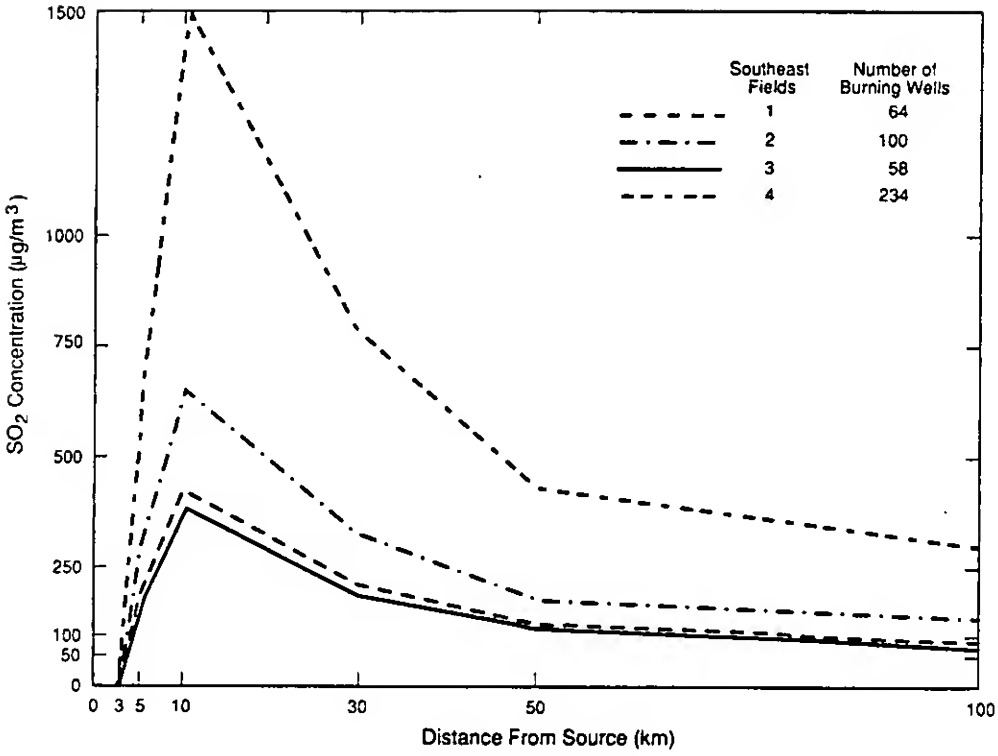

Figure E-1. SO_2 Concentrations Versus Distance from Sources for Four Cases.

Injury is related to rates of absorption and oxidation of sulfur dioxide to sulphite and sulfate by the plant. Desert plants have a number of characteristics that reduce their sensitivity. Anatomically, they have a waxy coating on leaves and stems reducing surface absorption, and under drought stress, the openings in the leaves are few and nearly closed, reducing diffusion into the leaf. Leafy structures are temporal in many woody plants, and they have minimal surface area. Physiologically, desert plants would have lower absorption because of low metabolic rates and a minimum of new growth tissues, which are most seriously affected. Damage is also reduced under the alkaline conditions in these deserts. No vegetation could be more resistant to atmospheric pollutants than the hard, woody, spiny, sparse, perennial shrubs of this desert. Although these gaseous plumes may be created during the winter period of growth when these desert annuals are more susceptible to damage, any effects would be temporary because the large reservoir of ungerminated seeds in the ground would not be affected and would reproduce in some following winter of abundant moisture. Trials have shown that weedy species, which include many of the genera of the annuals in this desert, are more resistant to atmospheric pollution that crop plants. The most sensitive vegetation of the region would be the cultivated plants under irrigation and the horticultural plants, including shade trees.

2. TERRESTRIAL ECOSTRESSES - HUMANS

Toxicology of Burning Oil Wells

Burning oil or fumes from a breached well would generate a plume containing a number of potentially hazardous components, including carbon monoxide and products of incomplete combustion, such as polyaromatic hydrocarbons, sulfur dioxide, and heavy metals. The air pollution generated by this source would be analogous to the reducing-type of smog occurring in London and Europe when adverse weather results in accumulation of sulfur dioxide and particulates from wood or coal burning. In one classic episode in London in 1952, 4,000 deaths were attributed to acute air pollution of this type.

As discussed below, the impact of burning oil on human or animal populations in Kuwait should be small. The reasons for the relatively small impact are the modest concentrations of the more toxic pollutants in the plume and the small target populations. It is probable that a small, sensitive subpopulation consisting of the elderly, infants, individuals with cardiovascular or pulmonary impairments, and some hypersensitive individuals would exhibit clinically detectable symptoms if exposed to the plume at optimal distance from the source. Symptoms would include irritation of eyes and throat and aggravation of bronchitis and asthma. Depending on how long the conditions of acute air pollution persisted, some increase in mortality attributable to air pollution would occur. However, the actual increase would be small because of the low concentration of contaminates expected to reach populated areas.

Characterization of Plume

The plume was characterized in terms of content of soot, CO, SO_2, and H_2S. Because the H_2S is released from wells in the absence of combustion, the concentration of H_2S would be inversely related to the concentration of the other hazardous components. The volatile components of the oil would be rapidly dispersed or would be consumed by fire. The oil also contains some heavy metals that would appear in the plume. The most toxic metal is vanadium at about 50 ppm. At levels expected in the plume, no toxic effects would be expected. The primary effect of the metals would be to catalyze the formation of sulfuric acid from SO_2. A number of volatile hydrocarbons are found in the oil, but these would be rapidly dispersed or consumed in the fire.

The ground-level concentration of pollutants is greatest 10 km from the source because the plume has not reached the ground level at distances nearer to the source.

Target Population

The 1985 census placed the population of Kuwait at 1,697,301, most of which is in coastal cities along the Persian Gulf. There is a small Bedouin population primarily in the southern Neutral Zone. The largest city is Salmya, near Kuwait City. Neither Salmya nor Kuwait City would, given prevailing wind conditions, be in the path of plumes from the West Field and Southeast Field.

Agriculture is minimal, although some areas just inland from the coast of the Persian Gulf have been identified as potentially viable zones for agriculture. Primary stock potentially at risk from the plume would be dairy cattle just outside of Kuwait City.

Assumptions

In the oil field models, the wells were assumed to be arrayed in a line. However, the wells may actually be clumped. Also, each major field was considered individually. The possibility of a combination of plumes from various sources was not considered. These factors would lead to an underestimating of the contaminant concentration. Also, prevailing winds are from the northwest and would carry the pollution away from population centers. However, winds from the south are not uncommon in the spring and summer and may occur any time of the year.

The maximum pollutant concentrations in the plume would occur at 10 km. Although major population centers are farther than 10 km from the source, the levels considered here are, for the most part, for the 10-km distance.

Toxic Potential by Pollutant

Table E-1 shows the ground-level concentrations at 10 km from the source for pollutants generated at each of three fields under the four stipulated scenarios for daytime conditions. Under the nighttime conditions, lower concentrations are expected at ground level.

Carbon Monoxide. According to the model, the carbon monoxide in the plume would be too low to have any effect. At any distance from the source given any scenario, the maximum level would be 6.3 ppm. Maximum concentrations downwind of the trenches are three times higher. The ACGIH Time Weighted Average for an 8-hour exposure of industrial workers is 50 ppm. A study in California cities obtained average levels of 10-20 ppms of CO in an 8-hour period.

SO_2 and Soot. These pollutants are considered together because of synergistic effects. The highest concentrations of these compounds occur for scenario #4, in the plume generated from the North Field where SO_2 reaches 2.3 mg/m^3 (.9 ppm)

and soot is 2.9 mg/m³. The maximum concentrations are seen at 10 km and diminish at greater distances.

These maximum levels are about half of the estimated pollution levels seen in the London incident of 1952. In the latter, 4.5 mg/m³ of particulates occurred with 1.34 ppm SO_2. Therefore, because of the lower pollutant concentration and because maximum concentrations would probably not impinge on populated areas, mortality at the level in the classic incident in London (4,000 dead) would not be expected. However, both concentrations downwind of the trench are nearly ten times higher. Hence, combatants unprotected by gas masks are at risk.

Table E-1. Summary of Pollutant Concentrations at 10 km from Source

	Scenario			
Field	1	2	3	4
		Soot (mg/m³)		
West	.12	.37	.10	.42
North	--	--	.57	2.9
Southeast	.52	.82	.47	1.9
Trench	14			
		SO_2 (ppm)		
West	.11	.11	.003	.13
North	--	--	.17	.87
Southeast	.16	.25	.14	.57
Trench	1.7			
		CO (ppm)		
West	.085	.80	.23	.91
North	--	--	1.4	6.3
Southeast	1.1	1.8	1.0	4.2
Trench	12			
		H_2S (ppm)		
West	.0009	.0021	.0112	.0027
North	--	--	--	--
Southeast	.00004	.00037	.00058	.00014
Trench	--			

Analyses of more recent morbidity data have shown correlation of mortality rates with air pollution in London and in West Germany (Wichmann et al., 1989). However, some studies have shown no correlation of air pollution with respiratory disease, general mortality, or hospital loads (Hompesch, 1989). Recent studies in England have indicated that excess mortality may occur when concentrations of smoke and SO_2 reach .75 mg/m^3 and .25 ppm, respectively (Casarelt and Doulls, 1986). Wichmann et al. (1988) showed impaired lung function in individuals with pre-existing disease at pollution levels of .08 ppm SO_2 in a 1987 air pollution episode. The levels of the pollutants in the plumes would be, therefore, high enough to affect human health.

The levels of SO_2 and particulates associated with increased mortality may occur in the vicinity of the northern wells in scenario #4 and may feasibly be obtained at 10 km from the southeastern wells in scenario #2. The plumes do not threaten major population areas at these distances, and the numbers of individuals involved would require further analysis, but there may certainly be some deaths of sensitive individuals.

The increased mortality is the result of the SO_2, which irritates the upper respiratory tract (URT), slows tracheo-mucous clearance and increases the excitability of bronchiolar smooth muscle. Animal studies have shown bronchiolar effects at 10 ppm for 18 days in rats and at 1 ppm for 1 year in dogs. However, in the form of sulfuric acid, increased airway responsiveness is seen at levels as low as .03 ppm. Pre-existing respiratory disease greatly increases the sensitivity to these pollutants. Humans show increased bronchiolar responsiveness to 5 ppm of SO_2. However, similar responses of asthmatic patients occur at .5 ppm (Sheppard et al., 1981).

Carcinogens. The risk from increased incidence of cancer depends on how long the pollution persists. Burning fuel contains a number of known carcinogens such as polyaromatic hydrocarbons and heavy metals, such as nickel. Increased instances of lung cancer are seen in areas of consistent air pollution from burning wood or coal (Chapman et al., 1988). Increased cancer has also been reported in firefighters (Heyer et al., 1990).

In the scenarios in Kuwait, the exposure time, even considering the possibility that the fires would take months to extinguish, would be relatively short, and the pollutant concentration would be low. Any increase in cancer incidence would be undetectable by current statistical methods.

Hydrogen Sulfide. Hydrogen sulfide is a poisonous gas that causes death by asphyxiation and inhibition of cellular respiration. Approximately 6% of the victims overcome by hydrogen sulfide and presenting at hospital emergency rooms die. The presence of hydrogen sulfide is a major hazard at oil refineries and textile manufacturers and in agricultural settings where manure is stored in enclosed areas.

Health effects have been reported at as low as 20 ppm, primarily as irritation of the eyes (Arnold et al., 1985). At 150 to 250 ppm, bronchitis and pulmonary edema occur. At 500 ppm, headache and nausea are expected, with sudden death possible at levels above 500 ppm. Levels of 4-5 ppm have been measured within oil refineries. The Threshold Limit Value is 10 ppm for hydrogen sulfide.

Data on the effects of chronic inhalation of hydrogen sulfide are limited, although chronic pulmonary edema has been reported at 35 ppm. In rats, teratogenic effects are seen at 100 ppm. Digestive disorders have been reported in animals at 15 mg/kg/day. All of these effects occur at levels well in excess of predicted exposure.

The levels of hydrogen sulfide in the plume from the oil are negligible. Even as close as .3 km from the source, no clinical symptoms would be expected from inhalation of the plume. The highest concentration of hydrogen sulfide is .32 ppm at 1 km in scenario #4. This would result only in a detectable odor (threshold of .1 ppm).

Conclusions

The primary toxicological effect would be a possible increased mortality in a small sensitive population from inhalation of sulfur dioxide and particulates. Because of the low exposure level and the small target population, the increased mortality may not be obvious except by retrospective analysis. Downwind of the trench, however, short-term exposures to soot and SO_2 would result in appreciable impact to the respiratory system of personnel without protective apparatus.

Quantification of risk in terms of deaths per 100,000 exposed would require additional information on population distribution and the effects of combined plumes from various sources. Combined pollutant concentrations from various sources would have to be considered.

3. MARINE ECOSTRESSES

Based on information we have received, a 20-million-barrel crude oil spill to the Persian Gulf is possible near Kuwait's coast. Ten million barrels could be released in the first 24 hours followed by another 10 million in the next 36 hours. The potential source is a combination of tankers and on-shore storage tanks located near Kuwait's coast. The magnitude of this potential oil spill exceeds, by a factor of five, any previous oil spill. Such an oil spill could disrupt the important fishing industry in the Gulf, shut down water desalination plants in Kuwait, Saudi Arabia, Bahrain, and Qatar that supply a large share of the area's water, and cause long-term damage to the Gulf's ecology.

Previous Oil Spills

The ten largest previous world oil spills, and the Exxon Valdez spill, are listed in Table E-2 (*World Almanac*, 1990):

Table E-2. Ten Largest Oil Spills

Name, Location	Year	Barrels
Ixtoc I, southern Gulf of Mexico	1979	4,000,000
Nowruz, northern Persian Gulf	1983	4,000,000
Atlantic Empress & Aegean Captain	1979	2,000,000
Castillo de Beliver, South Africa	1983	1,800,000
Amoco Cadiz, France	1978	1,600,000
Torrey Canyon, England	1967	900,000
Sea Star, Gulf of Oman	1972	800,000
Urquiola, Spain	1976	700,000
Hawaiian Patriot, northern Pacific	1977	700,000
Othello, Sweden	1970	600,000
Exxon Valdez, Alaska	1989	260,000

The first two, Ixtoc and Nowruz, were offshore wells that released oil over several months; the others were tankers that released oil over a few days. The Exxon Valdez spill was relatively small but had a cleanup cost estimated at $2B.

The Nowruz spill is of particular interest because it was in the Persian Gulf. We have been unable in the short term of this project to obtain accounts of scientifically determined quantitative effects from this spill, but news articles (*Newsweek*, 1983; and *Aviation Week and Space Technology*, 1983) reported a paralyzed shrimp industry and suspended operation of two Saudi desalination plants. Damage from this spill was probably minimized because it was in the northeastern part of the Gulf and a combination of northwesterly wind and currents carried the oil down the Iranian coast away from the Saudi coast, Qatar, and Bahrain where several water desalination plants are located. In a study of natural Gulf circulation, Pickett et al. (1984) point out that a spill near Kuwait would follow currents down the Saudi Coast and endanger the desalination plants.

Gulf Description

An oil spill in the Persian Gulf would be relatively serious because the Gulf is small and shallow, has slow circulation, and is very biologically productive. It is 500 miles long, 125 miles wide, and 300 feet deep at its deepest. Most of the Gulf is less than 100 feet deep, and much of its area near Kuwait, the Saudi coast, Quatar, Bahrain, and the UAE is less than 50 feet deep (Pickett et al., 1984). Currents provide a complete water change in roughly 3 years (*Encyclopedia Britanica*, 1982; Pilson,

1990). Slow circulation would make it difficult for the oil to disperse and would make it difficult for organisms from outside the Gulf to help reestablish lost species. On the other hand, relatively warm Gulf temperatures and high sunlight accelerate biodegradation and photochemical degradation of some oil spill components (Pilson, 1990; Burns, 1990). Because of its warm shallow waters, which receive nutrients from the Shatt Al-Arab, the Gulf is a very productive marine life area. The Arabian Sea, which includes the Gulf, is the highest marine life productivity area in the world (Burns, 1990).

Oil Spill Fate

We estimate that a 20-million-barrel spill can spread to cover an area 50 miles wide (nearly half the width of the Gulf) based on a very simple spreading algorithm from Fay (1971). It will probably travel south along the Saudi coast according to natural circulation studies by Pickett et al. (1984). NRC (1985) discusses potential fates of the oil spill and effects on marine life. Roughly half the oil will evaporate (the lighter, more volatile constituents), some will dissolve, some will be suspended as droplets, some will form a floating water-oil emulsion, and some will form fairly inert globs that initially float but gradually settle. The parts that dissolve or form small suspended droplets will be oxidized by biological or photochemical processes rather quickly (a few days) into other organic compounds (effect on marine life is presently unknown) carbon dioxide and water. The part that evaporates will be photochemically oxidized in the atmosphere. The part that settles will remain in the Gulf sediments for a very long time. The globs that settle contain mostly heavy oil compounds but also contain dissolved lighter compounds.

Possible Effects

Dissolved hydrocarbons are toxic to marine life and can cause some species to die over a short period of time. Toxicity is variable depending on species, developmental stage, and physical conditions. NRC (1985) lists lethal concentrations for some mollusk and crustacean larvae that range from 0.05 to 25 mg/L. If we use 1.0 mg/L as a lethal concentration, assume that 1% of the oil dissolves (this is a very rough guess) and assume that the Gulf is 50 feet deep, the 20-million-barrel spill could create a lethal area for mollusk and crustacean larvae 30 miles in diameter. Toxic conditions would probably last for a few days at most because the dissolved oil would be rapidly degraded.

Oil sediments, on the other hand, will persist for a long time and will enter the food chain through species such as shrimp, which feed on the Gulf bottom. Thus, there is the potential for long-term fishing industry disruption as well as general ecological disruption. Unfortunately, we are unable to quantify long-term effects at present. Models exist that attempt to project the fate of an oil spill and predict consequences to marine life and the marine ecology (Reed, 1990). Such a model can be

implemented in two to three months and may give a more quantitative view of possible effects than we have now.

The Gulf's Fishing Industry

The Gulf's fishing industry is fairly important. Table E-3, extracted from Unwin (1989), shows fishing industry statistics for the region:

Table E-3. Production and Consumption Data for the Gulf Region

Country	Fish and Shrimp Metric Tons	Percent of Consumption	kg per Capita
Qatar	2,700	17	7.3
Bahrain	7,900	33	22.5
Kuwait	8,700	25	4.4
UAE	85,000	100	53.1
Saudi Arabia	45,000	50	3.2

Desalination Plants

Water desalination plants are also very important. Table E-4, extracted from Unwin (1989), shows desalination statistics.

Table E-4. Desalinated Water Products: The Gulf

Country	Desalinated Water in GPD	GPD per Capita
Bahrain	30,000,000	85
Kuwait	96,000,000 (88% of use)	48
Saudi Arabia	570,000,000	41

There are three common types of desalination plants: reverse osmosis, flash evaporative, and ion exchange. All three will pass the light components of crude through with the desalinated water. Both the reverse osmosis and ion exchange types will get clogged by the heavier components of crude. Reverse osmosis plants are expected to clog in one to a few days depending on the concentration of oil. Their membranes can be cleaned using detergent in a roughly one week operation (Taylor, 1991).

Protecting desalination plants may be effective in keeping out floating oil, but not oil dissolved or suspended in the water column. Placing a ring of skirted booms around the plant inlet with a second ring of oil absorbing booms should keep most

of the floating oil out of the plant inlet. Placing vacuum trucks on barges inside the boom ring to skim floating oil will increase protection. This plan was suggested by Plotts (1991).

Power plants located near desalination plants depend on desalination for cycle makeup water. They are cooled directly by ocean water and do not depend on desalination plants for cooling. Oil in the cooling water will have little effect on performance, but losing the supply of makeup water, roughly 8 gal/h-MW (Hudson, 1991), will stop operations.

Oil Spill Treatment

It is possible that the oil spill will be ignited. Burning the oil is probably better for marine ecology than not burning it because burning helps remove the most volatile oil compounds that are the most soluble in water and hence the most toxic. Dispersants, while effective in deep water, should not be used in the shallow Gulf water or over reefs because they are more toxic than the oil (Eisler, 1975; Burns, 1990).

This Page is Intentionally Left Blank

NOMENCLATURE

Abbreviations and Symbols

AD	=	Aerodynamic Diameter
AMU	=	Atomic Mass Unit
bbl	=	barrel
b/d	=	barrels per day
^	=	indicates normalized variable
exp	=	base of natural logarithm (e)
g	=	gram
gal	=	gallon
GJ	=	gigajoules (10^9 joules)
GOR	=	Gas-to-Oil Ratio
GW	=	gigawatt (10^9 watts)
h	=	hour
K	=	Kelvin temperature scale
kg	=	kilogram
km	=	kilometer
l	=	liter
ln	=	natural logarithm
m	=	meter
Mbpd	=	million barrels per day
mg	=	milligram (10^{-3} g)
MJ	=	megajoule (10^6 joules)
μm	=	micrometer (10^{-6} m)
micron	=	micrometer (10^{-6} m)
min	=	minute
mm	=	millimeter
MMD	=	Mass Mean Diameter
nm	=	nanometer (10^{-9} m)
PDF	=	Probability Density Function
ppm	=	part per million
R	=	gas constant (1.987 calories/mole-K)
s	=	second
scf	=	standard cubic feet
URT	=	Upper Respiratory Tract
z	=	vertical coordinate

Acronyms

ACGIH	=	American Conference of Governmental Industrial Hygienists
IPSA	=	Iraqi Pipeline to Saudi Arabia
PCGC-2	=	Pulverized Coal Gasification & Combustion in 2 dimensions

Variables

A = area of pool (m^2)
B_{ext} = extinction cross section (m^2/g)
C = empirical coefficient (value of 10 to 15)
C_i = concentration of i^{th} component
C_p = ground-level concentration of pollutant (g/m^3)
d = droplet diameter (μm)
D = density conversion factor (m^3 of oil to kg of oil)
D_i = diffusion coefficient for i^{th} component (cm^2/s)
D_{10} = 10% passing grain size for sand (mm)
EF = pollutant emission factor (kg/kg)
ε = parameter used as an exponent
F_w = estimated blowout flow rate per well (kg/s)
h = thickness of oil slick (m)
H = height (m)
η = viscosity (centipoise)
k = permeability (mm/s)
L = depth of trench (m)
L_s = equivalent line source length normal to wind direction (m)
M = mass density (g/m^3)
M_c = column density (g/m^2)
m_d = droplet mass (g)
M_p = pollutant production rate (kg/s)
n = integer
n_w = number of wellheads burning in a given field
ϕ = elevation angle of the sun (degrees)
q = source release rate (g/m-s)
Q = flow rate (m^3/s)
Q_h = heat output rate (MW)
r = radius (m)
R = burning rate (m/s)
R_b = radius of burning portion of oil slick (m)
R_s = radius of oil slick (m)
R_v = visual range (km)
σ_z = vertical dispersion parameter (m)
t = time (s)
T = temperature (usually Kelvin)
τ = optical depth (dimensionless)
θ = angle between the normal to a line source and the wind direction (degrees)
U = surface wind speed (m/s)
v_b = burn rate of oil slick (m^3/s)
v_s = rate of oil spill (m^3/s)

V_m = molar volume (cm^3/mole)
V_{out} = volume (m^3)
W = width of trench (m)
y = dimensionless variable

This page is intentionally left blank

DISTRIBUTION

Federal Agencies

Maureen Crandall (60)
Room GA 301
Intelligence Dissemination Divison, IN 40
U.S. Department of Energy
P.O. Box 23865
Washington, DC 20026

Internal

3141 S. A. Landenberger (5)
3151 G. L. Esch (3)
6601 D. Engi (50)
8524 J. A. Wackerly (1)

This page intentionally left blank

Org.	Bldg.	Name	Rec'd by	Org.	Bldg.	Name	Rec'd by

Sandia National Laboratories